DEVELOPMENT AND EVALUATION OF AN IMPEDANCE CARDIOGRAPHIC SYSTEM TO MEASURE CARDIAC OUTPUT

AND

DEVELOPMENT OF AN OXYGEN CONSUMPTION RATE COMPUTING SYSTEM UTILIZING A QUADRUPOLE MASS SPECTROMETER

July, 1967

Performed under Contract No. NAS 9-4500
by
University of Minnesota
Minneapolis, Minnesota
for
NATIONAL AERONAUTICS AND SPACE ADMINISTRATION
Manned Spacecraft Center
Houston, Texas

NASA CR 92220

DEVELOPMENT AND EVALUATION OF AN IMPEDANCE CARDIOGRAPHIC SYSTEM TO MEASURE CARDIAC OUTPUT

AND

DEVELOPMENT OF AN OXYGEN CONSUMPTION RATE COMPUTING SYSTEM UTILIZING A QUADRUPOLE MASS SPECTROMETER

July 1967

Performed under Contract No. NAS 9-4500

by

University of Minnesota
Minneapolis, Minnesota

for

NATIONAL AERONAUTICS AND SPACE ADMINISTRATION
Manned Spacecraft Center
Houston, Texas

DEVELOPMENT AND EVALUATION OF AN IMPEDANCE CARDIOGRAPHIC SYSTEM TO MEASURE CARDIAC OUTPUT

and

DEVELOPMENT OF AN OXYGEN CONSUMPTION RATE COMPUTING SYSTEM UTILIZING A QUADRUPOLE MASS SPECTROMETER

July 1967

by

W. G. Kubicek, D. A. Witsoe, R. P. Patterson, M. A. Mosharrafa,
J. N. Karnegis and A. H. L. From*

University of Minnesota College of Medical Sciences
Minneapolis, Minnesota

*Heart Disease Control Program
US Public Health Service
Washington, D. C.

Performed under Contract No. NAS 9-4500

by

University of Minnesota
Minneapolis, Minnesota

for

NATIONAL AERONAUTICS AND SPACE ADMINISTRATION
Manned Spacecraft Center
Houston, Texas

FOREWORD

The research reported here was undertaken with the objective of developing instrumentation suitable for space flight to carry out in-flight experiments to assess the effects of space flight upon the circulatory and metabolic systems in human beings. The main effort in these experiments was directed toward developing a new method to measure cardiac output and to develop a system that could be manufactured for space flight that would measure the oxygen consumption rate.

Given the conditions that the skin of the astronauts could not be penetrated during space flight, any method of measuring cardiac output would require the use of some external technique. It was decided to pursue in depth the possibility of utilizing previously observed intrathoracic electrical impedance changes during the cardiac cycle as a means of determining stroke volume and cardiac output. At present the method as described here appears to be most useful to determine ratios of cardic output while the absolute values obtained by the impedance method probably contain a considerable error. Further research is under way to attempt to assess the scope and significance of this error. The results of these experiments also indicate that a new dimension of usefulness of the impedance method will be in research and possibly clinical application in the area of cardiac dynamics. It appears that the peak height of the first derivative of the impedance change waveform is related to the rate of energy release by the left ventricle. Further

investigation of this feature is also under way.

For the development of a space flight qualifiable oxygen consumption rate computing system the major effort in this investigation was directed toward developing a light weight, rapid response system for the analysis of expired air. The quadrupole mass spectrometer appears to be suitable for this purpose. With further development it can be miniaturized sufficiently for use in space flight. A prototype laboratory model is operational and has been incorporated into an oxygen consumption rate computing system as described in this report.

The contributions of Dr. Roy Mattson in the early phases of this project were of great value in initiating the sophisticated engineering necessary in this project.

Special acknowledgment is extended to Dr. Samuel M. Fox, III, Chief, Heart Disease Program, U.S. Public Health Service, for many helpful suggestions and encouraging advice to proceed with the investigation of the impedance system as a means of determining cardiac output. Grateful acknowledgment is also extended to Dr. Fox for providing the services of Dr. Arthur From for assistance in the experiments upon animals.

The technical assistance of Mr. Charles Dowd, Mrs. Georgia Luks, and Mr. Phillip Ewing is also gratefully acknowledged.

The financial and moral support of Dr. Sherman Vinograd, Dr. Charles Berry, Dr. Lawrence Deitlein, Dr. George Armstrong, Mr. William Judy, and many other NASA personnel is most gratefully acknowledged.

W. G. Kubicek

CONTENTS

CONTENTS (continued)

CONTENTS (continued)

CHAPTER ONE

EVALUATION OF THE IMPEDANCE METHOD OF MEASURING CARDIAC OUTPUT

SECTION I. A Comparison between Impedance and Dye Dilution Techniques for Estimating Cardiac Output

Summary -

A four electrode impedance plethysmographic system was developed which apparently monitors left ventricular output. Two band electrodes were placed around the subject's neck, a third band around the thorax at the level of the xiphisternal joint, and the fourth around the lower abdomen. The upper neck electrode and abdomen electrode were excited by a 100 kHz constant sinusoidal current and the resultant voltage (impedance) changes occurring with the cardiac cycle were monitored from the inner two electrodes. Stroke volume was calculated from the impedance change information using a formula relating impedance changes to volume changes in a conducting solid. A comparison study with simultaneous impedance and dye dilution measurements under rest and exercise conditions was carried out on 10 healthy young adult males. Results indicate that the impedance method predicts relative changes (ratios) in cardiac output with an accuracy of ±16 percent with 95 percent confidence.

Introduction -

Prior to the initiation of NASA Contract NAS 9-4500, research efforts by the University of Minnesota Physical Medicine & Rehabilitation Laboratories had indicated that impedance techniques may be applicable to the estimation of beat by beat cardiac output (3,4,5,8). A four band electrode

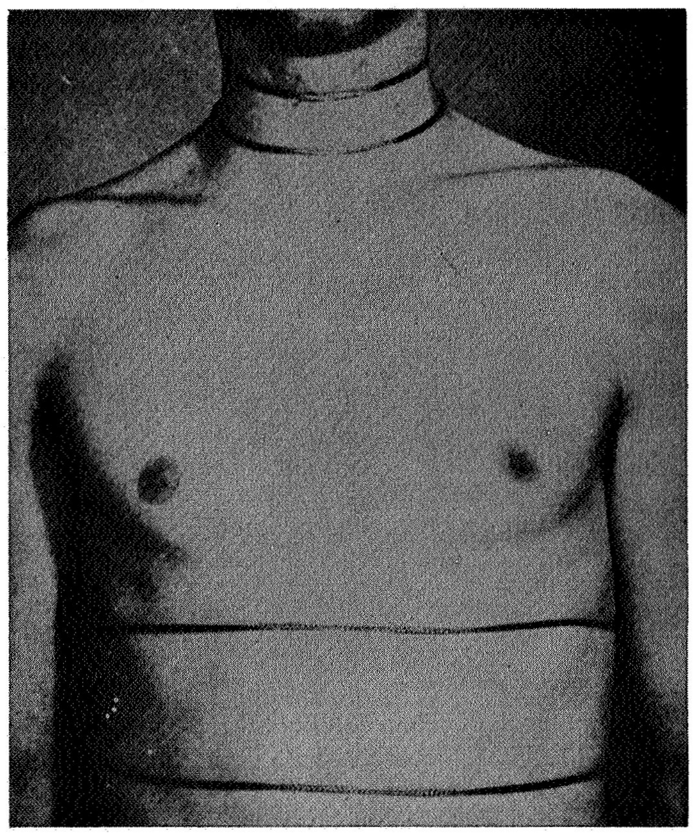

Fig. 1-1 Subject with four-band electrodes

impedance system had been used to estimate cardiac output values by an impedance technique. Two conductive strip electrodes approximately 6 mm wide were placed around the neck and two around the abdomen. The other two electrodes were spaced at least 2 centimeters away from the inner electrodes. The inner two electrodes were placed, one around the base of the neck and the second about two centimeters below the xiphisternal joint. A photograph of the subject with metallic bands in the position described above illustrates the position of the electrodes (fig. 1-1). The outer two electrodes were connected to a constant current source providing 6 milliamps, 100 kHz sinusoidal current. The other two electrodes were connected to a high impedance amplifier and suitable detection circuits to provide for the determination of the basic impedance between the two inner electrodes and also for the impedance change that occurred during the cardiac cycle. Cardiac output was then calculated from the impedance data with the aid of the formula shown below

$$\Delta V = \rho \frac{L^2}{Z_o^2} \Delta Z \qquad \text{equation 1-1}$$

ΔV = ventricular stroke volume (cc)

ρ = the electrical resistivity of blood at 100 kHz (average value 150 ohm-cm)

L = the mean distance between the two inner electrodes (cm)

Z_o = the basic impedance between the two inner electrodes (ohms)

ΔZ = extrapolated maximum impedance change during systole as described below.

In this earlier work the value of ΔZ was originally determined graphically by extrapolating the maximum decreasing slope of the impedance change waveform from the base of the curve at the start of systole to the end of ventricular systole as indicated by the second heart sounds. The extrapolation procedure is described in the ΔZ waveform of fig. 1-2.

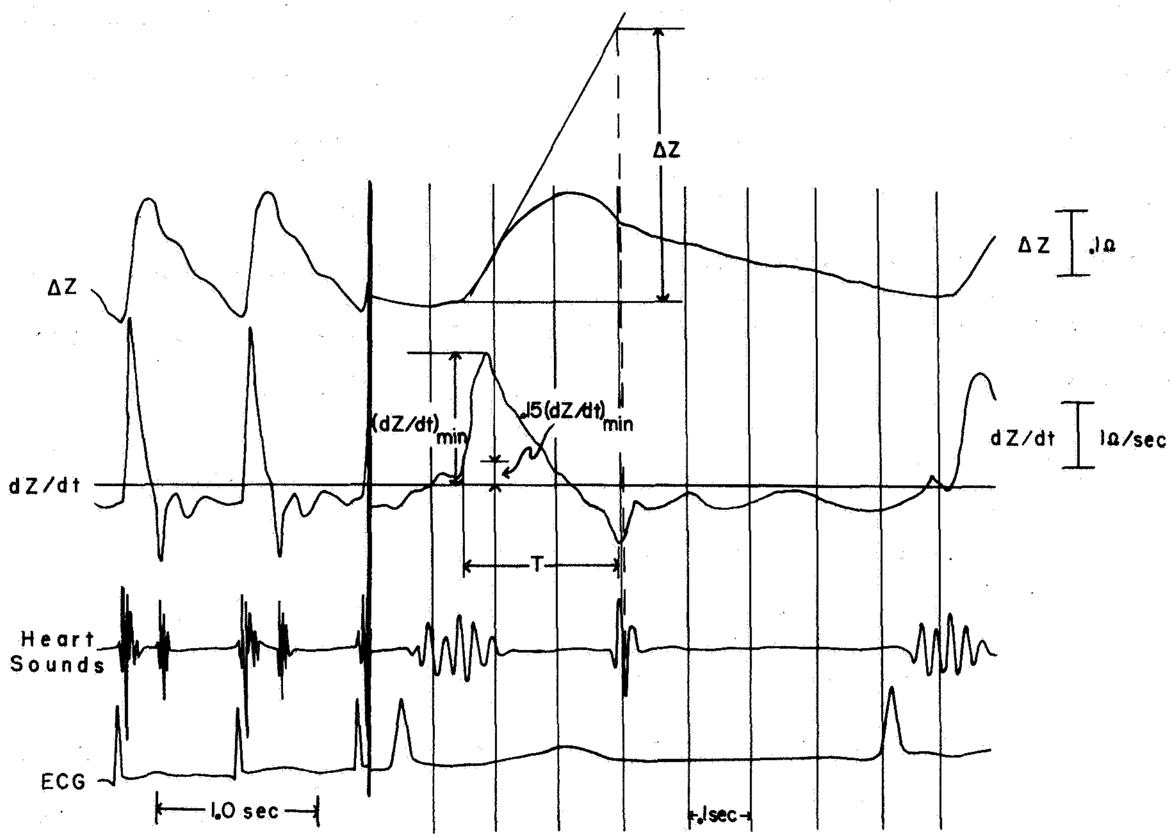

Fig. 1-2 Impedance Waveforms Depicting Analysis for Stroke Volume Estimation

The slope extrapolation procedure was subject to errors in that the drawing of the slope of the ΔZ waveform was dependent upon the judgment of the investigator and also the estimation of the end of systole by the second heart sound was often difficult or impossible when the subject was undergoing exercise or if there were valvular problems causing murmurs in the heart sounds. As part of the investigations under the current NASA contract, studies were carried out in which attempts were made to reduce the errors in calculating the maximum decreasing slope of the impedance change during systole. By taking the first time derivative of ΔZ, dZ/dt, it was possible to accurately determine the maximum slope of the impedance change waveform. It was also found that a characteristic peak in the dZ/dt waveform could be used to determine the end of left ventricular ejection. The ejection time, T, was measured from the occurence of 0.15 $(dZ/dt)_{min}$ to the positive signed peak occurring with the second heart sound as shown in fig. 1-2. The occurence of 0.15 $(dZ/dt)_{min}$ was chosen for the onset of ejection to eliminate from the ejection time determination the slow decrease in impedance that occurs with some individuals at the start of systole. The product of the negative peak of the first derivative and T was then used for the value of ΔZ in equation 1.

Equation 1 then takes the form,

$$\Delta V = \rho \frac{L^2 T}{Z_o^2} (dZ/dt)_{min} \tag{2}$$

where ρ, L and Z_o have been defined above in equation 1 and $(dZ/dt)_{min}$ is the peak value of the first time derivative of Z_o in ohms per second as shown in fig. 1-2. T is equal to the ventricular ejection time in seconds as described in fig. 1-2.

The average cardiac output can then be obtained by multiplying ΔV as determined by equation 2 by the pulse rate and averaging over four or five beats.

Methods -

To evaluate the impedance method for measuring cardiac output, a comparison study with simultaneous impedance and dye dilution measurements under rest and exercise conditions were carried out on ten healthy young adult males (7). A four electrode impedance system, as previously described, was used in this study. Electrodes for this study were made by wrapping 4 mm wide tinned copper braid shielding with a conductive cloth (Velcro hi-meg conductive pile B-22-11-WZ) and then sewing the electrodes on Velcro pile for backing. The electrodes were fastened together using Velcro #80 hook material. Both neck electrodes were sewn on a single two inch backing and each electrode used around the abdomen was sewn on a 1" backing. During the experiment the impedance change signal, the first derivative of the impedance change signal, heart sounds and ECG were recorded on a Precision Instrument model 200 FM magnetic tape recorder. Simultaneously the impedance change signal and the heart sounds were recorded on a Sanborn model 296 direct writing recorder. After the experiment, the data on magnetic tape were played back and graphically recorded on a Honeywell model 1108 Visicorder for analysis. Cardiac output was calculated from the impedance data by use of equation 2 and the average cardiac output was then obtained by multiplying the ΔV as determined by equation 2 by the pulse rate and averaging over 4 beats. The comparison dye dilution cardiac output values were obtained using the technique as follows:

The subjects were not premedicated. The catheters were inserted percutaneously with the subject supine on an x-ray table. The procedures were carried out using surgical sterile technique.

Two percent xylocaine was infiltrated over a basilic vein. A thin wall stainless steel needle was inserted into the vein in those subjects in whom it was of suitable size. A number five French standard woven nylon catheter was then passed through the needle and up the vein, the needle was then withdrawn over the catheter and out of the vein. If the vein was not of suitable size, Seldinger technique (9) was used with the vein being punctured by a teflon sleeved number 19 French percutaneous needle (Cook Catheter Co.). The steel needle and stylet were removed leaving the teflon part of the needle within the lumen of the vein. A teflon coated guide wire (Cook Catheter Co.) with a flexible tip was then passed through the plastic needle into the vein and the needle removed. A teflon radiopaque catheter (Cook Catheter Co.) was threaded over the guide wire and advanced into the vein. The catheter was 70 cm. long with an internal diameter of 1.16 mm. and an outer diameter of 1.5 mm. The nylon catheter, or the teflon catheter with its guide wire extended was then positioned under fluoroscopic control so that the tip was in the superior venacava.

Arterial intubation was done using the brachial artery, except once where the radial artery was used. The puncture site was infiltrated with 2 percent xylocaine. The artery was then cannulated using the teflon sleeved percutaneous needle described above. After removal of the inner steel needle and stylet, the plastic needle was anchored to the skin by one silk suture.

The teflon needle or catheter was attached directly to a densitometer (model X-302, Waters Co.) which in turn was connected to a constant flow infusion-withdrawal pump (model 600-900 Harvard Apparatus Co.). The sampling system was sterile so that blood withdrawn during a recording was then immediately infused. Patency of the arterial system was maintained by slowly infusing heparinized saline between measurements.

The venous catheter was carefully overfilled with the indicator, Cardiogreen dye. For each measurement one ml of the solution containing five mg of the dye was injected from a calibrated syringe. Arterial blood was sampled at a rate of 38.2 ml/min. The dye dilution curve was recorded on an electron beam recorder (model DR-8 Electronics for Medicine) with a paper speed of five mm/sec. The linear dye curve, and its electronically derived logarithm and integral, were simultaneously recorded. Dye calibrations for the linear deflection and its integral were done at the end of the procedure using the same connections that were used during the studies. The calibrations were done by preparing a 10 mg/L dye concentration in a blood sample. This dilution, as well as a blank, was prepared from a 50 ml sample of blood withdrawn before the first dye curve was done. All calibrations were done in duplicate. The densitometer had previously been shown to respond linearly to changes in the concentration of dye in the blood.

Cardiac output values were calculated by the Stewart-Hamilton formulas (10). The area under the linear dye curve was obtained from the integral deflection. The validity of these measurements was established by periodically checking these values against the areas obtained by planimetric integration of the curve. Recirculation of dye was excluded by using the linear part of the disappearance slope of the logarithm curve as presented mathematically by Hepner, et al (2).

After completion of the studies the catheters and needles were removed and the point of entrance compressed for a few minutes to prevent hematoma formation. The puncture sites were then covered by a band-aid.

Procedure -

Twelve comparison measurements were made between the impedance technique and the dye dilution method of measuring cardiac output of 10 young, normal Caucasian male subjects. The comparison measurements were made under the following experiment conditions:

ELAPSED TIME (minutes)	EXPERIMENTAL CONDITION
0-20	(1) 20 minute rest -- supine
22	(2) control measurement C_{1A} -- supine at rest

ELAPSED TIME (minutes)	EXPERIMENTAL CONDITION
25	(3) control measurement C_{1B}-- supine at rest
35	(4) control measurement C_{2A}-- sitting on bicycle at rest
38	(5) control measurement C_{2B}-- sitting on bicycle at rest
39	(6) start exercise on bicycle for 6 minutes with a work load of 30 watts/sq. M. pedaling 60 R.P.M.
43	(7) experimental measurement E_{1B}-- 4 minutes after start of exercise
45	(8) experimental measurement E_{1C} immediately (within 5 sec.) following 6 minute work period
45-65	(9) 20 minute recovery period after exercise -- sitting on a stool
67	(10) recovery measurement R_{1A} -- sitting on bicycle after exercise
70	(11) recovery measurement R_{1B} -- sitting on bicycle after exercise
71	(12) exercise on bicycle for 6 minutes at a work load of 60 watts/sq. M. pedaling at 60 R.P.M.
75	(13) experimental measurement E_{2B} -- 4 minutes after start of exercise
77	(14) experimental measurement E_{2C} immediately (within 5 secs.) following 6 min. work period
77-97	(15) 20 minute recovery period after exercise -- sitting on a stool
98	(16) recovery measurement R_{2A}-- sitting on the bicycle ergometer
101	(17) recovery measurement R_{2B}-- sitting on the bicycle ergometer

The impedance determined cardiac output measurements were made either near the time when the peak occurred in the dye dilution curve or immediately after recirculation appeared on the dye dilution curve. In the comparison measurements made after 6 minutes of work (E_{1C}, E_{2C}), the dye dilution curve was made with the subjects pedaling the bicycle and impedance measurement was made immediately (within 5 seconds) after they had stopped in order to eliminate motion artifacts. All of the impedance measurements were made with the subjects holding their breath.

Results -

Two approaches were taken to assess the value of the impedance method in predicting cardiac output. The first was to determine whether the impedance method could predict absolute cardiac output values comparable with those of a simultaneous dye dilution measurement. The second approach was to evaluate the impedance method's ability in predicting relative changes in cardiac output under various rest and exercise conditions.

In general, cardiac output values calculated by the impedance technique were larger than the simultaneous values obtained by the dye dilution technique, consequently the data were examined for a constant by which the impedance value could be divided to provide absolute value correlation with the simultaneous dye dilution values. The ratio between the impedance calculated cardiac output and the dye dilution cardiac output was determined for each simultaneous measurement.

Table 1-I Average Ratios of the Impedance Calculated Cardiac Output to Dye Dilution Cardiac Output for each Experimental Condition. Standard Deviations of a Sample are shown for the Various Averages.

$$\frac{\text{Z Cardiac Output}}{\text{Dye Cardiac Output}}$$

Subject	Supine	Sitting	Exercise I	Recovery I	Exercise II	Recovery II	Average	±S.D.
1	1.77	1.69	1.75	2.02	2.03	1.50	1.79	±.18
2	.63	1.51	.99	1.39	.91	1.44	1.14	±.32
3	1.43	1.38	1.08	1.45	1.25	1.35	1.32	±.13
4	1.22	1.11	1.20	1.17	1.22	.95	1.15	±.09
5	.87	1.14	.79	.94		.98	.94	±.12
6	1.20	1.33	1.21	1.31	1.49	1.16	1.28	±.11
7	.96	.91	.98	.91	.91	.91	.93	±.03
8	1.17	1.45	1.00	1.25	1.11	1.23	1.20	±.14
9	1.06	1.21	.98	1.23	.98	1.33	1.13	±.13
10	.72	.99	.73	.94	.70	1.45	.92	±.26
Average	1.10	1.27	1.07	1.26	1.17	1.23	1.18	

s = .24

s = .08

Table 1-I shows the average of these ratios for the various experimental conditions for each subject. The average of these ratios as shown in the lower right hand corner of Table 1-I was then used as a weighting constant. Each impedance calculated cardiac output value was divided by this weighting constant and plotted against the corresponding dye dilution value and is shown in fig. 1-3 as group corrected cardiac output. The dotted lines represent ±20 percent deviation from the perfect correlation 45° line.

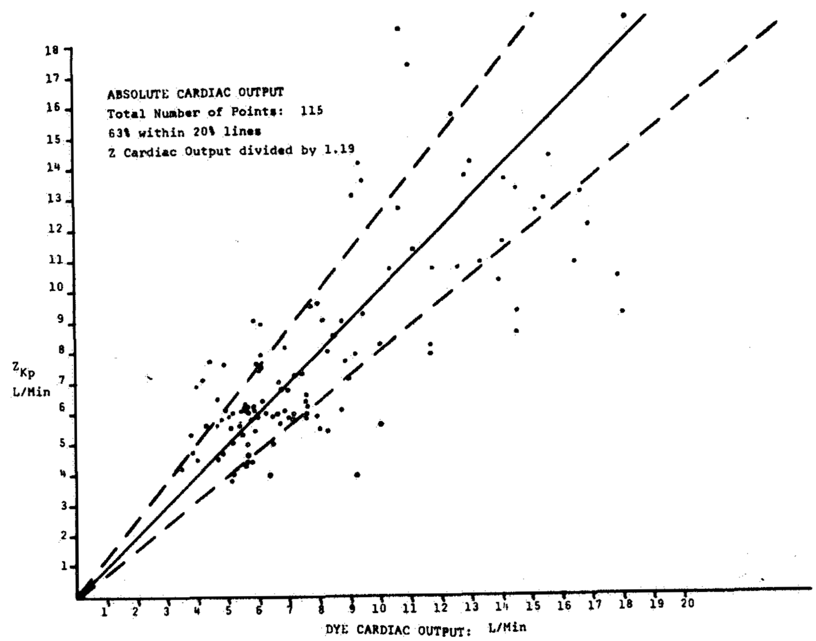

Fig. 1-3 Plot of group corrected cardiac output values

To assess the value of the impedance method in predicting the changes in cardiac output under rest and exercise conditions for an individual subject, a weighting constant for each subject was determined by taking the average of the ratios of the simultaneous impedance calculated cardiac output and dye dilution cardiac output (right hand column of Table 1-I).

Each subject's impedance calculated value was then divided by his particular weighting constant. The results of this comparison are shown in fig. 1-4 as individual corrected cardiac output. The cardiac output values appearing in figs. 1-3 and 1-4 were calculated by use of the peak negative value of the derivative multiplied by T (fig. 1-2).

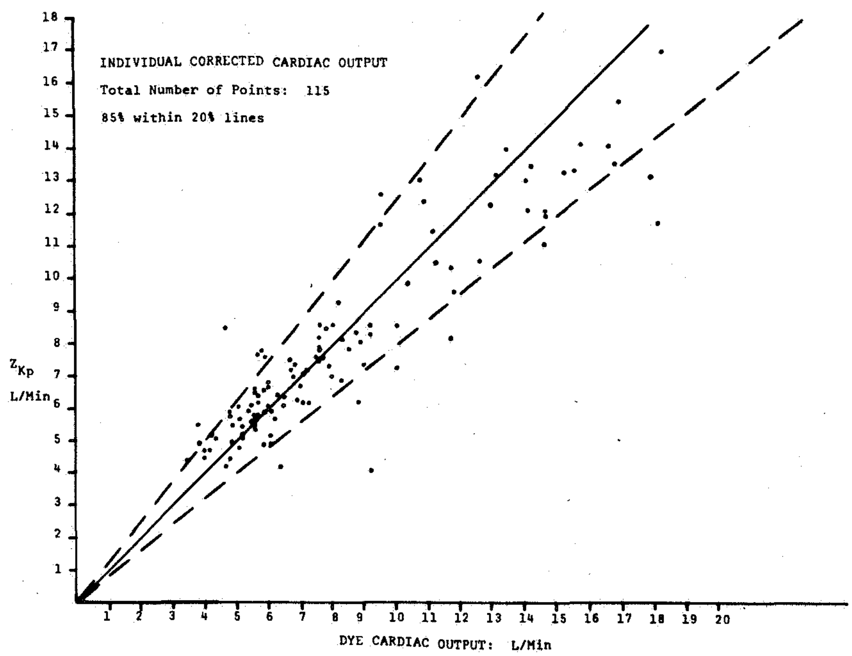

Fig. 1-4 Plot of individual corrected cardiac output values

Graphs of normalized dye dilution cardiac output and impedance values were plotted for each subject for the various experimental conditions. The group average for each experimental condition as determined from the individual subject graphs was then calculated and plotted as a composite graph for both impedance and dye methods of calculating cardiac output as shown in fig. 1-5. This graph indicated the average response of the entire group to changes in cardiac output as predicted by the impedance and dye techniques.

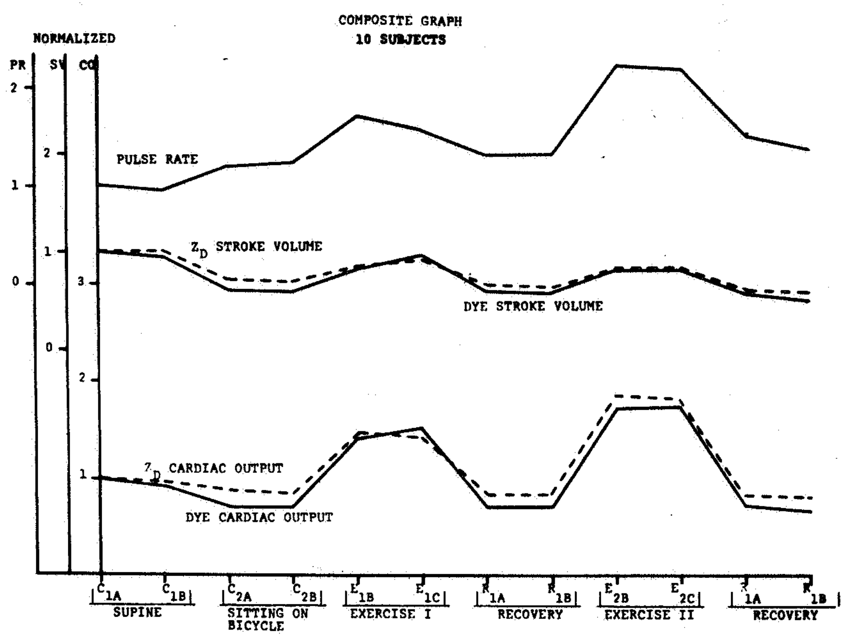

Fig. 1-5 Normalized graph of the average cardiac output values, stroke volumes and pulse rates for ten subjects

A further statistical analysis of the data was performed using the variance of the paired impedance and paired dye values for each experimental rest condition (supine, sitting on the bicycle and recovery). The reproducibility values were calculated, using only paired rest conditions and not paired exercise conditions (E_{1B}, E_{1C} and E_{2B}, E_{2C}) in order to reduce as far as possible variations in estimating true cardiac output between paired measurement and thus give a better estimate of measurement error. The following summarizes the techniques and results of this analysis. A more complete discussion is given in Appendix I.

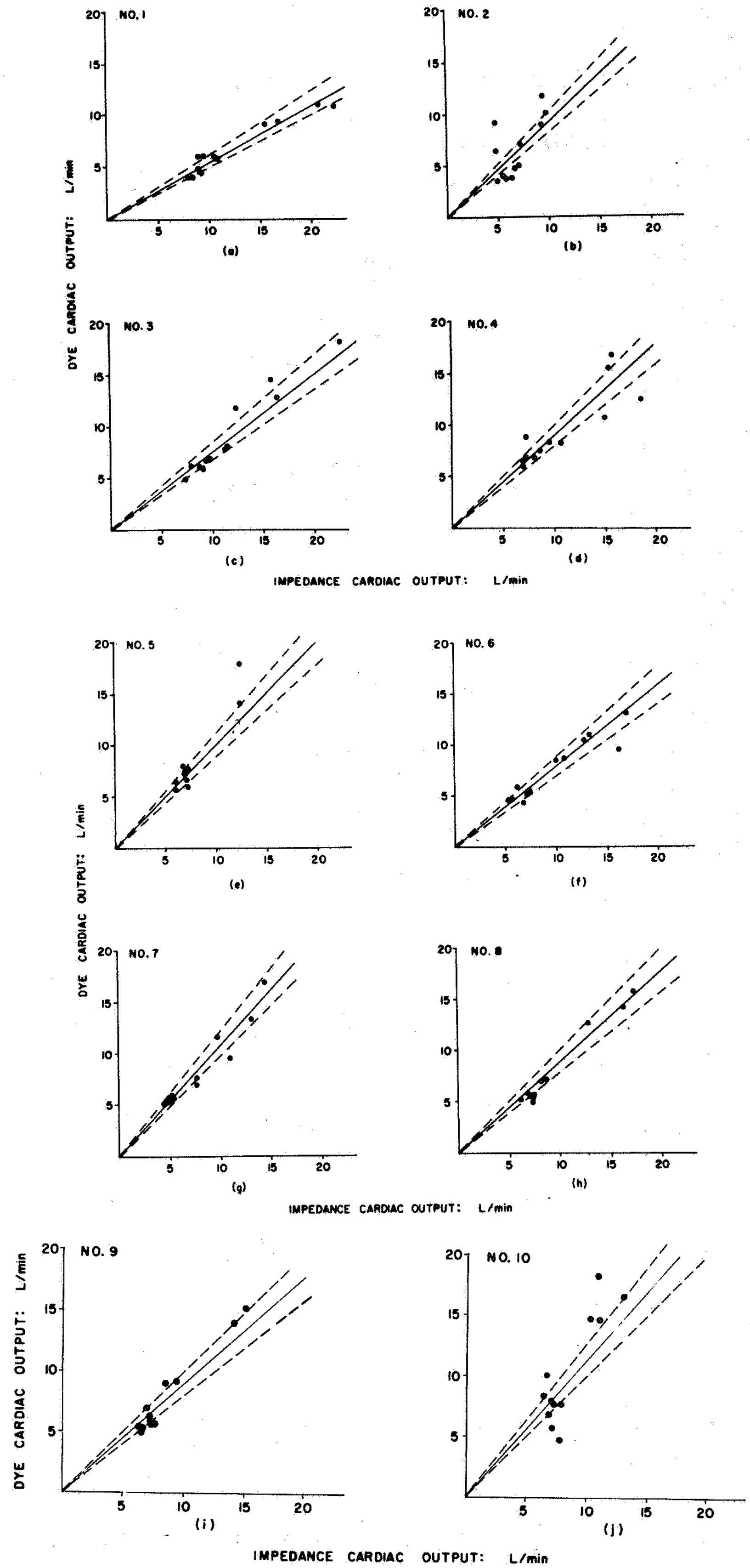

Fig. 1-6 Individual subject scatter plots with best fitting straight line and theoretical scatter reference lines as described in text.

Scatter plots of the impedance-dye comparison data for each subject are shown in figs. 1-6(a) through 1-6(j). The solid lines are the "best fitting" straight lines through the origin. The dashed lines are calculated to theoretically contain 68% of the points assuming the scatter about the solid line is due only to measurement error of the two techniques. Since figs. 1-6(a-j) are plots from ten different subjects it is obvious that different people have different curves relating their dye readings and impedance readings. Each graph has scatter, of course, but the analysis performed suggests that there is no more scatter than can be explained by the measurement errors of the two techniques and a true curve is a straight line (different for each subject) through the origin.

This conclusion was reached by the following argument: transforming both measurements by taking logarithms, lines through the origin with slopes S_i on the original scale became lines of unit slope with intercepts log S_i on the log scale. The residual variance of log dye for a given log impedance is then the sum of the replication variance for log impedance. The estimates of these replication variances are .00197 and .00056, respectively; they were obtainable because almost every observation was repeated and the estimated variances would then be pooled (1). Thus the standard deviation of log dye for a given log impedance is $\sqrt{.00197 + .00056} = .0503$, so it follows that approximately 68% of the observations on the log scale should fall within .0503 of a line with unit slope and intercept log S_i.

Since $\log^{-1} .0503 = 1.12$ and $1/1.12 = .89$, 68% of the original observations should lie between the lines:

$$y = 1.12S_i x \text{ and } y = .89S_i x.$$

These lines are the dashed ones in figs. 1-6(a-j).

The S_i were estimated by the rule:

$S_i = \log^{-1}$[ave log dye -ave log impedance]. It may be noted that most of the points do lie within the dotted boundaries, whereas the measurement errors of both dye and impedance imply that 32% should be outside. We conclude that it is very plausible that the true graph of each subject is approximately a straight line through the origin.

If it were a fact that the true graph for each subject is a straight line through the origin, an experimenter would not need to have calibrated his subject, i.e., determine the true line, to know that a ratio of two impedance readings at different conditions conditions would estimate the ratio of cardiac outputs. Assuming the variation of each of the two impedance readings to be that only of measurement error, it turns out that the ratio of the two readings is accurate to within 17% with 95% confidence. Proceeding in a similar fashion, it turns out that the ratio of two dye readings is accurate to within 33% with 95% confidence. The implications of the previous two sentences are that the ratio of two impedance readings might be a more accurate measure of the ratio of cardiac outputs than the ratio of dye measurements.

Discussion -

A visual comparison of the difference in the scatter of data points presented in figs. 1-3 and 1-4, as group corrected and individual corrected impedance cardiac output values, indicates subject to subject variation in the impedance data. The subject to subject variation is also illustrated in the right hand column of Table 1-I where the average weighting constant for each subject is shown along with the standard deviation of these weighting constants. Future investigations will be aimed at determining a universal correction factor or subject parameter that may reduce or eliminate the subject to subject variation, and consequently will allow estimation of absolute cardiac output values with higher accuracy than is now obtainable.

The composite graph (fig. 1-5) suggests that, on the average for all 10 subjects, the experimental impedance method provided the same physiological information concerning relative changes in cardiac output as the reference dye dilution technique.

The data obtained in this study indicate that the reproducibility of single impedance observations of cardiac output is greater than for a similar value obtained by the dye dilution technique. Likewise the results indicate that the ratio of two cardiac output values obtained by the impedance method is more accurate than a similar ratio obtained by the dye dilution technique in predicting true dye cardiac output ratios. This finding should have application in situations where the relative change in cardiac output is an important parameter and where the absolute values of cardiac output are of secondary value.

REFERENCES

1. Dixon, W.J., and Massey, F.J.: Introduction to Statistical Analysis, McGraw-Hill Company, 1957.

2. Hepner, C.F., James, G.W., Jacobs, J.E., Kezdi, P., and Wessel, H.U.: Automatic Computation of the Area under Indicator Dilution Curves. IEEE Trans on Communicat and Elect, 89:541-544, 1964.

3. Kinnen, E., Kubicek, W.G., Hill, P., and Turton, G.: Thoracic Cage Impedance Measurements: Tissue Resistivity in Vivo and Transthoracic Impedance at 100 kc. Technical Documentary Report No. SAM-TDR-64-5, USAF School of Aerospace Medicine, Brooks Air Force Base, Texas, March 1964.

4. Kinnen, E., Kubicek, W.G., and Patterson, R.: Thoracic Cage Impedance Measurements: Impedance Plethysmographic Determination of Cardiac Output (A Comparative Study). Technical Documentary Report No. SAM-TDR-64-15, USAF School of Aerospace Medicine, Brooks Air Force Base, Texas, March 1964.

5. Kinnen, E., Kubicek, W.G., and Witsoe, D.: Thoracic Cage Impedance Measurements: Impedance Plethysmographic Determination of Cardiac Output (an Interpretive Study). Technical Documentary Report No. SAM-TDR-64-23, USAF School of Aerospace Medicine, Brooks Air Force Base, Texas, May 1934.

6. Kinsman, J.M., Moore, J.W., and Hamilton, W.F., Studies on the Circulation. I. Injection Method. Physical and Mathematical Considerations. Amer. J. Physiol. 89:322-39, 1929.

7. Kubicek, W.G., Karnegis, J.N., Patterson, R.P., Witsoe, D.A., and Mattson, R.H.: Development and Evaluation of an Impedance Cardiac Output System. Aerospace Medicine, 37:1208-1212, 1966.

8. Patterson, R., Kubicek, W.G., Kinnen, E., Witsoe, D. and Noren, G.: Development of an Electrical Impedance Plethysmograph System to Monitor Cardiac Output. Proceedings of the First Annual Rocky Mountain Bioengineering Symposium, 1964.

9. Seldinger, S.I.: Catheter Replacement of the Needle in Percutaneous Arteriography. A new technique. Acta. Radiol., [Ther.] (Stockholm), 39:368-376, 1953.

10. Stewart, G.N.: The Output of the Heart in Dogs. Amer. J. Physiol., 57:27-50, 1921.

Appendix I

A Statistical Analysis of the Comparison Study between the Dye Dilution and Impedance Methods of Estimating Cardiac Output

James Boen, Ph.D.
Dept. of Biostatistics
University of Minnesota School of Public Health

Suppose that we address ourselves to the estimation of ratios of cardiac outputs. That is, given two impedance method cardiac output readings, z_1 and z_2, at different physiological levels, with what accuracy does z_2/z_1 estimate the ratio of the two "true" cardiac outputs for that individual. (We do not, of course, know what the true cardiac output for anyone at anytime is, but we "define" it as the [conceptual] average of an infinite number of dye measurements). Let z_{it} denote the impedance measurement on individual i at time t and let d_{it} denote the dye measurement on individual i at time t. Then

$$\frac{z_{it_1}}{z_{it_2}} = \frac{d_{it_1}}{d_{it_2}} \text{ exactly for all i, } t_1\text{, and } t_2 \text{ if, and only if,}$$

the graph of z vs d is a straight line through the origin for person i. That is, there exists a positive constant a_i such that $d_{it} - a_i z_{it}$ for all t>0. A glance at figs. 1-6(a) through 1-6(j) (the z vs d plot for each of the 10 subjects of the study) makes it clear that all the points do not lie on a straight line, let alone through the origin. However, there is certainly measurement error in both z and d, so that it is natural to ask whether the matter could be explained by measurement error of the two techniques. If it is assumed that the percent error for each type of measurement is constant, it follows that Var $(\log z_{it}) = \sigma^2_{\log z}$ and Var $(\log d_{it}) = \sigma^2_{\log d}$ are independent of the level of cardiac output. If there exists a_i such that the long run average of z_{it}, call it Z_{it}, is related to the long run average of d_{it}, call it D_{it_1}, by the equation $D_{it} = a_i Z_{it}$, then we have that $\log D_{it} = \log a_i + \log Z_{it}$. Let $\log d_{it} = \log D_{it} + \delta_{it}$ and $\log z_{it} = \log Z_{it} + \zeta_{it}$ where the δ's and ζ's are random variables with expectation 0 and variances $\sigma^2_{\log d}$ and $\sigma^2_{\log z}$, respectively. Then it follows that $\log d_{it} = \log a_i + \log Z_{it} - \delta_{it} + \zeta_{it}$ so that the conditional variance of $\log d_{it}$ for a given $\log z_{it}$ is $\sigma^2_{\log d} + \sigma^2_{\log z}$ since δ_{it} and ζ_{it} are assumed to be stochastically independent. Thus approximately 68% of the observations should fall within $\sqrt{\sigma^2_{\log d} + \sigma^2_{\log z}}$. Equivalently, transforming back from the log scale, about 68% of the observations should fall between

$D = a_i[\log^{-1}(\sqrt{\sigma^2_{\log d} + \sigma^2_{\log z}})]Z$ and

$D = a_i[\log^{-1}(\sqrt{\sigma^2_{\log d} + \sigma^2_{\log z}})]^{-1}Z$

Using $\overline{\log d_{it}} - \overline{\log z_{it}}$ as an estimate of $\log a_i$, we have an estimate of a_i; $\sigma^2_{\log d}$ and $\sigma^2_{\log z}$ are estimated by pooling the variances obtained from the duplicate measurements of z and d in non-exercise positions. In our case the estimates turned out to be $\hat{\sigma}^2_{\log d} = .00197$ and $\hat{\sigma}^2_{\log z} = .000562$ so that the estimate of $\sqrt{\sigma^2_{\log d} + \sigma^2_{\log z}}$ is .0503. Since $\log^{-1}.0503 = 1.12$ and $[\log^{-1}.0503]^{-1} = .89$, we would expect that 68% of the observations for individual i should lie within $D = a_i 1.12Z$ and

$D = a_i(.89)Z$ if the only errors are measurement errors. A survey of figs. 1-6(a-j) suggests that the model might well explain the graphs since it looks easily as though 2/3 of the observations lie, on the average, within the boundary lines.

The final statistical point is that of the error of z_{it_2}/z_{it_1}; to calculate it we transform back to the log scale. Assuming the variation of z_{it_2} and z_{it_1} to be only measurement error, as argued by the previous paragraphs, it follows that z_{it_2} and z_{it_1} are independent.
Now $\mathrm{Var}(\log z_{it_2} - \log z_{it_1}) = 2\,\sigma^2_{\log z}$, so about 68% of the observed $\log z_{it_2} - \log z_{it_1}$, lie within $\sqrt{2}\,\sigma_{\log z} = .0332$, and 95% lie within $2\sqrt{2}\,\sigma_{\log z} = .0664$ of $\log z_{it_2} - \log z_{it_1}$. Thus about 68% of the observed z_{it_2}/z_{it_1} lie within $1.08(z_{it_2}/z_{it_1})$ and $(1/1.08)(z_{it_2}/z_{it_1})$ and 95% lie within $1.17(z_{it_2}/z_{it_1})$ and $1/1.17(z_{it_2}/z_{it_1})$. Hence the z-method gives ratio measurements within 8% with 68% confidence and within 17% with 95% confidence. Proceeding in a similar fashion, it follows that the d-method gives ratio measurements within 15% with 68% confidence and within 33% with 95% confidence. The implications of the previous two sentences are that: z_{it_2}/z_{it_1} might be a more accurate measure of D_{it_2}/D_{it_1} than d_{it_2}/d_{it_1}. For single observations the dye values were within 11% with 68% confidence and 23% with 95% confidence.

In summary, the statistical argument is as follows. If we knew that the curve calibrating z to d for a given person were a straight line through the origin, an observed z-ratio would estimate the same thing as an observed d-ratio. The evidence that they are nearly straight lines through the origin consists of noting that the variation about the fitted lines is roughly that expected from the measurement errors in both z and d. It is important to bear in mind that the scatter in the graphs is due to both z and d measurement error.

SECTION II. Evaluation of the Impedance Cardiac Output Method by Other Laboratories

Summary -

Impedance cardiac output systems were delivered and installed at the University of Alabama and Duke University for evaluation of the impedance cardiac output technique. A comparison study between the impedance cardiac output method and indicator dilution technique was carried out on 13 healthy male subjects by the Duke University Department of Medicine. In addition beat by beat impedance stroke volumes were compared with simultaneous stroke volumes obtained by the pressure gradient technique on two patients. Results on the 13 subjects with one control and one elevated cardiac output measurement agree with the University of Minnesota findings that at present the impedance method is most reliable for determining ratios of cardiac output. Impedance-pressure gradient comparisons of beat by beat stroke volumes resulted in correlation coefficients of .91 and.93 also suggesting that the impedance technique may be a reliable indication of relative changes in cardiac output. These results agree with University of Minnesota findings.

Introduction -

To provide proper evaluation of the impedance method for measuring cardiac output comparison studies should be carried out by several impartial laboratories. As a first step the NASA requested the University of Minnesota Laboratories to deliver impedance cardiac output systems to Dr. Glenn Foster, University of Alabama Medical Center and to Dr. Joseph C. Greenfield, Jr., Duke University, Durham, North Carolina. The units were installed and instructions given for determining cardiac output by University of Minnesota personnel. The two laboratories were to compare the impedance method with the indicator dilution technique or other accepted techniques on patients and/or subjects. The reports of results were then to be transmitted to the University of Minnesota.

At the time of delivery of the units the technique for calculating impedance cardiac output was by graphical extrapolation of the impedance waveform ΔZ, as described in equation 1, Section I, Chapter One. Subsequently all comparisons reported by these laboratories were obtained by this technique, rather than the calculation method using the first time derivative, dZ/dt (equation 2, section I, chapter 1).

Results of the comparison study at Duke University have been reported to the University of Minnesota and are summarized in the following paragraphs. The University of Alabama has apparently decided not to pursue the comparison study since there has been no communication to the University of Minnesota.

Methods

Simultaneous indicator dilution curves (dye) and impedance records were obtained in 13 healthy male subjects before and after intravenous infusion of isoproterenol. Cardiac output was also measured simultaneously by dye and impedance methods in 24 patients, 9 had mitral valve disease, 4 aortic valve disease, 5 hypertensive heart disease, 2 chronic lung disease, 2 myocardial disease, and 2 had only arrhythmias. Six of the patients had atrial fibrillation and in two of these impedance stroke volume was compared to simultaneous direct measurement of stroke volume by the pressure gradient technique (1).

A Medtronic impedance cardiac output system model 2110 with four electrodes was used according to the University of Minnesota methods described in section I of this chapter. The impedance change signal from the inner two sensing electrodes was displayed on an oscilloscope and recorded by Honeywell Visicorder together with EKG and a phonocardiogram from the second left interspace. All measurements were made during relaxed mid-expiratory apnea. The value of the maximum impedance change was determined graphically and the stroke volume was calculated according to equation 1, section 1 of this chapter. For all impedance cardiac output determinations stroke volume was taken as the mean for ten consecutive heart beats. Indicator dilution curves were obtained following injection of indocyanine green with the Colson-Gilford densitometer. In the patients undergoing diagnostic cardiac catheterization the dye was injected into either the right heart or main pulmonary artery and sampled from the left radial artery. In the other subjects the dye was injected into the median cubital vein and arterial blood was sampled from a brachial artery.

Results -

Simultaneous measurements of impedance and dye dilution cardiac output before and after isoproterenol in 13 subjects gave 26 paired values for cardiac output. The resulting regression equation was:

impedance cardiac output = 2.93 + 0.86 L/min with a standard error of 2.33 liters per minute and a correlation coefficient r = 0.68. The results of the study on 13 subjects is summarized in fig. 1-7.

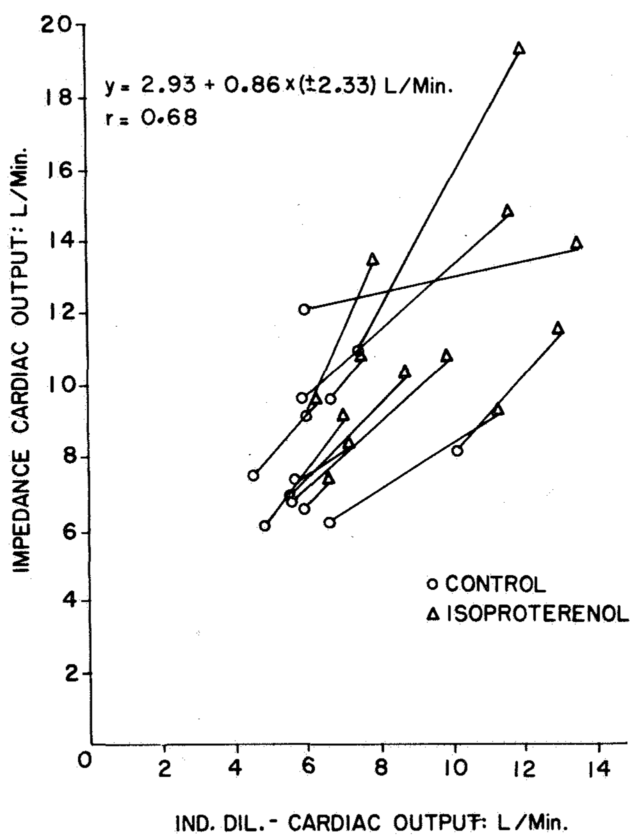

Fig. 1-7 Cardiac Output Response to Isoproternal as Measured by Impedance and Dye Method in 13 Healthy Subjects

In the 24 patients reasonable correlation was found by inspection. All values except four fell within the standard confidence limits derived from the normal subjects but the mean was nearer to the line of identity. Two of the four had significant aortic regurgitation and one had mitral regurgitation and severe pulmonary hypertension. In these three the impedance estimation exceeded the dye estimate considerably. In three other patients with less severe mitral regurgitation the ratio of the impedance and dye estimates was close to unity. One patient with pure aortic stenosis and another with a similar degree of aortic stenosis but with mild regurgitation also gave ratios close to unity. In one patient with ischemic heart disease the dye estimate greatly exceeded the impedance estimate. In the six patients with atrial fibrillation impedance stroke volume was found to vary with the preceding cycling, the relationship differing slightly in each patient.

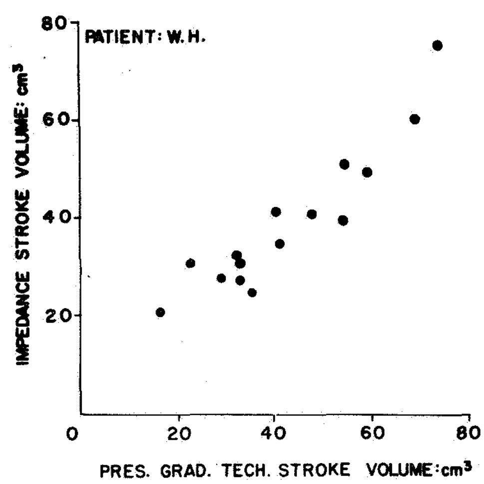

Fig. 1-8 Comparison of Impedance and Pressure Gradient Technique Estimations of Stroke Volume

In the two patients in whom the stroke volumes for individual beats were estimated simultaneously by impedance and pressure gradient techniques resulting correlation coefficients were $r = 0.91$ and $r = 0.93$ for each patient. Results of comparison between the pressure gradient technique and the impedance technique for estimating stroke volume on one patient is shown in fig. 1-8.

Discussion by Dr. Joseph C. Greenfield, Jr., Duke University

These preliminary findings in a small group of subjects support a direct relationship between stroke volume and thoracic electrical impedance during the first part of a cardiac cycle. From the present study the correlation between the dye and the impedance cardiac output appears to be less than published estimates for indicated dilution techniques and the Fick method. However the beat to beat correlation of impedance stroke volume with that measured directly by the pressure gradient technique appeared to be closer than the correlation of impedance and dye cardiac output. Nevertheless, much larger samples are required to allow a more accurate statistical analysis. Clearly close attention to technique particularly electrode placement and respiration is necessary to minimize variation, both in individuals and from patient to patient. An atraumatic method of estimating cardiac output and beat to beat changes in stroke volume is attractive in a number of fields, particularly physiological monitoring, coronary care facilities and hospital outpatient use. The method deserves further evaluation.

Discussion -

The findings of Dr. Greenfield are in agreement with those results found by our laboratory in a comparison study on human subjects (Chap. 1, Sect. I). Results in fig. 1-7 are comparable to the University of Minnesota findings. The variety of slopes of the lines connecting two cardiac output levels for the 13 different subjects is characteristic of the results found on 10 University of Minnesota subjects (figs. 1-6a through 1-6j). Since there are only two levels of cardiac output, one control and one resulting from isoproterenal, (fig. 1-7) it is impossible to determine an actual regression line for each subject and subsequently to determine if a regression line would pass through or near the axes of origin. The reproducability of each method cannot be tested from the limited data available.

Dr. Greenfield's results obtained by comparison of impedance stroke volumes with pressure gradient technique stroke volumes (fig. 1-8) on an individual subject are similar to those obtained by the University of Minnesota when comparing impedance stroke volumes against simultaneous beat by beat electromagnetic flowmeter stroke volumes on dogs (Chap. 1, Sect. III). Fig. 1-8 suggests that the impedance techniques could be used to monitor relative changes in stroke volume and cardiac output and yield essentially the same information as the pressure gradient technique.

It is of interest to note that impedance cardiac output values obtained on patients with severe aortic regurgitation were considerably higher than those measured by the dye method. Chapter Four of this report describes animal experiments in which the results indicated that the peak value of dZ/dt, the first derivative of the thoracic impedance waveform, was linearly related to peak flow in the ascending aorta. Further dog experiments suggested that the aorta may be the site of origin of the impedance waveform. If the preceding inferences are correct then the patient with aortic regurgitation would be expected to have a lower cardiac output as measured by the dye method while peak aortic flow may be high and thus reflected in the peak value of dZ/dt. Since the peak value of dZ/dt multiplied by the ejection time is equivalent to the extrapolated value of ΔZ as used by Greenfield in calculating impedance stroke volume, the impedance cardiac output values could be larger than the dye method values. This would be due to the probability that the impedance method also measures at least part of the regurgitation of blood back into the left ventricle.

The results determined by Greenfield are in agreement with those obtained by the University of Minnesota.

REFERENCES

1. Barnett, G.O., J.C. Greenfield Jr., and S.M. Fox, III. The Technique of Estimating the Instantaneous Aortic Blood Velocity in Man from the Pressure Gradient. American Heart Journal, 62:359, 1961.

SECTION III. Comparison of the Impedance Method with Electromagnetic Flowmeter Measurements on Dogs

Summary -

The impedance plethysmographic method for estimating, beat by beat, stroke volume in dogs was compared with simultaneous beat by beat stroke volumes obtained from analog integration of ascending aortic flow waveforms as measured by an electromagnetic blood flowmeter. Ranges of stroke volume were produced by paired pulse pacing of the heart in four dogs and by injection of Isoproterenol in a fifth dog. A typical result is given by the least squares equation:

Impedance stroke volume = (1.30 flowmeter stroke volume - 3.35)cc

with a correlation coefficient of .97 and a standard error of estimate of 2.7 cc. over a range of stroke volumes from 10 to 38 cc. as measured by the flowmeter. The offset or intercept (-3.35 cc) is attributed to a random error in estimating zero flow of the flowmeter waveform. Comparison of the least squares regression lines between experiment showed an unexplainable unique slope for each animal. Subsequently the impedance technique should be valid under the conditions of the experiments for estimating relative changes of beat by beat stroke volume and cardiac output.

Introduction -

An attractive feature of the impedance method for monitoring cardiac output is its beat by beat estimation of stroke volume. If such a technique can be documented to yield accurate results then transient responses of the heart can be easily observed. Validation of the impedance method should ideally be by comparison with an accepted beat by beat technique for monitoring cardiac output. Unfortunately however, the two most generally accepted techniques for monitoring cardiac output, indicator dilution and Fick technique yield only average values over several steady state cardiac cycles. Documentation of the impedance technique in humans can then at best be done by averaging the impedance stroke volumes over a time interval and assuming that the corresponding accepted method measurement reflected the same cardiac cycles.

An alternative approach to evaluation of the beat by beat impedance method is a comparison with beat by beat techniques applicable on experimental animals. The electromagnetic flowmeter is a generally accepted technique for determining pulsatile flow and thus providing a means for beat by beat evaluation of the impedance technique. The purpose of the study described in this section was to compare stroke volume estimations by the impedance technique with simultaneous stroke volumes computed from electromagnetic flowmeter waveforms. Since the impedance technique is basically a stroke volume estimation method (as opposed to minute cardiac output from the indicator dilution method) the best evaluation technique was to vary stroke volume over a wide range rather than varying cardiac output since under some conditions cardiac output changes might reflect only pulse rate changes.

Methods -

Experiments were performed on 20 kilogram male mongrel dogs anesthetized with pentobarbitol at the rate of 30 mg/kg. Following a left thoracotomy an electromagnetic flowprobe (Biotronex Laboratory Inc. Model 410 Blood Flowmeter) was acutely implanted on the ascending aorta to monitor left ventricular output. In addition electrode leads for a Medtronic Inc. Model 5837 paired pulse pacemaker were sewn into the left atrium to control heart rate. After closure of the chest the animals were placed on a continuous suction to eliminate any pneumo-thorax and band electrodes for the impedance measurements were attached (see Chap. 1, Section I for electrode configuration). The instrumented animals were allowed to stabilize for about one hour before measurements were made.

The experimental protocol was basically the recording on magnetic tape of aortic flow, impedance change, ΔZ, the first derivative of ΔZ, dZ/dt, and the ECG over a wide range of pulse rates as controlled by the paired pulse pacemaker. Stroke volumes were then computed by standard analog computer techniques from the aortic flow waveforms. Since the peripheral resistance of the animal was relatively constant under the experimental conditions, the cardiac output remained nearly constant and thus the stroke volumes were inversely proportional to pulse rate. Using this technique, stroke volumes differing by a factor of three to four were attainable over a pulse rate range of 60 to 180 bpm on the individual animal.

To evaluate the effects of changing peripheral resistance on the impedance estimation of stroke volume one experiment was performed in which an Isoproterenal injection was coupled with the cardiac pacing. Low stroke volumes were first obtained by pacing the heart at 175 and 195 bpm then mid range stroke volumes were recorded from the control condition when the animal was not being paced. Following the control measurements, elevated stroke volumes and pulse rates were obtained by injection of 30 gamma of Isoproterenol. All measurements in these experiments were taken at resting expiratory level of respiration (controlled by a positive pressure respirator) such that thoracic impedance variations due respiration would not affect the cardiogenic impedance signal used to calculate stroke volume.

Results -

Linear relationships were found to exist between impedance calculated stroke volume and the simultaneous stroke volume computed from aortic flow waveforms. Figures 1-9 to 1-12 are the results obtained by controlling heart rate with pacing while fig. 1-13 depicts the data from the experiment in which Isoproterenol was used to elevate stroke volume. The results presented here are from five of eleven experiments in the study. Technical problems such as poor flow waveforms prohibited evaluation on two dogs in the pacing series and the remaining four experiments with Isoproterenol resulted in only a small range of stroke volumes such that a comparison between methods would have little statistical significance.

Least squares regression lines, standard error of estimate (S.E.E.) and correlation coefficients (R) have been calculated for each experiment and are indicated on the figures. Ideally all regression lines would have the same slope and pass through the origin of the graphs but it is obvious from the figures that these conditions do not exist. All of the regression lines intercept X or Y axis near the origin (none greater than 2.8 cc) and there is no trend toward either axis, i.e. three intercept the X axis and two intercept the Y axis. All factors contributing to this non zero intercept error can not be defined but a major contribution probably results from the

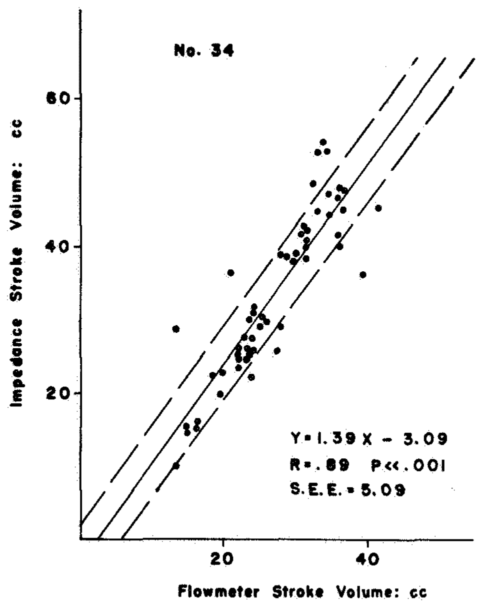

Fig. 1-9

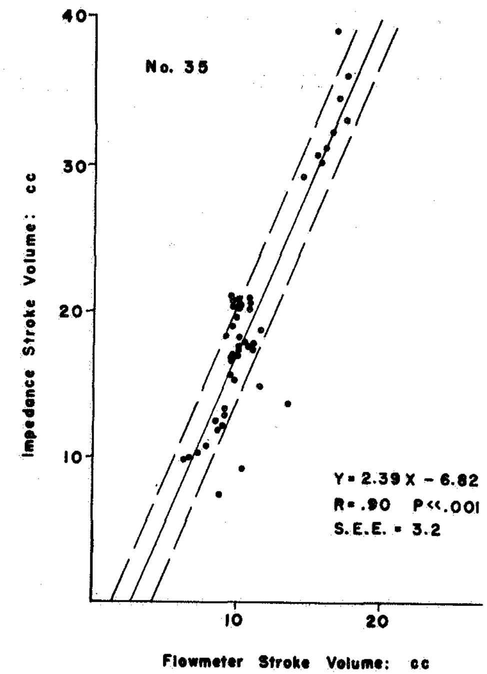

Fig. 1-10

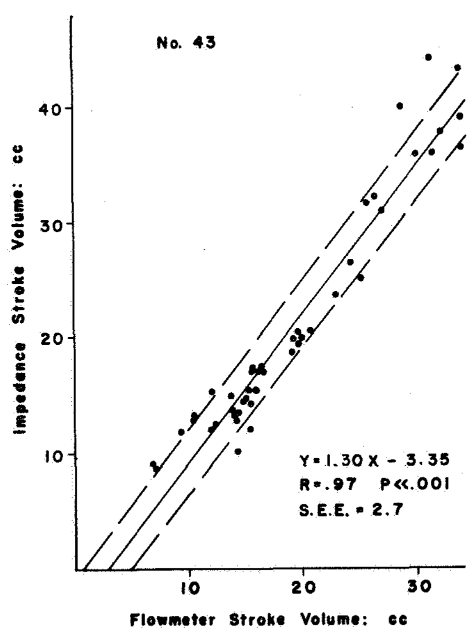

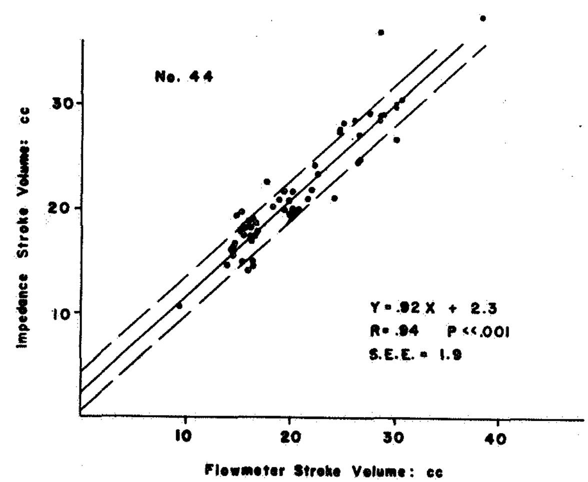

Fig. 1-12

Fig. 1-11

Fig. 1-9 to 1-12 Comparison of impedance estimated stroke volume with stroke volume computed from ascending aorta flow; range of stroke volumes obtained by paired pulse pacing of heart.

inability to accurately determine the absolute zero flow condition of the aortic flow waveform.

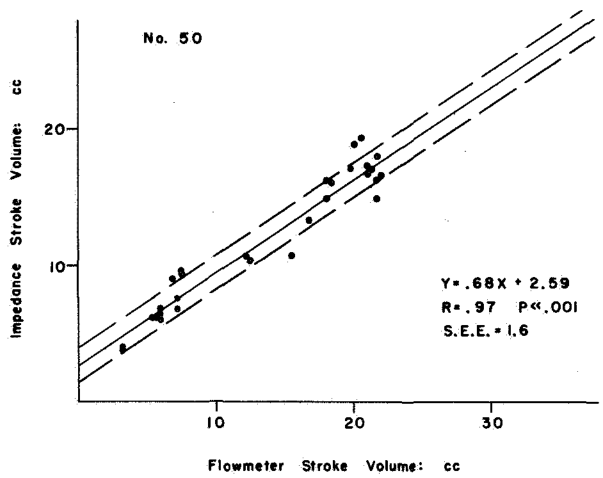

Figure 1-13 Impedance flowmeter stroke volume comparison, elevated stroke volumes obtained by isoproterenal injection

Accurate integration for stroke volume is dependent on the computer operator's ability to determine the zero of the flow waveform and since the regression line intercepts are scattered about the axes of origin the random error in estimating zero flow could be the cause of the intercept scatter.

The variations between animals in slope of the regression lines between the impedance values and those obtained by the accepted method, (flowmeter) are not unique to this study. Similar variations were found between the comparisons obtained in a human study described in Section I of this chapter where the indicator dilution method was used as a standard. At the present time these slope variations cannot be explained. Slope variation was also observed between dogs in a study comparing peak aortic flow to peak derivative of thoracic impedance, dZ/dt, although linear relationships were found to exist (Chap. 5 Sect I).

Discussion -

The correlation between the impedance determined stroke volumes and those obtained from flowmeter waveforms is greater than that obtained from the comparison study on humans in which the impedance method was compared with the indicator dilution technique (Chap. 1 Sect I). The better correlation and smaller scatter in these experiments probably results from comparing the beat by beat impedance method with another beat by beat technique as opposed to comparison with an averaging technique. Although the range of stroke volumes obtained by pacing the heart (dogs 34, 35, 43, 44) were determined from discrete levels of constant cardiac output where an averaging technique would be valid, the data range of interest is that obtained by injection of Isoproterenol, dog 50, where stroke volumes were changing with every beat. Under such conditions the correlation was not diminished, thus the potential use of the impedance technique in investigation of transient response of the heart becomes quite attractive.

At present the application of the impedance technique for monitoring cardiac functions appears to lie in the estimation of relative changes in stroke volume and cardiac output. The results presented indicate that a satisfactory linear relationship exists between the impedance data and flowmeter determined stroke volumes. Subsequently the impedance technique would be a reliable indication of cardiac output or stroke volume relative changes under the conditions of the described experiments. Although the impedance method is limited now to estimation of relative changes it remains a simple and bloodless technique and can be applicable in many situations where accepted techniques cannot be used and absolute values of cardiac output are not essential.

It is suggested that further evaluation of the impedance method should be carried out under conditions of widely varying peripheral resistance. This evaluation could be performed on animals with electromagnetic flowmeters and on cardiac patients in shock where response to treatment could be monitored by both a reference indicator dilution measurement and the impedance method.

CHAPTER TWO

ELECTRODES FOR AN IMPEDANCE CARDIAC OUTPUT SYSTEM

The measurement of thoracic impedance for use in estimating cardiac output requires a four electrode configuration. The placement of electrodes on a subject and the electrical and mechanical properties of electrodes are important to the obtaining of artifact and systematic error free data. Investigations of electrode placement and materials have resulted in a tape-on, disposable, four-band electrode configuration which should be suitable for clinical, research laboratory and in-flight measurements.

SECTION I. <u>An Electrode Placement Study</u>

Summary -

Impedance method cardiac output values are dependent on the separation between the neck bands of a four-band configuration when the separation is less than 3 cm. in normal adults. There was no variation in calculated cardiac output due to neck band separation when the bands were positioned 3 or more centimeters apart. With closely spaced neck bands, the nonlinear relationship between Z and L near electrode I accounts for the dependence of calculated cardiac output on band separation.

A cross-harness electrode has been designed for use as electrode II. The cross-harness electrode is positioned five or more centimeters from band electrode I thus eliminating

the dependence of the calculated cardiac output on neck band separation. Similar values of impedance determined cardiac output are found with the cross-harness configuration and the four-band configuration with neck electrodes separated by three or more centimeters.

Introduction -

In the use of a four-band electrode configuration to measure cardiac output by the impedance method, the separation between the neck band electrodes deserves attention as a significant variable. Cardiac output measurements previous to this investigation were made with neck bands held at a separation of two centimeters by sewing them to a cloth backing. The purpose of this investigation was to determine the relationship of the separation between neck electrodes to impedance method cardiac output values. As a result of the investigation a cross-harness electrode configuration was developed which eliminated the problems of band separation.

A. The Neck Band Configuration

Experimental Method - A sketch of the four-band electrode configuration used in the investigation is shown in fig. 2-1.

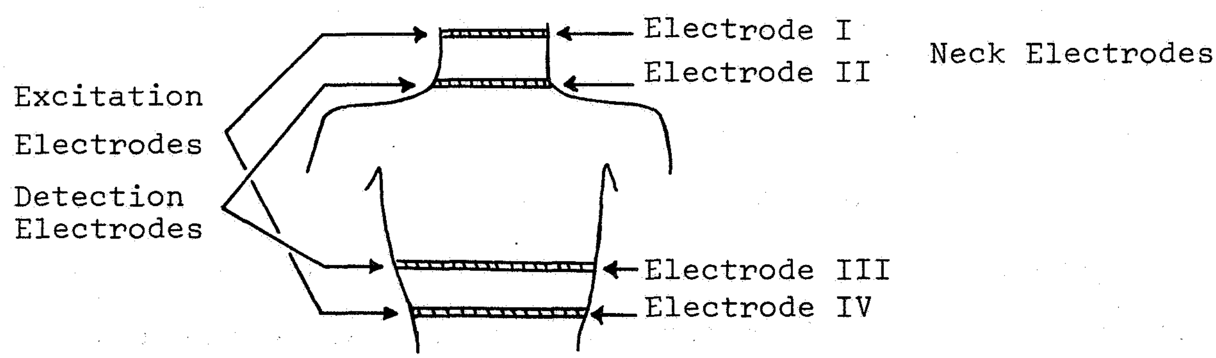

Fig. 2-1 Four-Band Electrode Configuration

Electrodes I and IV are the current excitation electrodes, and II and III are the detecting electrodes.

By using the impedance information described in chapter one, cardiac output by the impedance method is calculated from the equation:

$$C.O. = \frac{\rho L^2}{Z^2}\Delta ZPR \qquad \text{Equation 2-1}$$

Where C.O. = cardiac output (liters/min.)

PR = pulse rate

ρ, L, ΔZ, and Z are defined in equation 1-1, section I.

Impedance method cardiac output measurements were made with various distances between electrodes I and II by moving electrode I with respect to electrode II which was taped in position. The average separation of bands I and II is noted as d_{12}.

Measurements were made on the following male adults:

Table 2-I: Physique of the Subjects

	Subject 1	Subject 2
Age	26 years	32 years
Height	68 1/2 years	69 1/2 years
Weight	164 pounds	170 pounds
Surface Area	1.88m^2	1.94m^2
Thorax Length, L	33 cm.	31 cm.

Results -

A plot of the equation (1) cardiac factors $\rho L^2 Z^{-2}$ and (ΔZxPR) as a function of neck band separation is shown in fig. 2-2.

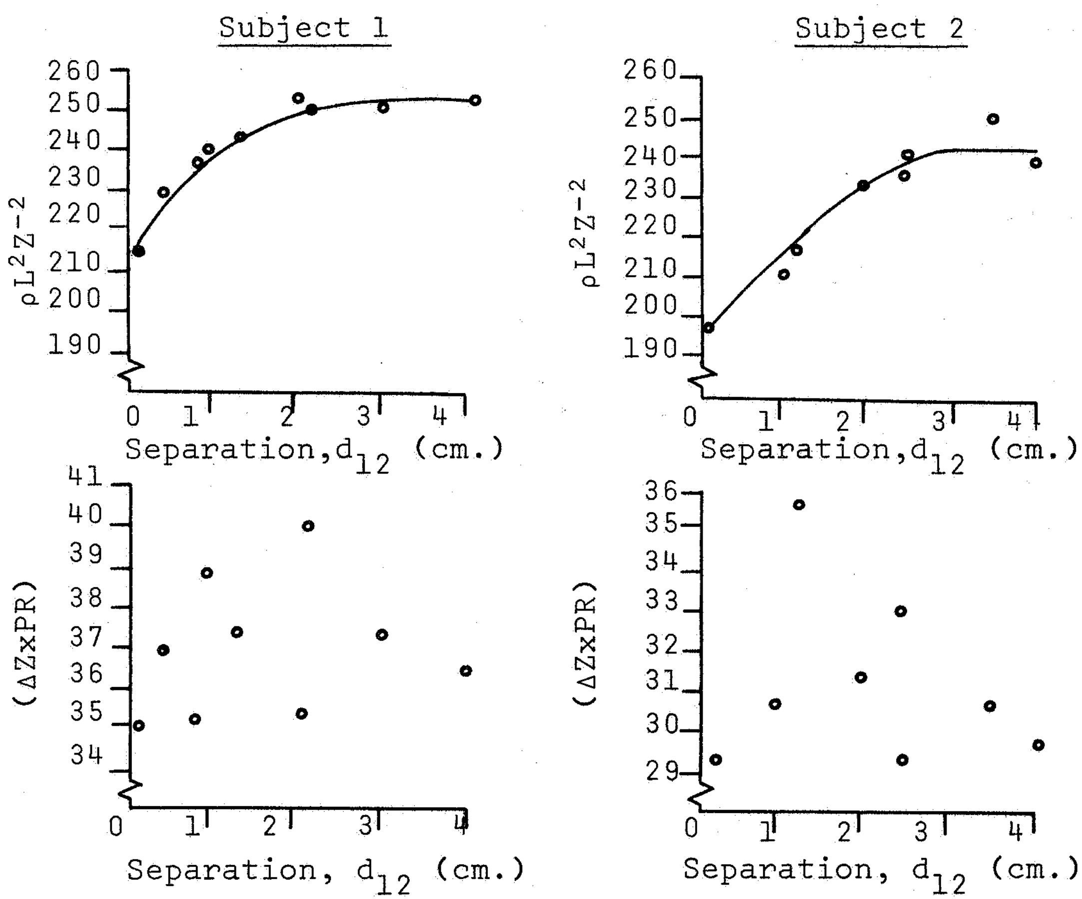

Fig. 2-2 Plots of Cardiac Factors Versus Neck Band Separation

Fig. 2-2 indicates that the cardiac factor, Z^{-2}, depends on the neck band separation, d_{12}, and a curve approximating the data was drawn. The randomness of the factor, (ΔZxPR), indicates that it has no dependence on d_{12}. Thus impedance calculated cardiac output values are apparently dependent on the separation of electrode bands I and II as seen in fig. 2-3.

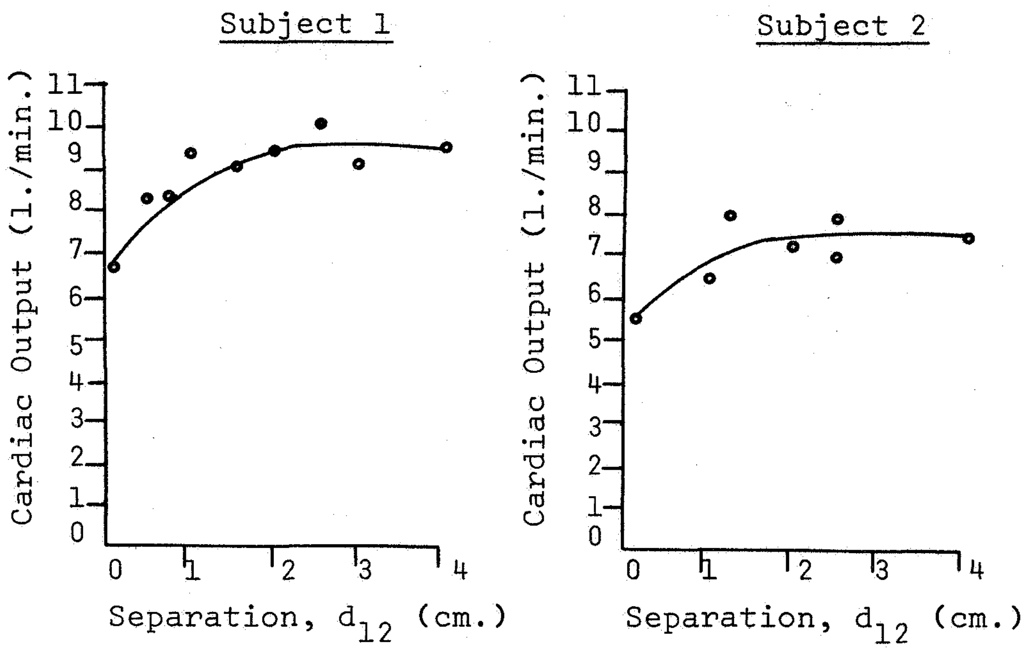

Fig. 2-3 Cardiac Outputs Versus Band Separation

Discussion -

Averages of cardiac output should remain constant for a resting subject if the positions of electrodes II and III are not changed. However, by removing the cloth backing on the neck electrodes and allowing electrode I to move while the others remain fixed, changes in the impedance calculated cardiac output were observed without apparent physiological reasons.

The normalized curves of fig. 2-4 show the comparison of cardiac output values from fig. 2-3 with the cardiac factor $\rho L^2 Z^{-2}$ values from fig. 2-2. Fig. 2-4 indicates that cardiac output and $\rho L^2 Z^{-2}$ have the same dependence on d_{12}.

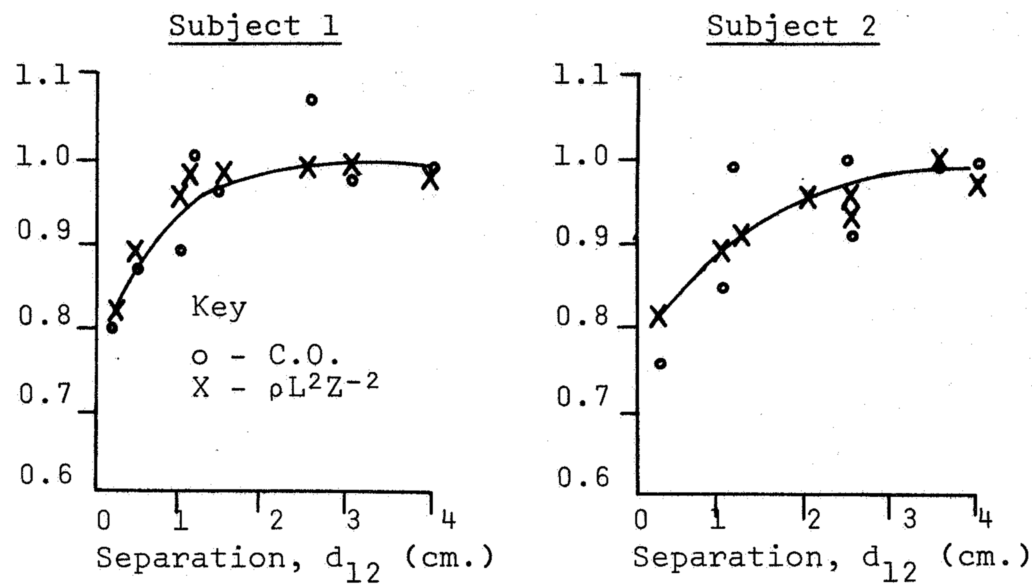

Fig. 2-4 Normalization Curves for Cardiac Output and $\rho L^2 Z^{-2}$

The factor (ΔZxPR) is not dependent on d_{12} since the normalized curves of C.O. and Z^{-2} appear to coincide. For this reason (ΔZxPR) will be assumed independent of d_{12}. Variations in (ΔZxPR) are then caused by actual beat-by-beat fluctuations in cardiac output.

Before a discussion on the reasons for the dependence of Z^{-2} on d_{12}, it will be determined whether the random variations in (ΔZxPR) have as large an effect on cardiac output measurements as do the variations in Z^{-2}.

The average values of (ΔZxPR) and its standard deviations along with the values of C.O. and $\rho L^2 Z^{-2}$ at d_{12} = 0 and at d_{12} = 3 are given in Table 2-II.

Table 2-II: Cardiac Variables

	Subject 1		Subject 2	
	Average	Std. dev., s	Average	Std. dev., s
$(\Delta Z x PR)$	37.2	±2.2	31.2	±2.1
	$d_{12} \simeq 0$	$d_{12} = 3$	$d_{12} \simeq 0$	$d_{12} = 3$
$\rho L^2 Z^{-2}$	216	255	198	248
C.O.	7.6	9.5	5.7	7.8

Now the contributions of the factors Z^{-2} and $(\Delta Z x PR)$ on cardiac output measurements can be shown. First, Z^{-2} is varied by its value at $d_{12} = 3$ to its value at $d_{12} \simeq 0$, while the variable $(\Delta Z x PR)$ is held at its mean value and C.O. changes are noted.

The difference in the values of C.O. at the two positions represents C.O. change due to Z^{-2}. The calculations are shown in Table 2-III.

Table 2-III

Effect of Z^{-2} on Cardiac Output
Using the Average Value of $(\Delta Z x PR)$

Subject 1

$$\text{C. O. } (d_{12} \simeq 0) = \rho L^2 Z^{-2}(\Delta Z x PR) = (.216)\ (37.2) = 8.0$$

$$\text{C.O. } (d_{12} = 3) = (.255)(37.2) = 9.5$$

$$\text{C. O. } (d_{12} = 3) - \text{C.O.}(d_{12} \simeq 0) = 9.5 - 8.0 = 1.5$$

Subject 2

$$C.O.(d_{12}\approx 0) = \rho L^2 Z^{-2}(\Delta Z x PR) = (.198)(31.2) = 6.2$$

$$C.O.(d_{12}=3) = (.248)(31.2) = 7.7$$

$$C.O.(d_{12}=3) - C.O.(d_{12}\approx 0) = 7.7-6.2 = 1.5$$

The mean value (ΔZxPR) is varied one standard deviation, while the variable Z^{-2} is held at its value at $d_{12}=3$, and C.O. changes are noted (Table 2-IV). The difference in the C.O. values represents changes due (ΔZxPR).

Table 2-IV

Effects of (ΔZxPR) on Cardiac Output Using the Value of Z^{-2} at d_{12} = 3 cm.

Subject 1	Subject 2
$\overline{C.O.}=\rho L^2 Z^{-2}(\Delta ZxPR)=(255)(37.2)=9.5$	$\overline{C.O.}=\rho L^2 Z^{-2}(\Delta ZxPR)=(248)(31.2)=7.7$
$C.O.(\text{at } s)=\rho L^2 Z^{-2}\left|(\overline{\Delta ZxPR})+s(\Delta ZxPR)\right|$	$C.O.(\text{at } s)=\rho L^2 Z^{-2}\left|(\overline{\Delta ZxPR})+s(\Delta ZxPR)\right|$
$C.O.(\text{at } s)=(255)(37.2+2.2)=10.0$	$C.O.(\text{at } s)=(248)(31.2+2.1)=8.3$
$C.O.(\text{at } s)-\overline{C.O.}=10.0-9.5=0.5$	$C.O.(\text{at } s)-\overline{C.O.}=8.3-7.7=0.6$

The results from Tables 2-III and 2-IV show that the maximum variation in Z^{-2} has three times the effect on cardiac output changes as do beat-by-beat variations of one standard deviation in (ΔZxPR).

To explain the increase in thorax impedance, Z, as the separation of the neck bands, d_{12}, decreases, the neck was modeled as a homogeneous cylinder of resistivity ρ . Electrode I is an excitation band on the surface of the cylinder, and generates the potential detected at electrode II. Fig. 2-5 shows that as electrode I moves closer to electrode II, the surface potential no longer remains a linear function of d_{12}.

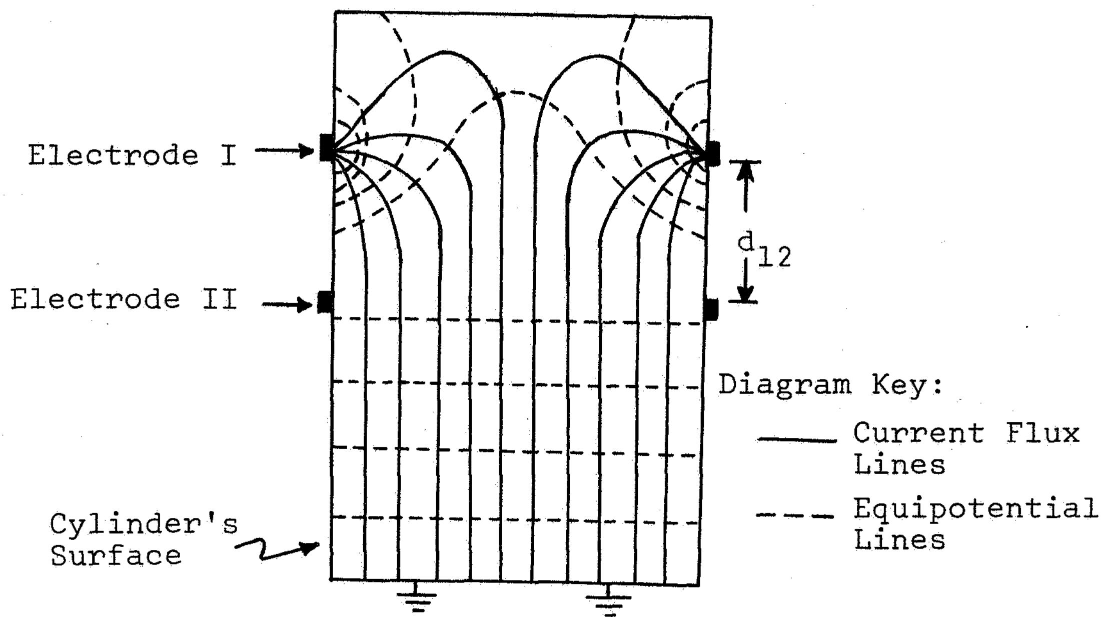

Fig. 2-5 Equipotential Surfaces in a Cylinder (lateral Cross-Sectional Plane)

Based on the shape of the equipotentials shown in fig. 2-5, an expected curve for measured thoracic impedance Z between electrodes II and III as a function of d_{12} is shown in fig. 2-6. (Recall that electrode I is driven by a constant current source and Z is the thoracic impedance between equipotential planes).

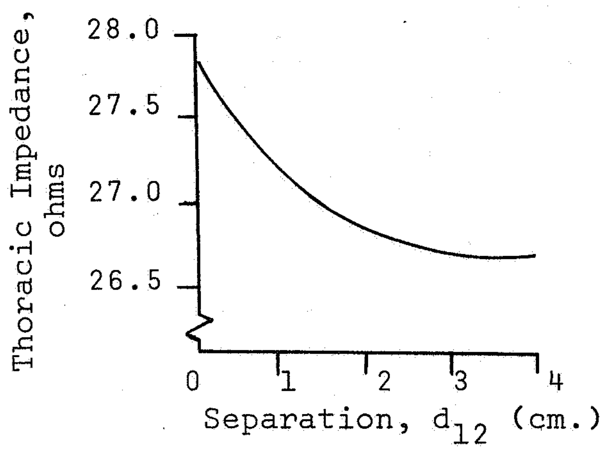

Fig. 2-6 Measured Thorax Impedance as a Function of Neck Band Separation

In an attempt to show that the effect of d_{12} on Z is not a unique characteristic of the neck, the four-electrode band configuration was put on the arm and the leg. Bands I and II were positioned on the upper arm or thigh, separated by distance d_{12} and bands III and IV were placed on the lower arm or calf.

The plot of the normalized impedance between electrodes II and III (fig. 2-7) shows the dependence of Z on d_{12} and that the arm having the smaller cross-sectional area also has the lower breaking point. This would indicate that for subjects with smaller diameter necks, it is possible to use a smaller separation between the neck bands without introducing variations in cardiac output measurements due to $Z^{-2}(d_{12})$.

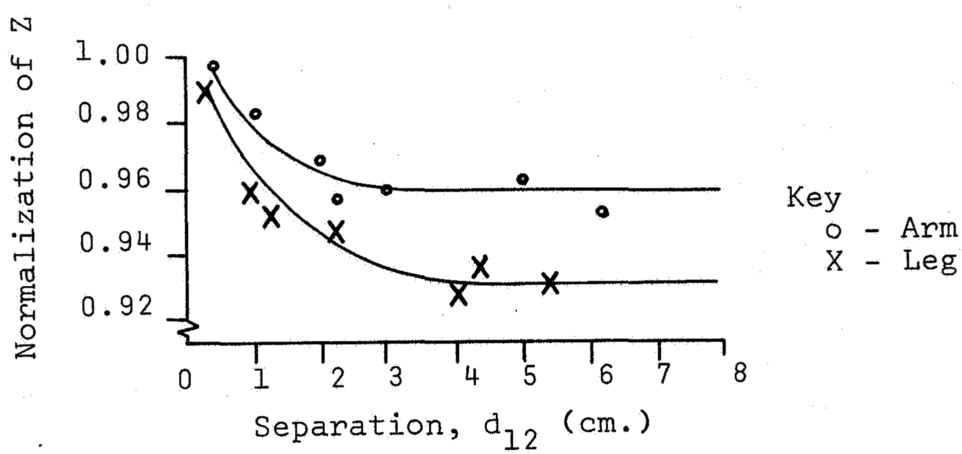

Fig. 2-7 Normalized Extremity Impedance

B. The Cross-Harness Configuration

The cross-harness electrode configuration was developed as a result of the investigation into the effect of the separation of the neck bands on cardiac output measurements using four-band impedance plethysmography. The four-band electrode configuration is shown in fig. 2-1 of the previous section of this report. The advantages of the cross-harness configuration (fig. 2-8) over the four-band electrode configuration are the stabilization of the position of the second electrode, and the insurance that electrode I is greater than 2 or 3 centimeters above electrode II (where $\Delta C.O./\Delta d_{12} \approx 0$). These advantages eliminate variations in calculated cardiac output values caused by the neck band separation. Another advantage of the cross-harness is an improvement in neck mobility.

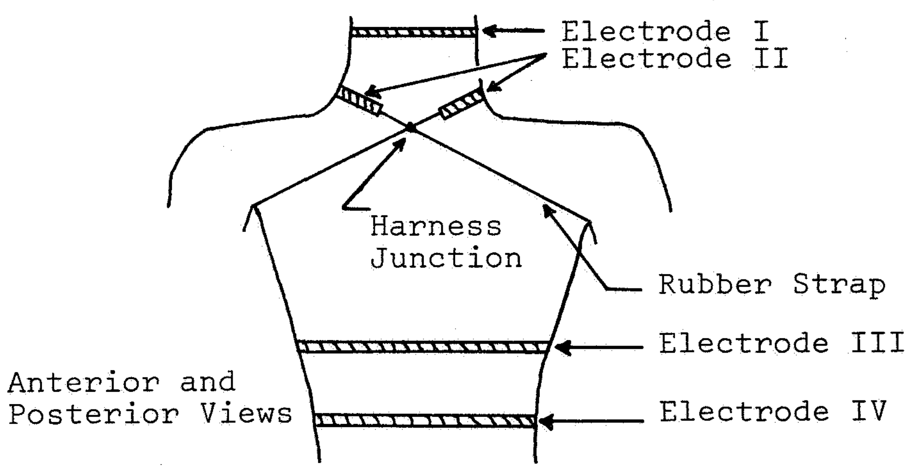

Fig. 2-8 Cross-Harness Configuration

Design of the Cross-Harness -

The design criterion of the cross-harness electrode configuration was that the second electrode lies on an average equipotential line generated by the current excitation (I and IV) electrodes. Electrodes I, III, and IV are the same as those used in a four-band electrode configuration. The average equipotential lines must be those established in the absence of the second electrode. Then, the second electrode should cross equipotential lines, a new equipotential line would be established and this is undesirable because the thoracic potential field would be dependent on the position of the second electrode.

Equipotential lines were measured on a subject using the impedance system with the four-band configuration, except electrode band II was replaced by a detecting probe. The contract area of the probe was large enough, so that skin impedance could be neglected as it is with a band electrode. The surface area of the probe (1/2 cm. x 4 cm.) times the resistivity (1) of the skin (220 ohm-cm.$^{-2}$) was small compared to the input impedance (3 x 10^5 ohms) of the detecting amplifier in the impedance plethysmograph. Equipotential lines were drawn and labeled with their corresponding impedance values (fig. 2-9).

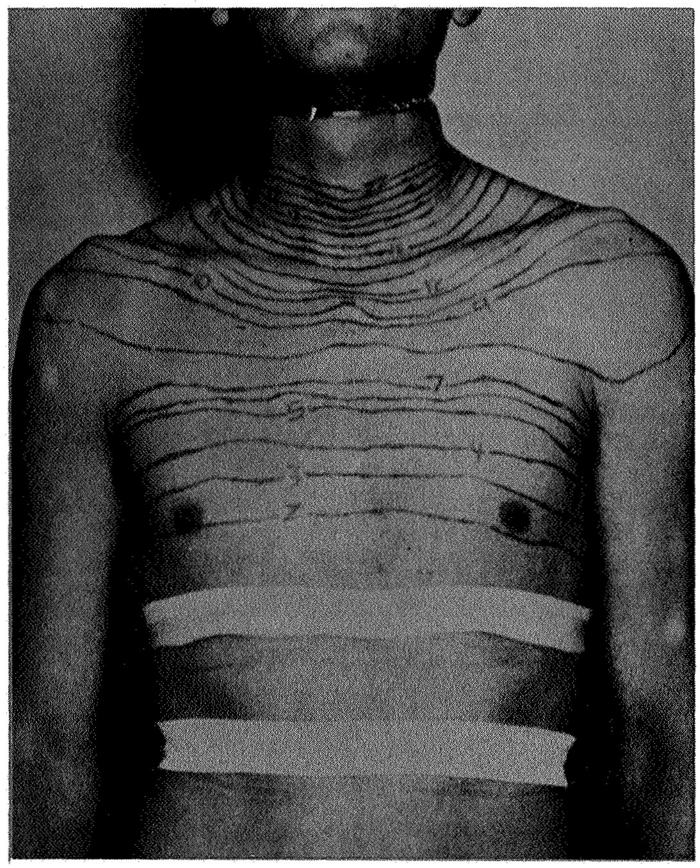

Fig. 2-9 Equipotential Lines on a Young Adult Male

The cross-harness was placed on a subject who had equipotential lines drawn on him to observe how well the second electrode would conform with the equipotential lines. A solid band was used for the second electrode which extended from the anterior to the posterior harness junctions and over both sides in the neck-shoulder region. It was observed that the second electrode lies on an equipotential line along the top on the shoulder, but near the harness junction it crosses equipotential lines. To experimentally determine how far the end of the second electrode should be from the harness junction, measurements of thorax impedance were made as equal segments of the second band were removed starting at the harness joint and working upward to the top of the shoulders (fig. 2-10).

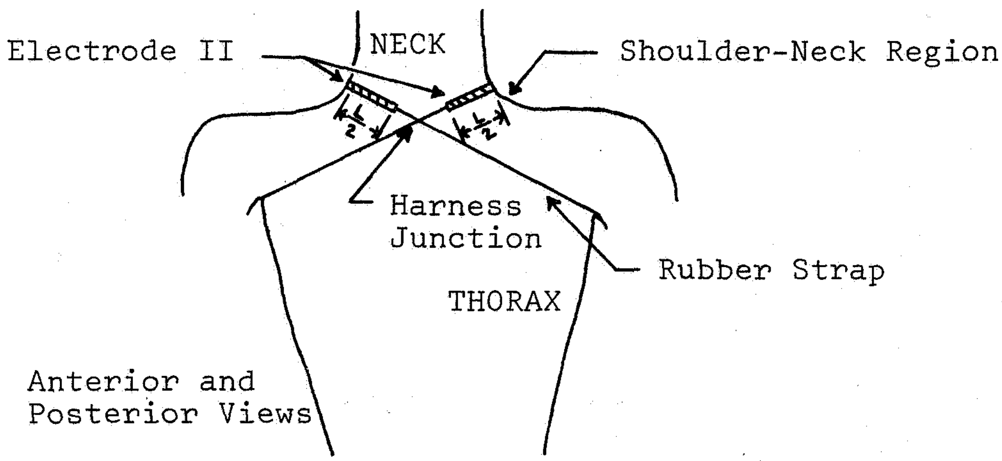

Fig. 2-10 The Second Electrode of the Cross-Harness Configuration

One centimeter segments were removed from the front and band ends of the electrode until the length, L, of the second electrode over both shoulders was reduced from 20 to 2 centimeters. A plot of the thorax impedance, Z, versus the length, L, of the second electrode over each shoulder is shown in fig. 2-11.

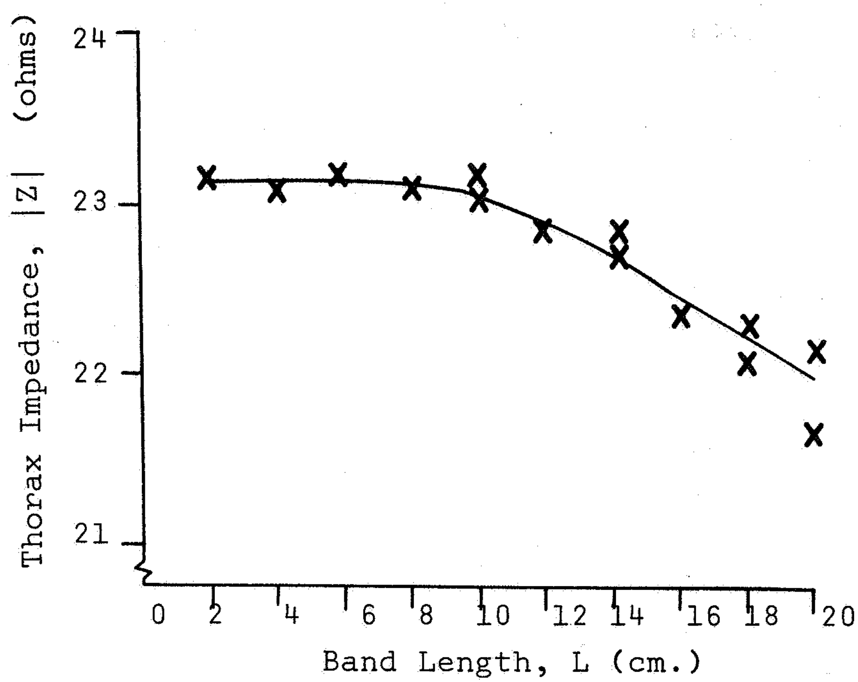

Fig. 2-11 Thorax Impedance Versus Length of the Second Electrode

Figure 2-11 indicates that for a length, L, between 2 and 10 centimeters, the second band would lie on an equipotential line. A 10 centimeter strap over each shoulder is used in the present design.

Results and Discussion -

For calculation of cardiac output by equation 2-1 with cross-harness configuration data, the thoracic length L was measured as the mean distance between electrode III and the cross-harness electrodes. Calculated cardiac output values, using the cross-harness configuration, were equivalent to values obtained from the four-band configuration with a separation of three or more centimeters between the neck bands.

In the investigation of the effect of neck-band separation on cardiac output measurements using the four-band configuration, electrode I was moved with respect to the other electrodes which were taped in position. Figure 2-3 shows that cardiac output measurements are independent of the position of electrode I, if a separation d_{12} of more than 2 or 3 centimeters is maintained. The separation between the first and second electrode is greater than 5 centimeters with the cross-harness configuration. Thus, one advantage of the cross-harness configuration over the four-band configuration is the insurance that electrode I is greater than 2 or 3 centimeters above electrode II (where $\Delta C.O./\Delta d_{12} \approx 0$).

When the second band of the two neck bands was not taped in position, slippage upward of this band was noted with neck motion. Slippage rate was enhanced by oils in the electrode paste, neck movements, and by the tapered region of the lower neck where electrode band II should be placed to maximize d_{12} (i.e. d_{12}>3 centimeters).

REFERENCES

1. Kinnen, E., Kubicek, W.G., Hill, P., and Turton, G.: Thoracic Cage Impedance Measurements: Tissue Resistivity in Vivo and Transthoracic Impedance at 100 kc. Technical Documentary Report No. SAM-TDR-64-5, USAF School of Aerospace Medicine, Brooks Air Force Base, Texas, March 1964.

SECTION II. Electrode Materials

Summary -

Based on the results of the work described in sections I and II of this chapter an electrode configuration has been developed that is considered to be the best available at this time for use with the impedance cardiac output system.

The configuration employs the band electrode placement described in chapter one with the stipulation that at least 3 cm. separates the neck electrodes.

The band configuration has been chosen over the harness electrode described in section I of this chapter because of the ease in donning and doffing and the greater degree of freedom allowed by the band configuration as opposed to the harness arrangement.

The preferred electrode material for the band electrodes is the 3M Company 1 mil aluminum deposited on a polyester film and bonded to an adhesive back. The electrode is lightweight, comfortable, and possesses adequate electrical characteristics. The cost of this electrode material is low thus making the electrodes disposable after one use.

Introduction -

To obtain meaningful artifact free information concerning intrathoracic impedance information, the excitation and sensory electrodes of a four electrode impedance system (cf. chapter one) must have electrical properties compatible with the system and must not affect the signals of interest. The electrodes must also provide minimum discomfort to the subject or patient in clinical, research or inflight environments. The following criteria were deemed necessary for an acceptable electrode.

1. Electrode to skin interface impedance must be low such that (a) it is negligible compared to the current source output impedance and sensing amplifier input impedance and (b) changes in the interface impedance due to motion, etc. reflect impedance changes which are negligible compared to the cardiogenic impedance variations of interest.
2. The dc resistance of a 0.25 X 36 inch electrode should be one ohm or less to minimize voltage gradients along the electrode.
3. Motion between the electrode and skin surface must be eliminated.
4. The electrodes must be lightweight, comfortable, and impose a minimal restriction on the movements of the subject.

Materials and Methods -

The following materials were investigated as possible candidates for electrode construction: (all electrodes have a .25 inch wide conductive medium)

1. Conductive Velcro (Velcro Hi-Meg conductive pile V-22-11-WZ, Velcro Corp., New York, N.Y.) with 4 mm wide braided copper center

2. 3M Aluminum Christmas wrap (3M Company, St. Paul, Minnesota).
3. Schjeldahl Mylar-Aluminum deposited film, .35 mil Mylar, .18 mil aluminum (G.T. Schjeldahl Co., Northfield, Minnesota).
4. 3M copper strip with a 3M conductive adhesive (3 mil copper with a pre-applied 2-3 mil conductive adhesive).
5. 3M Polyester laminate-gold deposited film
6. 3M Polyester laminate-aluminum deposited film 3.6 mil polyester, 1.0 mil aluminum

The 3M aluminum Christmas wrap and the 3M gold deposited film were eliminated as usable materials because of their high d.c. resistance values. The gold film was a vapor deposited material and had a resistance of 3.4 ohms for a 12 X 1.25 inch strip. To obtain a gold film electrode with acceptable d.c. resistance characteristics would most likely incur a prohibitive price.

Mechanical Properties

All of the deposited metal film materials were quite resistant to fatigue stresses, possessed a moderate amount of elasticity, and were comparatively lightweight, although these properties were not quantitated.

The copper strip electrode was stiff and uncomfortable and although an adhesive was used the material did not easily conform to the surface of the body.

Construction of Electrodes

1. Conductive Velcro

These electrodes had been used extensively by this laboratory (chapter one) before the onset of the study described here. The construction is shown below.

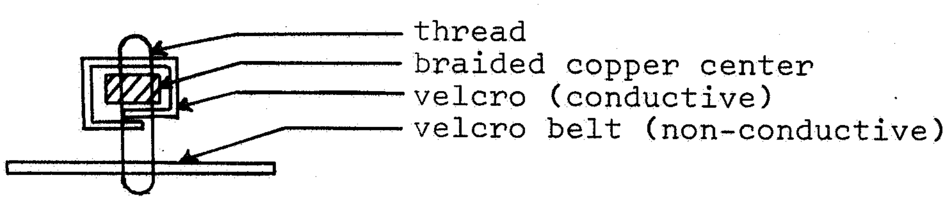

Cross-Section

2. Metal film deposited electrodes

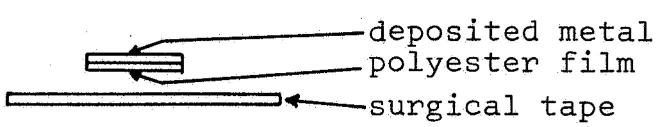

Cross-Section

The advantages of this electrode is ease in fabrication, expandability, patient comfort, lightweight and disposable.

3. Copper strip with light silver doped conductive adhesive

The copper strip electrode supplied by the 3M Company consisted of a 3 mil copper band with an adhesive doped with silver particles. The adhesive was approximately 2-3 mils thick and uniformly applied to the band by machine. As described previously, the copper strip electrode was stiff and cumbersome.

Impedance Characteristics of Electrodes at 100 kHz

To evaluate the skin-electrode interface impedance of the various electrode materials, a General Radio Type 1605 Impedance Comparator was used to measure the total thoracic impedance between band electrodes. The measurement circuit is shown below.

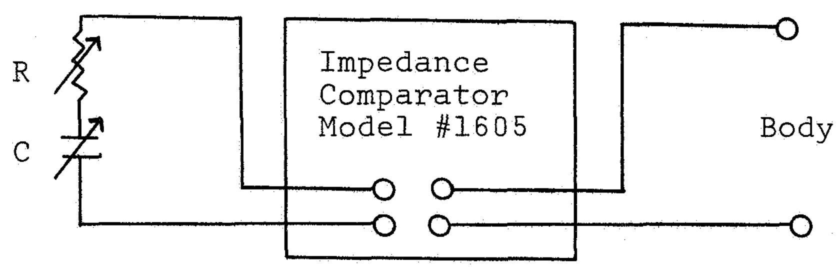

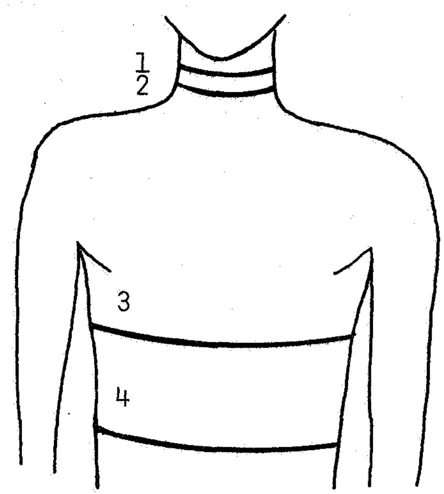

To eliminate differences in measured total thoracic impedance due only to electrode placement variations when comparing different materials the position of the four-band electrodes was inscribed on the skin surface. Measurements of thoracic impedance were made between band locations 1 and 4 and between 2 and 3. The tabulated results are shown in Table 2-V.

TABLE 2-V

Type of Electrode	No. of Subjects Tested	Electrodes 1-4			Electrode 2-3			dc Resistance of 0.25 X 36" electrode
		RΩ	X_cΩ	ZΩ	RΩ	X_cΩ	ZΩ	
Velcro without conductive paste	6	74.0	46.2	87.4	53.8	37.8	80.5	1Ω
Velcro with conductive paste	6	50.0	13.0	51.6	37.3	11.7	39.6	≈1Ω
Schjeldahl .18 mil Al on .35 mil Mylar	3	49.2	16.5	52.0	37.0	14.6	39.9	1Ω
Cu with silver doped adhesive	1 (limited material)	187.0	325.0	372.0	143.4	265.0	304.0	
3M 1.0 mil Al on 3.6 mil polyester film	2	44.7	21.5	49.7	33.3	17.6	37.9	0.2Ω

Discussion -

Electrode-skin interface impedance was found to be minimal with the Velcro and conductive paste, Schjeldahl aluminum deposited Mylar and 3M aluminum deposited polyester film electrodes. The Velcro electrode has several disadvantages in that the conductivity of the conductive pile was found to decrease with use and the conductive paste must be used to minimize the interface impedance. The aluminum deposited electrodes were also more comfortable than the Velcro and the feature of being lightweight and disposable is quite attractive.

The 3M Company has supplied us, and more recently the NASA, with prefabricated one mil aluminum deposited polyester film on a newly developed semi-porous type backing according to our specifications. The porous backing allows the skin to breath and should result in additional comfort for the subject. This electrode system appears to be the most desirable of those evaluated since electrode-skin interface impedance and dc-resistance was minimal, the electrodes are comfortable, and prefabrication with quality control by the 3M Company provides uniform quality electrodes.

CHAPTER THREE

INSTRUMENTATION FOR IMPEDANCE CARDIAC OUTPUT SYSTEM

SECTION I University of Minnesota Breadboard Impedance Cardiograph (ZCG)

Summary -

A four electrode impedance cardiograph was designed to accurately measure and record Z_o, ΔZ, and dZ/dt. The unit operates satisfactorily with dry disposable tape on electrodes. The system has an accurate and convenient null balance readout system for Z_o and automatic balancing to obtain ΔZ. The output impedance of the current source and input impedance of the voltage recording amplifier are large enough to eliminate any significant error that might be caused by electrode-tissue interface impedance changes that could occur with the cardiac cycle.

Introduction -

In order to successfully record impedance information from the thorax it is necessary to have an impedance cardiograph (ZCG) with a high level of electrical and operational performance. The ZCG described in this section has the necessary electrical specifications to accurately record the impedance information related to cardiac activity using dry disposable tape on electrodes employing a four electrode technique. The system was designed with an automatic balance and a switch operated manual balance to give good operational performance. An accurate readout of the mean thoracic impedance Z_o was provided for laboratory use. The system has electrical outputs and calibration for Z_o, the mean thoracic impedance; ΔZ, the thoracic impedance change; and dZ/dt, the first time derivative of the impedance change, which are the parameters necessary to compute cardiac output using the impedance technique. For research purposes the system has an electrical output for d^2Z/dt^2, the second time derivative of the impedance change.

System Requirements and Design

The fundamental four electrode measurement technique is shown in fig. 3-1. A 100 kHz current from a constant current source flows between electrodes 1 and 4. A voltage V_t is

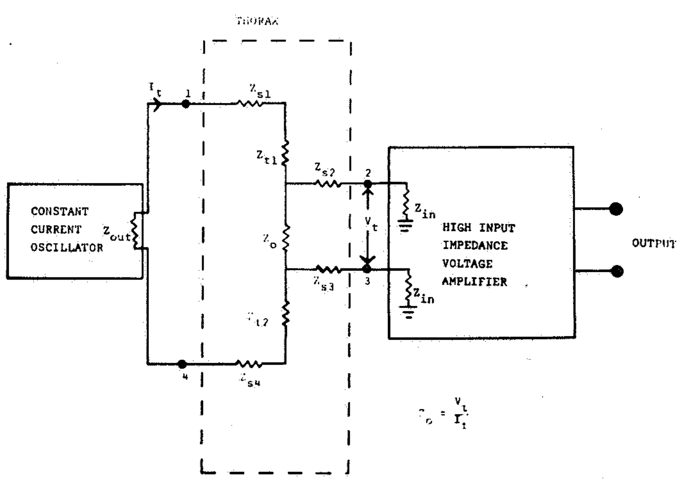

Fig. 3-1 Basic four electrode measurement technique indicating impedances of electronic circuitry, thorax and electrode-skin interface as described in text.

picked up from inner electrodes 2 and 3 which reflects the voltage across Z_o. The impedances Z_{s1}, Z_{s2}, Z_{s3}, and Z_{s4} represent the impedance of the skin and electrode tissue interface for the respective electrodes, Z_{t1}, and Z_{t2} are the impedances of the thorax between band electrodes 1 and 2 and band electrodes 3 and 4 respectively. Now if the output impedance of the current source Z_{out} is >> $Z_{s1} + Z_{t1} + Z_o + Z_{t2} + Z_{s4}$ and $Z_o << Z_{s2} + Z_{s3} + Z_{in}$ for all measurement conditions then the current from the current source I_t is approximately equal to the current through the thoracic impedance Z_t. Also, if the input impedance of the voltage amplifier Z_{in} is >> $Z_{s2} + Z_{s3}$ then the voltage between electrodes 2 and 3 is equal to the voltage across the internal thoracic impedance Z_o. For these conditions Z_o would be equal to V_t/I_t independent of Z_{s1}, Z_{s2}, Z_{s3}, Z_{s4}, Z_{t1}, and Z_{t2}.

Hill, et al (1), stated that very large impedance signals occur at the electrode-tissue interface thereby causing impedance plethysmography signals indicating volume change to be in error. Recording the impedance change occurring during the cardiac cycle on the thorax between electrodes 1 and 4 or electrodes 2 and 3, the largest typical value seen is ΔZ = 0.2 ohm out of an approximate total impedance Z = 50 ohms. With this information and knowing the output impedance of the current source and input impedance of the voltage amplifier, the maximum impedance error signal using the four electrode impedance technique can be calculated assuming the entire impedance change to be at the electrode-tissue interface. For example, if the output impedance of the current source is 100K ohms and electrode tissue interface change is 0.2 ohms

then $$\frac{\Delta i}{I_t} = \frac{Z_o}{Z_o + Z_{s1} + Z_{t1} + Z_{t2} + Z_{s2}} - \frac{Z_o}{Z_o + Z_{s1} + Z_{t1} + Z_{t2} + Z_{s2} + \Delta Z}$$

where Δi = the output current change

I_t = the current output

$$\frac{\Delta i}{I_t} = \frac{100K}{100K + 50 + .2} - \frac{100K}{100K + 50 + .2} \approx (2)10^{-6}$$

or $\Delta i/I_t$ = .0002%

This .0002 percent current change would reflect itself as a .0002 percent impedance change. If it is assumed that $Z_o + Z_{s2} + Z_{s2} << Z_{in}$, the input impedance of the voltage amplifier then it can be shown that a .0002 percent change in the recorded voltage would occur with a .2 ohm impedance change at the electrode-tissue interface. Using the four electrode system on the thorax a typical impedance change value is .2 ohm out of a 25 ohm thoracic impedance or a .8 percent change. Since this value is much greater the total of .0004 percent change that occurs with a .2 of an ohm change at the electrode-tissue interfaces it can be assumed that the maximum typical electrode-tissue interface impedance change error can be neglected as a source of error in the ΔZ thoracic impedance signal if the output impedance of the current source and input impedance of the voltage amplifier is 100K ohms. The high output impedance of the current source and high input impedance of the voltage recording amplifier also makes the ZCG ΔZ output less sensitive to other non-periodic electrode-tissue interface impedance changes such as might occur with subject movement.

In order to simplify the recording of a ZCG, an automatic balance system and an accurate readout system for Z_o, the mean thoracic body impedance was incorporated into the system.

The following objectives were pursued in designing the unit:

(1) A floating constant current source oscillator with an output impedance of 100K ohms.

(2) A differential input voltage amplifier with an input impedance of 100K ohms and a common mode rejection ratio of 50 db.

(3) A system accuracy for Z_o of 1 percent

(4) System linearity for Z_o of .5 percent

(5) Calibrated outputs for ΔZ, and dZ/dt

(6) Low noise output for dZ/dt

(7) Automatic rebalancing of Z_o

(8) A rapid manual rebalance of Z_o

(9) An accurate readout system for Z_o

Fig. 3-2 shows a block diagram of the impedance plethysmographic system. As seen in the figure, 100 kHz constant amplitude current is fed to the thorax. The output of the current source is connected to the thorax by means of coaxial cables with electrically driven shields to reduce the effective cable capacity and thereby maintain high output impedance at the electrodes. In the present system the output impedance of the current source is 100K ohms measured at the distal ends of the cables at the electrode terminals.

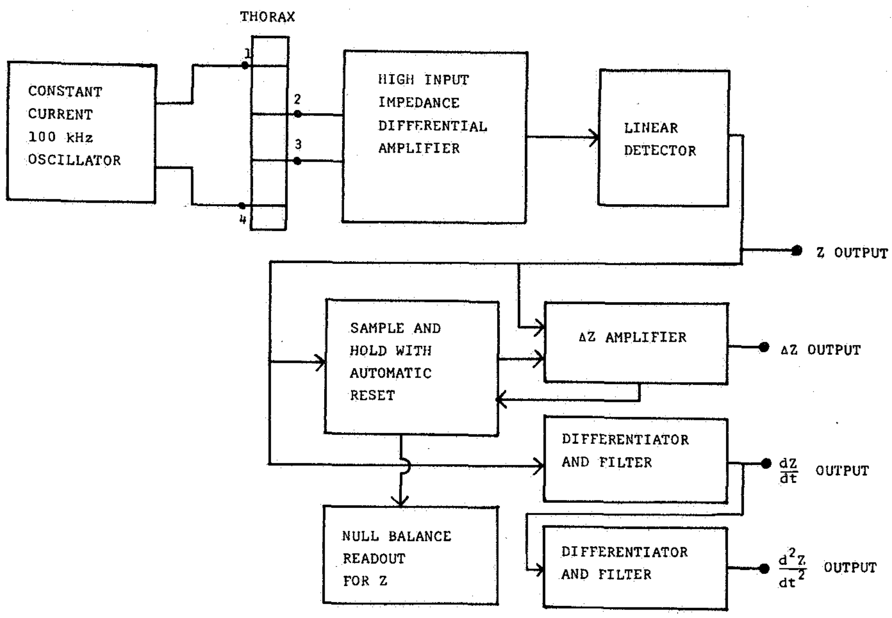

Fig. 3-2 System block diagram

The voltage is recorded from the thorax by a differential amplifier with coaxial leads. The differential input impedance of the amplifier is 100 K ohms when measured at the cable ends using 100 kHz current. Positive feedback is used on the input to reduce the effects of cable capacity. The common mode rejection ratio is a minimum of 50 db at 100 kHz when measured at the electrode terminals of the cables.

The output of the differential amplifier is fed to a linear detector. The output of the detector is fed to a long term stable sample and hold circuit and to the ΔZ amplifier. The ΔZ amplifier has an input from the sample and hold circuit. In the ΔZ amplifier the two inputs are subtracted to give the ΔZ output.

The sample portion of the sample and hold circuit can be operated either manually by a switch or automatically. The automatic operation is achieved by sensing the output of the ΔZ amplifier and then sampling when the absolute value of the output exceeds an adjustable preset limit. This allows the system to record the small ΔZ changes due to the cardiac signal, but if respiration, movement or other artifact causes a larger change in ΔZ, the system will automatically rebalance in approximately 40 milliseconds. The output of the detector is also fed to two analog differentiators to give the first and second time derivatives. The null balance circuit connected to the sample and hold output, nulls an accurate D.C. voltage against the output of the sample and hold circuit to accurately measure the value of the mean impedance Z_o.

Circuit Design -

Drawing 3-4 shows the circuit diagram for the constant current source and driven shield circuit. Transistor Q_1, is used in a Colpitts oscillator circuit. In order to achieve amplitude stability, the standard Colpitts circuit was modified by adding Zener diode controlled negative feedback. Transistor Q_2 is used as a high input impedance buffer to the output stage. The high output impedance current source oscillator is achieved by using the collector of transistor Q_3 as a current source. The 100 kHz current is coupled to the body using transformer TR1, a signal from each side of the output transformer is picked up by field effect transistors Q_4 and Q_5 and amplified with near unity voltage gain to provide a low impedance output signal to drive the shields of the output cables.

Drawing 3-1 shows the input circuitry and 100 kHz filter. Transistors Q_{10}, Q_{11}, Q_{12}, and Q_{13} form two symmetrical buffer amplifiers for the integrated differential operational amplifier OP1.

The buffer amplifiers are used to achieve the high input impedance and also to provide the positive feedback necessary to reduce the effects of cable capacity. The adjustable capacitors from the collector of the second stage Q_{12}, Q_{13}, to the base of the first stage Q_{10}, Q_{11}, are used to provide the positive feedback. The capacitors for each stage with their respective input cables in place are adjusted to reduce the effects of the shunting capacitance caused by the cable. The output of each amplifier is fed to the differential operational amplifier OP1 to achieve a common mode rejection of 50 db. The output of OP1 is connected to operational amplifier OP2. The amplifier acts as a 100 kHz band pass filter to eliminate interfering signals.

Drawing 3-2 shows the linear detector the sample and hold circuit, and the automatic rebalance circuit. The output of OP2 is connected to OP3 which serves as a linear detector. The linear detection operation is achieved by placing diodes in the feedback loop of the operational amplifier. The high gain of the operational amplifier greatly reduces the nonlinear effects of the diode which normally accompany a detection process using only diodes. The output of the detector is connected to operational amplifier OP4 which serves as a low pass filter and amplifier. The output voltage of OP4 is fed to (a) operational amplifier OP5, the sample and hold amplifier, (b) the ΔZ amplifier OP6, and (c) OP7, the first differentiator. Operational amplifiers OP6, OP7, OP8, and OP9 are shown in drawing 3-3. The holding operation by OP5 is achieved by switching a capacitor charged to a voltage proportional to Z_o around the feedback loop of the high input impedance operational amplifier. The amplifier OP5 has field effect input transistors which have very low offset currents. The sample and hold operation is performed by a switch for manual operation or by a relay for automatic operation. The output from the sample and hold amplifier is fed to the ΔZ operational amplifier, OP6. The ΔZ operational amplifier is operated in the summing mode with input signals from OP4 which contains the total time varying impedance signal and from OP5 which is the output signal of the sample and hold amplifier that represents impedance Z_o. Because the sample and hold amplifier inverts the signal, the ΔZ amplifier subtracts the mean impedance Z_o value held by the sample and hold amplifier from the total time varying impedance. The ΔZ amplifier output represents the small time varying impedance of the thorax ΔZ. The output ΔZ amplifier is connected to a comparator circuit which operates a relay when an adjustable present limit has been exceeded at the ΔZ output. The limit adjustment is made with potentiometer R_1, as shown in drawing 3-6. This performs the automatic rebalancing necessary for compensation of changes in Z_o that occur with respiration or motion. The relay is connected to the sample and hold circuit. When the relay is energized the sample and hold circuit will sample the output of OP4 to obtain a new mean value for Z_o and thereby return the output of the ΔZ amplifier to near zero.

The total time varying impedance output from OP4 is fed to operational amplifier OP7 which takes the first time derivative of the time varying impedance. This amplifier also filters the signal. The output of OP7 is fed to operational amplifier OP8 which gives at its output the second time derivative of the impedance signal.

Transistors Q_{14}, Q_{15}, and Q_{16} are used to form a sawtooth waveform generator that is used for calibration of the first derivative shown in drawing 3-5. The period and amplitude of the calibration signal is adjusted to give a derivative output square pulse amplitude equal to 1 ohm per second.

Connected to the Z_o output is a null balancing circuit which is used to obtain an accurate readout of the mean impedance Z_o as shown in drawing 3-6. The circuit nulls the output of Z_o against a Zener controlled reference voltage using calibrated potentiometer R_2. The value of Z_o can be directly read from the face of R_2. Switch S_3 is used to connect the meter to either a low or high sensitivity scale. Switch S_4 is used to connect the instrument to the subject or to a fixed calibrating resistance of 25.5 ohms. The calibrating resistance can be paralleled using the switch with two different resistances to give .1 ohm steps on the ΔZ output. Switch S_2 is used to switch in the sawtooth waveform for the derivative calibration. Also shown in drawing 3-6 are the interconnections between electronic circuit cards.

The system has four output signals, Z_o, ΔZ, dZ/dt, and d^2Z/dt^2. The voltage output for Z_o is 1 to 10 volts corresponding to an Z_o of 10 to 100 ohms, for ΔZ the output is 5 volts/ohm change at the input, for dZ/dt the output is .5 volt/ohm per sec change of impedance at the input and for d^2Z/dt^2 the output is .005 volts/ohm per sec^2 change at the input. When the system is connected to a normal subject, the ΔZ, dZ/dt and d^2Z/dt^2 outputs will be in the range of 0-2 volts.

The specifications of the system are as follows:

Current source output impedance	100K ohms
Differential input impedance	100K ohms
Accuracy of Z_o	1 percent
Linearity of Z_o	.5 percent
Range of Z_o measurement	15 to 80 ohms
Automatic balance time	40 ms
ΔZ bandwidth (3db)	60 Hz
dZ/dt bandwidth (3 db)	40 Hz
Noise output of dZ/dt	100 mV peak to peak

REFERENCE

1. Hill, R. V., Jansen, J. C., and Fling, J. L.: Electrical Impedance Plethysmography: A critical analysis. J Appl Physiol 22:161-168 1967.

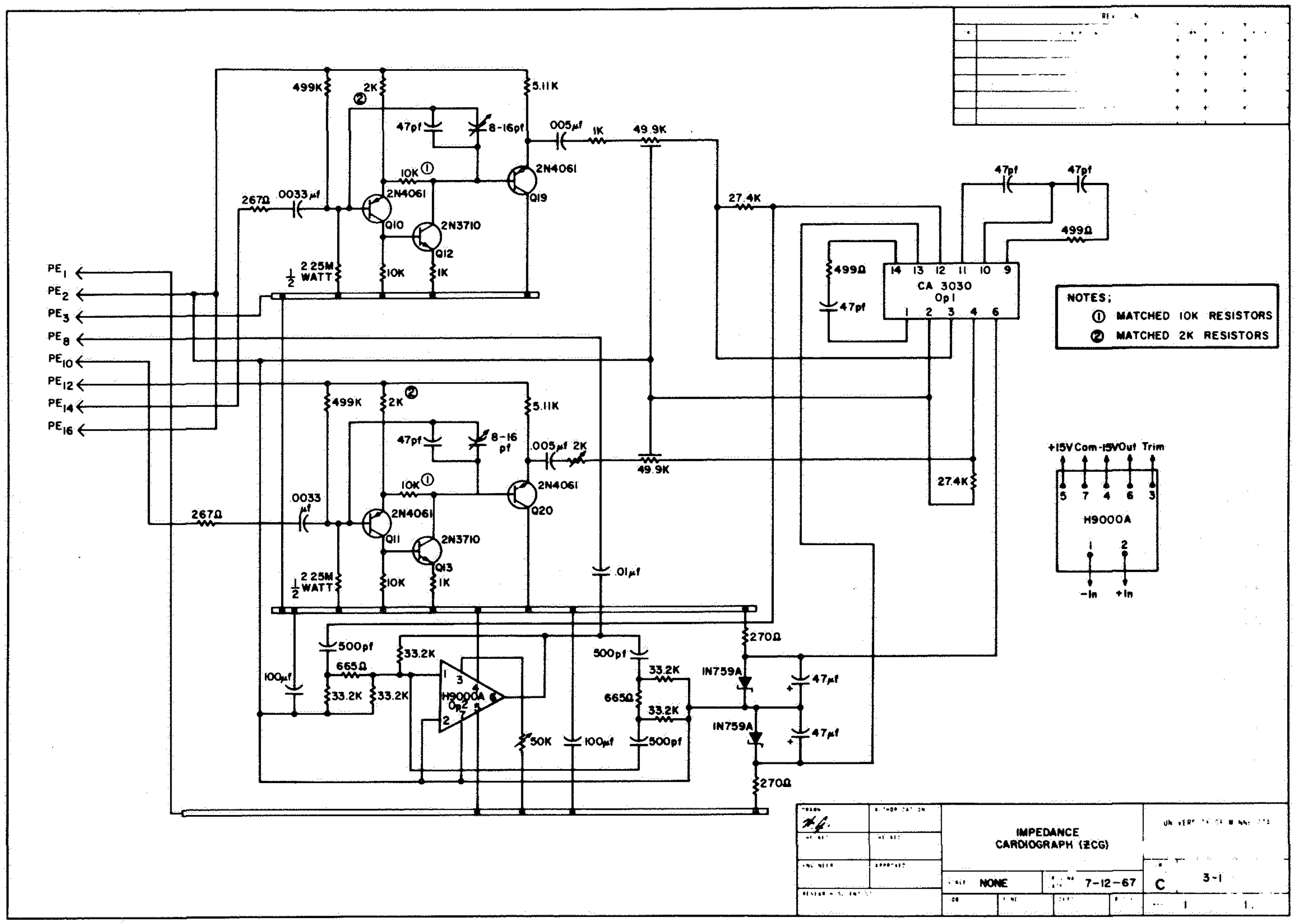
NOTES;
① MATCHED 10K RESISTORS
② MATCHED 2K RESISTORS
CA 3030
Op1
H9000A
+15V Com -15V Out Trim
-In +In
2N4061
2N3710
Q10
Q11
Q12
Q13
Q19
Q20
IN759A
PE1
PE2
PE3
PE8
PE10
PE12
PE14
PE16
IMPEDANCE
CARDIOGRAPH (ZCG)
NONE
7-12-67
C
3-1

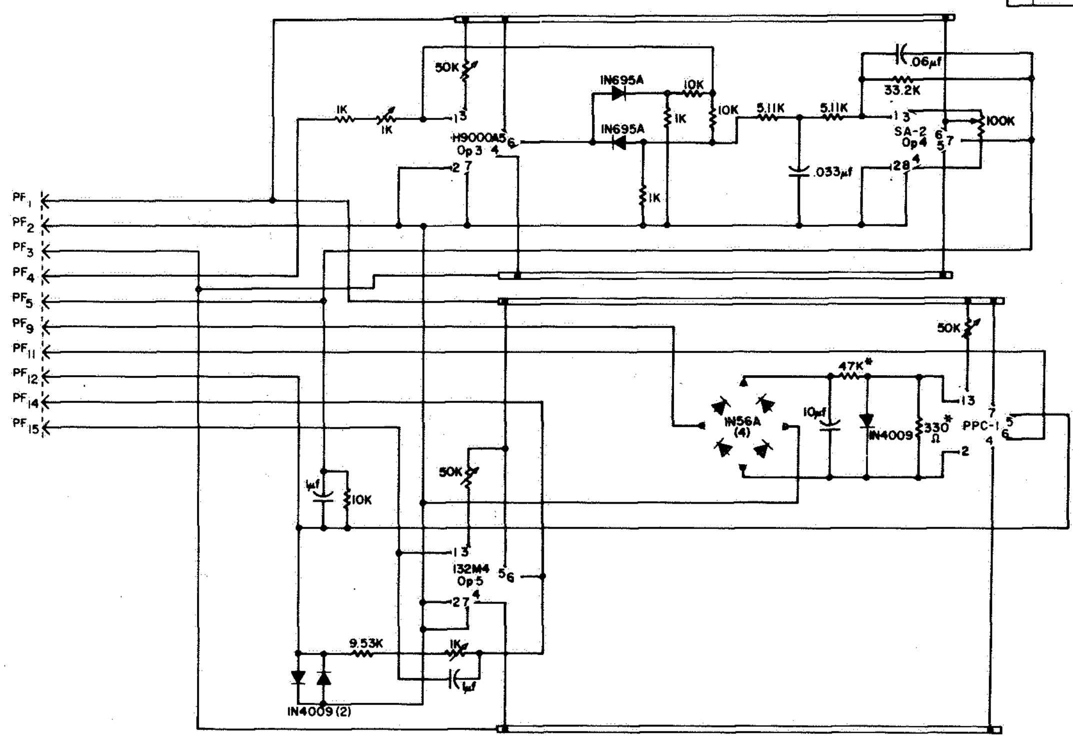

NOTES;
ALL RESISTORS ARE 1%, $\frac{1}{8}$ WATT METAL FILM EXCEPT FOR* WHICH ARE 5%, $\frac{1}{4}$ WATT CARBON.

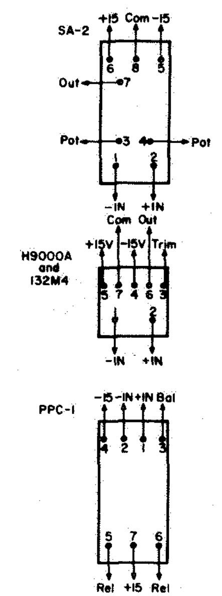

IMPEDANCE
CARDIOGRAPH (ZCG)

NONE 7-7-67 C 3-2

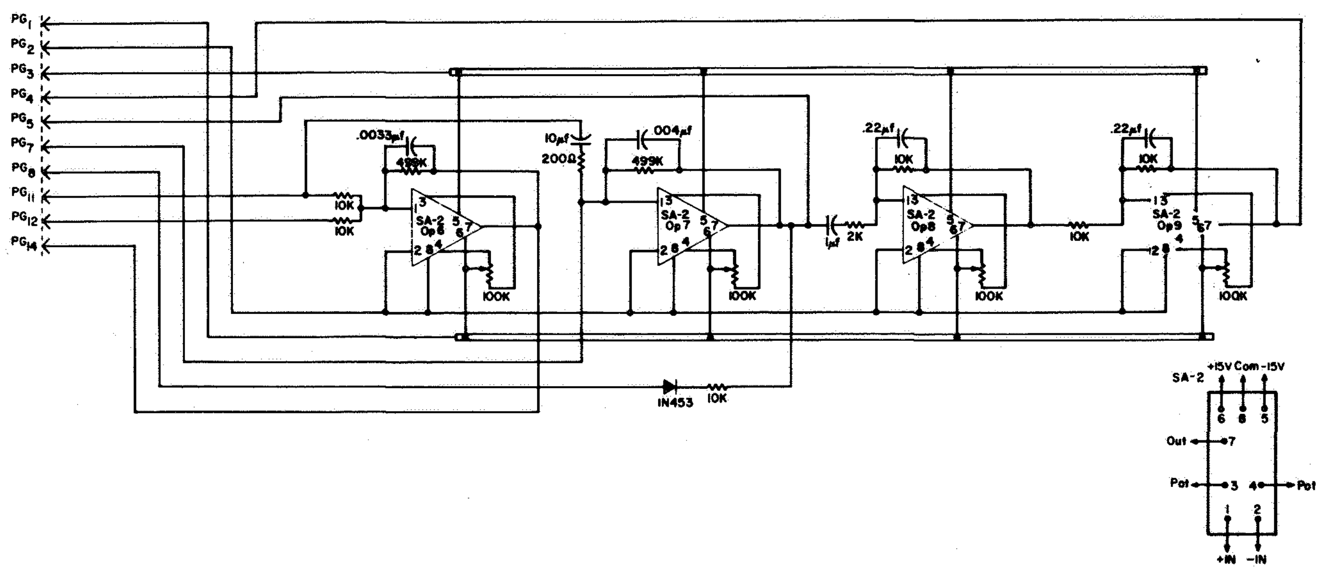

REVISIONS

IMPEDANCE CARDIOGRAPH (ZCG)

NONE 7-5-67 C 3-3

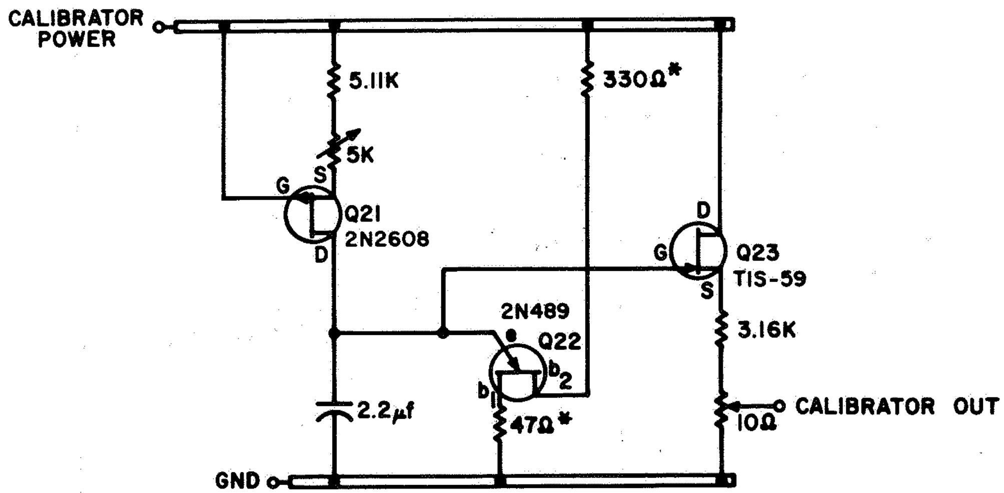

REVISIONS				
LTR	DESCRIPTION	DWN	DATE	APPROVED

NOTES;

ALL RESISTORS ARE 1% METAL FILM, $\frac{1}{8}$ WATT EXCEPT* WHICH ARE 5% CARBON, $\frac{1}{4}$ WATT.

DRAWN M. G.	AUTHORIZATION	IMPEDANCE CARDIOGRAPH (ZCG)			UNIVERSITY OF MINNESOTA
CHECKED	CHECKED				
ENGINEER	APPROVED	SCALE NONE	ORIGINAL DATE 6-30-67		DWG SIZE B — 3-5
RESEARCH SCIENTIST		JOB	FUND	DEPT / BUDGET	SHEET 1 OF 1

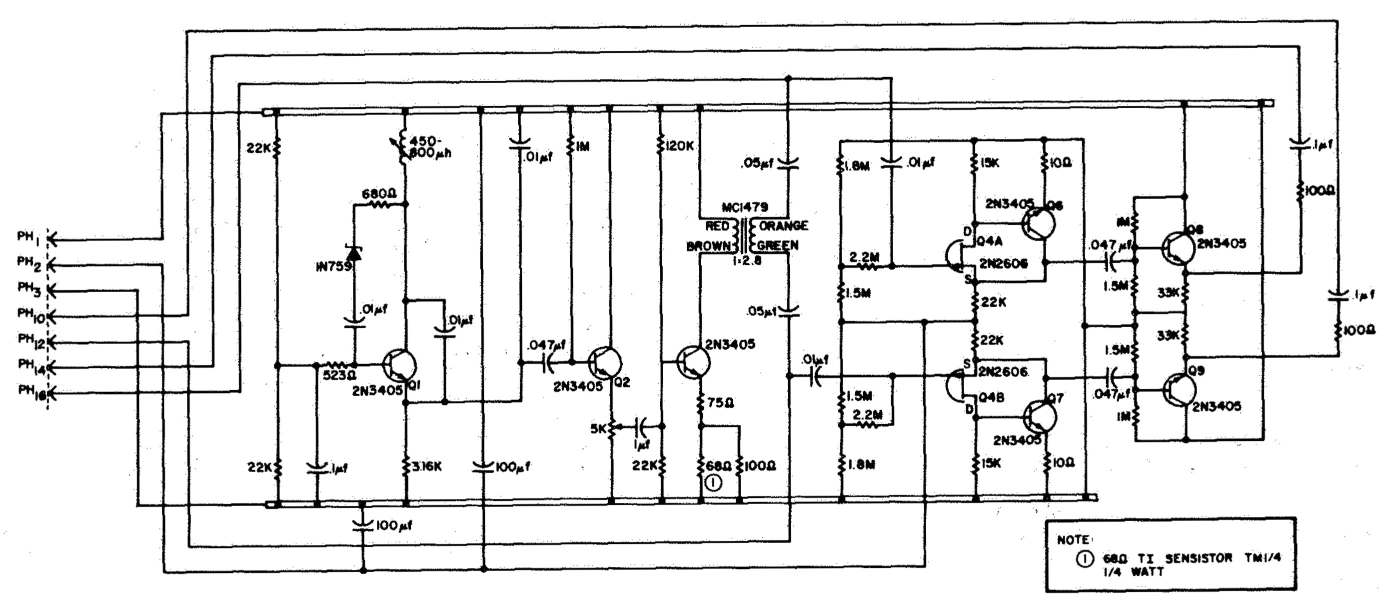

IMPEDANCE CARDIOGRAPH (ZCG)

NONE

7-12-67

C

3-4

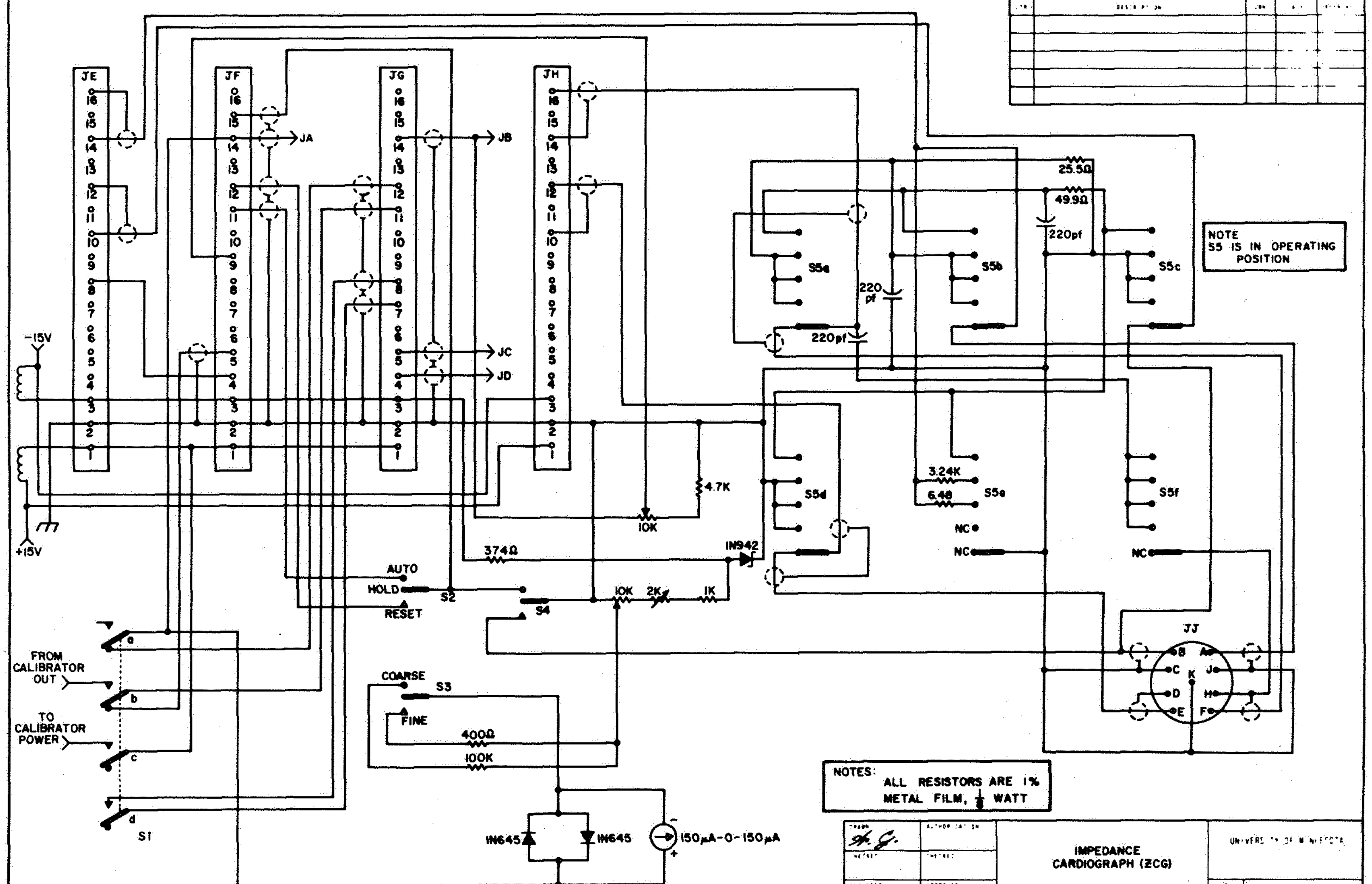

NOTE
S5 IS IN OPERATING POSITION

NOTES:
ALL RESISTORS ARE 1% METAL FILM, 1/8 WATT

REVISIONS

IMPEDANCE CARDIOGRAPH (ZCG)

SCALE NONE

7-12-67

C

3-6

SECTION II. Evaluation of an Inflight ZCG Breadboard

Summary -

Assistance was given the NASA in the testing and evaluation of Spacelabs breadboard ZCG system. Initial testing of Spacelabs, Inc. breadboard ZCG in our laboratory showed that the system had a number of problems. After discussing these problems with the NASA and Spacelabs Inc. in conferences at Houston, a majority of the problems were resolved. The major problem still unresolved is the amount of allowable noise on the first derivative of ΔZ.

Discussion -

In order to aid the development of flight hardware, assistance was given to the NASA in the design, testing and evaluation of a ZCG system produced by Spacelabs Inc. The assistance was given to the NASA in the testing and evaluation of Spacelabs Inc. proposed ZCG flight hardware in two ways. One way was the actual testing of Spacelabs ZCG breadboards in our laboratory. The other way was by attending conferences held by the NASA at Houston to discuss the problems encountered with the Spacelabs hardware and attempt to resolve these problems by discussing them with Spacelabs representatives.

The initial tests of the Spacelabs ZCG breadboard showed a number of problems. As the testing proceeded it was found that a number of these problems could be traced to faulty construction and wiring. A number of the wiring errors were corrected in our laboratory. After the correction of these problems, three specifications showed large deviations from the desired value. They were a) low output impedance of the current source measured at the end of the subject cables, b) low differential input impedance measured at the end of the subject cables, c) excessive noise on the first derivative output and d) the ECG R spike appearing on the first derivative output.

A number of trips were made to Houston to meet with representatives of the NASA and Spacelabs, Inc. in an attempt to resolve the problems. After the discussions with Spacelabs, Inc. personnel concerning the problems, Spacelabs made modifications in the existing breadboards. As a result of the modifications, the problems with low differential input impedance and ECG R spike on the first derivative output were resolved. Spacelabs reported that the maximum output impedance of the constant current source they could obtain was 60K ohms. The desired value would be 100K ohms. It was agreed that this value would be acceptable. The problems with noise on the first derivative were not significantly changed after the modifications. This problem was also compounded by the fact that it is difficult to define the noise in a manner that would indicate its effect in reducing the accuracy of the cardiac output measurement. The approval to begin flight prototype construction was given by the NASA before this problem was completely resolved. No further work on the evaluation was done after approval to start flight prototype hardware construction was given to Spacelabs. Inc.

SECTION III. Digital Computer Program for Computation of Cardiac Output by the Impedance Method (ZCG)

Summary -

A digital computer program was developed to compute beat by beat stroke volume and cardiac output from ZCG information. The computer samples the Z_o and dZ/dt output from a ZCG and finds $(dZ/dt)_{min}$ and τ. With this information and the value for L and ρ, the program computes cardiac output and stroke volume in real time. The present program has been tested only on a limited number of subjects and under limited conditions. Therefore, additional work is needed to assure operation on a large number of subjects and under various conditions.

Introduction -

The stroke volume and cardiac output information given by the ZCG is of a beat by beat nature. To obtain accurate average values and to continuously observe beat by beat stroke volume and cardiac output changes that occur under various conditions, it is necessary to compute a large number of beats. This section describes a preliminary digital computer program that will compute cardiac output and stroke volume in real time on a beat by beat basis.

The program was developed on a Spear micro-LINC computer. Fig. 3-3 shows a typical dZ/dt waveform recorded from four-band electrodes as was described previously (Chapter One, Section I). The stroke volume and cardiac output were

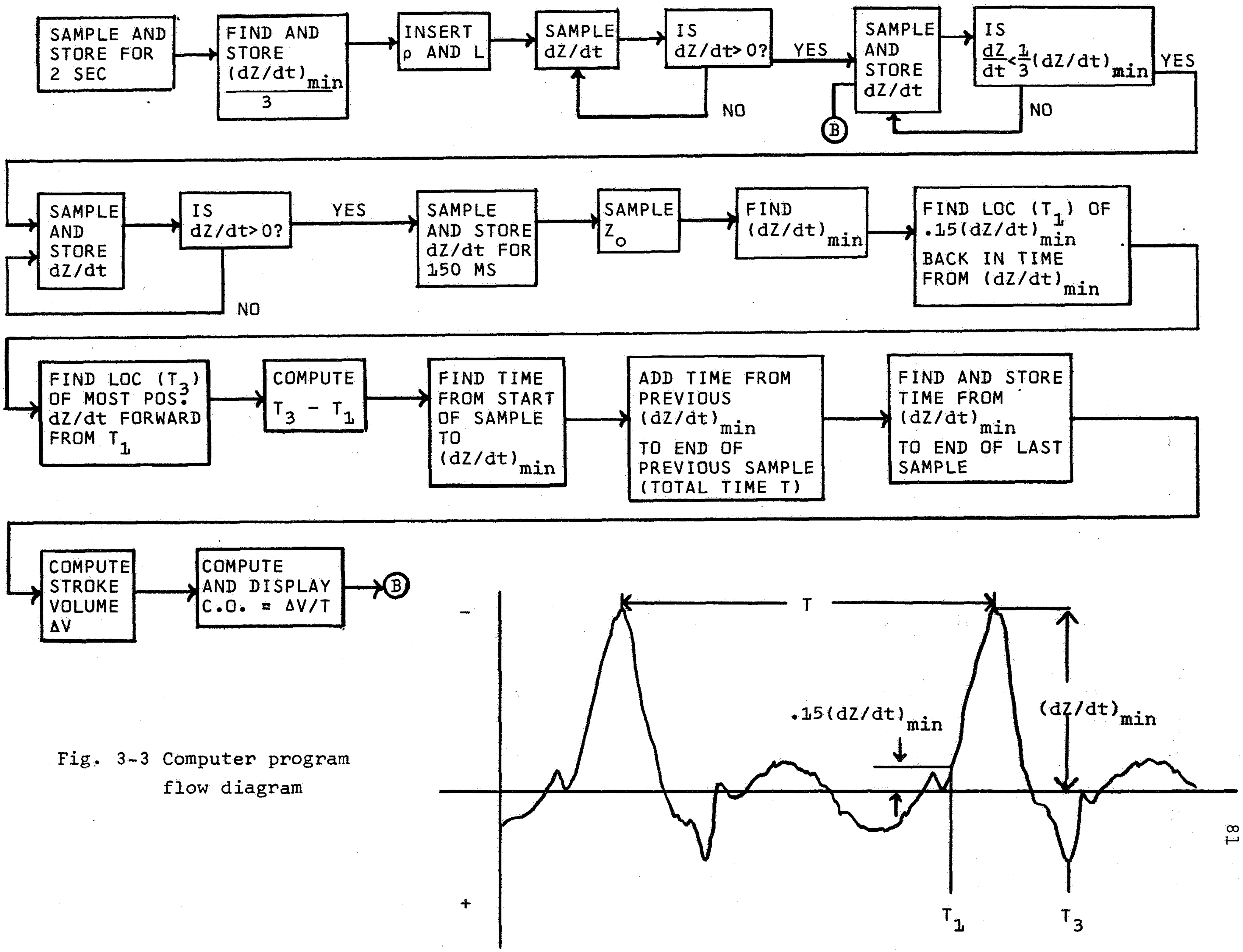

Fig. 3-3 Computer program flow diagram

calculated using the standard formula as described below:

$$\Delta V = \rho \frac{L^2 \tau}{Z_o^2} (dZ/dt)_{min}$$

and $C.O. = (\Delta V)(T)$

ΔV = stroke volume (cc)

ρ = resistivity of blood at 100 kHz and 37.5°C (150 ohm-cm)

L = mean distance between pick up electrode (cm)

Z_o = impedance between pick up electrodes (ohms)

$(dZ/dt)_{min}$ = minimum value of first time derivative of Z (ohms per sec)

τ = $(T_3 - T_1)$ = ventricular ejection time as determined from the dZ/dt waveform

T = the time interval between heart beats in minutes

C.O. = cardiac output (cc per min)

Fig. 3-3 shows the minimum value of dZ/dt, T_1, T_3, and T. The difference between T_1 and T_3 is the ventricular ejection time. T_1 is found by going back in time down the dZ/dt waveform as shown in Fig. 3-3 from $(dZ/dt)_{min}$ to $.15(dZ/dt)_{min}$. This is done to eliminate from the ejection time determination the slow decrease in impedance that occurs with some individuals at the start of systole. T_3, the end of systole is indicated by the peak positive dZ/dt after $(dZ/dt)_{min}$. The program was developed using only impedance information and does not require the ECG for timing. A simpler program could be developed using the ECG for timing but it could put a restriction on the use of the program in some applications.

Program Description -

The program starts by sampling dZ/dt for 2 seconds as shown in fig. 3-3. It then finds $(dZ/dt)_{min}$ and divides it by 3 (in fig. 3-3 negative dZ/dt is above the zero line). Next the constants ρ and L are entered. The computer then starts sampling dZ/dt and looking for a positive dZ/dt value. When it finds a positive value it starts sampling and storing. The computer is now looking for the start of the next complete systole. Referring to the waveform shown in fig. 3-3, it can be seen that dZ/dt is positive only in the last part of systole or during diastole. If it is assumed that the computer found the positive value occurring during the latter part of systole then from fig. 3-3 it can be seen that the next negative value of dZ/dt will occur during diastole. The normal subjects tested to date have shown negative dZ/dt values during diastole to be greater than 1/3(dZ/dt) min. Therefore, since the computer is looking for the start of a systole it jumps over any dZ/dt until it is less than $1/3(dZ/dt)_{min}$ of the previous beat. After it finds a dZ/dt less than $1/3(dZ/dt)_{min}$ it assumes it is in a systolic ejection period and it begins to look for a zero crossing which will occur after $(dZ/dt)_{min}$. When the computer finds a zero crossing it samples for 150 ms more which is enough time to cover a complete systolic ejection period. After a 150 ms it samples the Z line to obtain Z_o. The computer then finds $(dZ/dt)_{min}$ and the location in memory of $.15(dZ/dt)_{min}$

by going back in time down the dZ/dt waveform from $(dZ/dt)_{min}$ as shown in fig. 3-3. Because the sampling rate is constant and the samples are stored in consecutive location in the memory, their position in the memory will be an indication of their occurrence in real time. After T_1 is found it goes forward in time and finds the location in the memory of the most positive dZ/dt value in the current samples which corresponds to T_3. The computer then calculates $T_3 - T_1$ to obtain the systole ejection time τ. At this point the computer has all the information necessary to compute stroke volume.

The computer then proceeds to obtain T in order to compute heart rate per minute. It computes the time from the start of the sampling and storing period to $(dZ/dt)_{min}$ and adds to it the time from the previous $(dZ/dt)_{min}$ to the end of the previous sample period. The latter time interval will be in error on the first beat because of the delay necessary for the computer to find the start of systole. The computer then stores the time from the $(dZ/dt)_{min}$ of the present beat to the end of the current sample for use in calculating T for the next beat. The stroke volume and cardiac output is then calculated and the value of cardiac output is displayed on a cathode ray tube as a point on a graph. The computer then jumps to point B in the flow chart to start the next beat. The time for all the calculations is less than the sampling rate, therefore no time is lost.

The present program has some deficiencies that need further work. For example, if some motion artifact causes a large

$(dZ/dt)_{min}$ it is possible that the program would stop calculating. Also, other changes in the waveform that may be apparent after testing a large number of individuals may require changes in the present criteria or the addition of new criteria.

CARDIAC OUTPUT COMPUTER PROGRAM

```
     [PATERSON
     [HEARTBEAT ANALYSIS
     [NOVEMBER 1966
     [CLEAR MEMORY
0020        SETi1
0021        1000
0022        CLR
0023        STA 1
0024        XSKi1
0025        JMPp-2
0026        SETi1
0027        2000
0030        STA 1
0031        XSKi1
0032        JMPp-2
0033        SETi15
0034        777
     [SAMPLE 1024 POINTS
0035 #1C SETi3
0036        3777
0037        SAM 10
0040        STAi3
0041        JMP9A
0042        XSK 3
0043        JMPp-4
     [FIND MAXIMUM
0044        SETi3
0045        3777
0046        CLR
0047        STC8A
0050 #1A XSKi3
0051        JMPp+2
0052        JMP1E
0053        LDA 3
0054        COM
0055        ADD8A
0056        APOi
0057        JMP1A
0060        LDA 3
0061        STC8A
0062        JMP1A
     [DIVIDE MAX BY 3
0063 #1E LDA
0064        8A
0065        MUL
0066        8B+4000
0067        STC8C
     [WAIT FOR NEGATIVE VALUE
0070 #1D JMP9A
0071        SAM 10
0072        APOi
0073        JMP1D
     [START STORING
     [INSERT CONSTANTS
0074 #1Z RSW
0075        STC8G
0076        LSW
0077        STC8H
0100 #1F SETi4
0101        3777
0102 #1G JMP9A
0103        SAM 10
0104        STAi4
0105        COM
0106        ADD8C
0107        APOi
0110        JMP1G
0111        LDA
0112        4
0113        STC8D
0114        SETi5
0115        -10
0116        JMP9A
0117        SAM 10
0120        STAi4
0121        XSKi5
0122        JMPp-4
0123 #1J JMP9A
0124        SAM 10
0125        STAi4
0126        APOi
0127        JMP1J
     [SAMPLE 150 MS AFTER ZERO CROSS
0130        SETi5
0131        -113
0132        JMP9A
0133        SAM 10
0134        STAi4
0135        XSKi5
0136        JMPp-4
     [SAMPLE Z1
0137 #2A SAM 11
0140        STC8E
0141        ADD4
0142        STA
0143        8L
0144        COM
0145        ADAi
0146        2000
0147        STC10
     [FIND MAX
0150 #2B SETi7
0151        3777
0152        CLR
0153        STC8A
0154 #2C XSKi10
0155        JMPp+2
0156        JMP2D
0157        LDAi7
0160        COM
0161        ADD8A
0162        APOi
0163        JMP2C
0164        LDA 7
0165        STC8A
0166        ADD7
0167        STC8F
0170        JMP2C
     [DIVIDE BY 3
0171 #2D ADD8A
0172        MUL
0173        8B+4000
0174        STC8C
     [FIND T1
0175        ADD8C
0176        SCR 1
0177        STC8J
```

```
0200 0200      SET 12
0201 0201      8F
0202 0202 #2G LDAi
0203 0203      -1
0204 0204      ADD12
0205 0205      STC12
0206 0206      LDA 12
0207 0207      COM
0210 0210      ADD8J
0211 0211      APO
0212 0212      JMP2G
0213 0213      LDA
0214 0214      12
0215 0215      STC8K
     0216 [FIND T3
0216 0217 #2H SET 12
0217 0220      8F
0220 0221      ADD8L
0221 0222      COM
0222 0223      ADD12
0223 0224      STC14
0224 0225      STC8M
0225 0226 #2K XSKi14
0226 0227      JMP P+2
0227 0230      JMP2L
0230 0231      LDAi12
0231 0232      COM
0232 0233      ADD8M
0233 0234      APO
0234 0235      JMP2K
0235 0236      LDA 12
0236 0237      STC8M
0237 0240      ADD12
0240 0241      STC8N
0241 0242      JMP2K
     0243 [COMPUTE T3-T1
0242 0244 #2L LDA
0243 0245      8K
0244 0246      COM
0245 0247      ADD8N
0246 0250      STC8P
     0251 [COMPUTE T
0247 0252 #2M ADD8P
0250 0253      ADAi
0251 0254      -2000
0252 0255      ADD8R
0253 0256      STC8S
0254 0257      ADD8P
0255 0260      COM
0256 0261      ADD8L
0257 0262      STC8P
     0263 [COMPUTE NUMERATOR
0260 0264 #2P ADD8G
0261 0265      JMP7X
0262 0266      STC8X
0263 0267      ADD8H
0264 0270      JMP9C
0265 0271      ADD8H
0266 0272      JMP9C
0267 0273      ADD8A
0270 0274      JMP9C
0271 0275      ADD8P
0272 0276      JMP9C
0273 0277      ADD8X
0274 0300      STC8T
0275 0301      ADD1
0276 0302      STC8U
     0303 [COMPUTE DENOM
0277 0304      ADD8E
0300 0305      JMP7X
0301 0306      STC8X
0302 0307      ADD8E
0303 0310      JMP9C
0304 0311      ADD8S
0305 0312      JMP9C
0306 0313      ADD8X
0307 0314      STC8V
0310 0315      ADD1
0311 0316      STC8W
     0317 [USE DIVIDE ROUTINE
0312 0320      ADD8T
0313 0321      STC7A
0314 0322      LDAi
0315 0323      3777
0316 0324      STC7B
0317 0325      ADD8V
0320 0326      STC7C
0321 0327      JMP7P
     0330 [COMPUTE EXPONENT
0322 0331      LDA
0323 0332      8W
0324 0333      COM
0325 0334      ADD8U
0326 0335      ADD7E
0327 0336      ADAi
0330 0337      -6
0331 0340      ATR
0332 0341      ADAi
0333 0342      343
0334 0343      STCP+3
0335 0344      ADD7F
0336 0345      COM
0337 0346      0
     0347 [STORE FINAL VALUE IN 02,03
0340 0350      STAi15
0341 0351      STAi15
0342 0352      STAi15
0343 0353      STAi15
0344 0354      XSK 15
0345 0355      JMP1Z
0346 0356      HLT
     0357 E400
0400 0360      CLR
0401 0361      SNS 3
0402 0362      JMPP+4
0403 0363      SETi12
0404 0364      777
0405 0365      JMP5B
0406 0366      SNS 4
0407 0367      JMPP+4
0410 0370      SETi12
0411 0371      3777
0412 0372      JMP5B
0413 0373      SNS 5
0414 0374      JMP400
0415 0375      SETi12
0416 0376      2777
0417 0377 #5B SETi17
```

```
0400      -1000
0401      LDAi2
0402      DIS 2
0403      XSKi17
0404      JMPP-3
0405      JMP400
0406 [DELAY-DISPLAY
0407 #9A SET 17
0410      0
0411      SETi2
0412      -20
0413      LDAi1
0414      DIS 1
0415      XSK 1
0416      JMPP+3
0417      SETi1
0420      777
0421      XSKi2
0422      JMPP-7
0423      SNSi0
0424      JMP10
0425      JMP17
0426 [UTILITY ROUTINE
0427 #9B SET 17
0430      0
0431      JMP7X+2
0432      MUL
0433      8X+4000
0434      JMP7X+2
0435      STC8X
0436      JMP17
0437 [STORAGE
0440 #8A 0 [CURRENT MAX
0441 #8B 1252 [ONE THIRD
0442 #8C 0 [THRESHOLD
0443 #8D 0 [T1 LOCATION
0444 #8E 0 [T2
0445 #8F 0 [LOC OF CURRENT PEAK
0446 #8G 0 [RHO
0447 #8H 0 [L
0450 #8J 0 [0.15 PEAK
0451 #8K 0 [T1 LOC
0452 #8L 0 [LOC LAST SAMPLE
0453 #8M 0 [TEMP MIN
0454 #8N 0 [T3 LOC
0455 #8P 0 [T3-T1
0456 #8R 0 [1ST PART OF T
0457 #8S 0 [T
0460 #8T 0 [NUMERATOR
0461 #8U 0 [EXP NUM
0462 #8V 0 [DENOM
0463 #8W 0 [EXP DENOM
0464 #8X 0 [WORK SPACE
0465 [ARITH
0466 [ARITHMETIC ROUTINES
0467 [G.FELLOWS-SEPT 66
0470 [AXBIC
0471 [C MUST BE POSITIVE
0472 [A IN 7A,B IN 7B, AND C IN 7C
0473 [FIXED RESULT IN 7D
0474 [EXPONENT OF RESULT IN 7E
0475 [MANTISSA OF RESULT IN 7F
0476 #7A 0
0477 #7B 0
0504 0500 #7C 0
0505 0501 #7D 0
0506 0502 #7E 0
0507 0503 #7F 0
0510 0504 #7G 0  [MANT A
0511 0505 #7H 0  [MANT B
0512 0506 #7J 0  [MANT C
0513 0507 #7K 0  [EXPON DENOM
0514 0510 #7L 0  [TEMP STORE
0515 0511 #7M 0  [MANT RECIP
0516 0512 #7N 0  [EXPON NUMER
0517 0513 #7P LDA
0520 0514     0
0521 0515     STC7V
0522 0516     LDA
0523 0517     7A
0524 0520     AZEi
0525 0521     JMP6A
0526 0522     JMP7X
0527 0523     STC7G
0530 0524     ADD7B
0531 0525     AZEi
0532 0526     JMP6A
0533 0527     JMP7X+2
0534 0530     STC7H
0535 0531     ADD1
0536 0532     STC7N
0537 0533     ADD7C
0540 0534     AZEi
0541 0535     JMP6B
0542 0536     JMP7X
0543 0537     STC7J
0544 0540     ADD1
0545 0541     STC7K
     0542 [RECIPROCAL OF C
0546 0543 #7Q LDAi
0547 0544     4000
0550 0545     STC7L
0551 0546     STC7M
0552 0547     SETi1
0553 0550     -12
0554 0551 #7R ADD7J
0555 0552     COM
0556 0553     ADD7L
0557 0554     APO
0560 0555     JMP7T
0561 0556     ROL 1
0562 0557     STC7L
0563 0560     LDAi
0564 0561     1
0565 0562     ADD7M
0566 0563     ROL 1
0567 0564     STC7M
0570 0565     XSKi1
0571 0566     JMP7R
0572 0567     JMP7U
0573 0570 #7T CLR
0574 0571     ADD7M
0575 0572     ROL 1
0576 0573     STC7M
0577 0574     ADD7J
0600 0575     SCR 1
0601 0576     STC7J
0602 0577     XSKi1
```

```
0603  0600       JMP7R
      0601  [MULTIPLY MANTISSAS
0604  0602  #7U  ADD7M
0605  0603       SCR 1
0606  0604       ADAi
0607  0605       1
0610  0606       STC7M
0611  0607       LDA
0612  0610       7G
0613  0611       MUL
0614  0612       7H+4000
0615  0613       JMP7X
0616  0614       MUL
0617  0615       7M+4000
0620  0616       JMP7X+2
0621  0617       STC7F
0622  0620       ADD7K
0623  0621       COM
0624  0622       ADD1
0625  0623       ADD7N
0626  0624       ADAi
0627  0625       -2
0630  0626       STC7E
0631  0627       ADD7E
0632  0630       APO
0633  0631       JMP7W
0634  0632       ADAi
0635  0633       SCR
0636  0634       STC7S
0637  0635       ADD7F
0640  0636  #7S  0
0641  0637       STC7D
0642  0640  #7V  JMP
0643  0641  #7W  LDAi
0644  0642       3777
0645  0643       STC7D
0646  0644       JMP7V
      0645  [FLOAT
0647  0646  #7X  SETi1
0650  0647       0
0651  0650       STC7Y
0652  0651       LDA
0653  0652       0
0654  0653       STC7Z
0655  0654       ADAi
0656  0655  #7Y  0
0657  0656       APO
0660  0657       JMP7I
0661  0660       POL 1
0662  0661       APOi
0663  0662       JMPp+3
0664  0663       POR 1
0665  0664  #7Z  JMP
0666  0665       XSKi1
0667  0666       JMPp-6
0670  0667  #7I  POL 1
0671  0670       APO
0672  0671       JMPp+3
0673  0672       POR 1
0674  0673       JMP7Z
0675  0674       XSKi1
0676  0675       JMPp-6
      0676  [NUMERATOR IS ZERO
0677  0677  #6A  CLR
0700  0700       STC7D
0701  0701       JMP7V
      0702  [DENOM IS ZERO
0702  0703  #6B  LDAi
0703  0704       3777
0704  0705       STC7D
0705  0706       JMP7V
0706  0707
```

CHAPTER FOUR

ORIGIN OF IMPEDANCE VARIATIONS DURING THE CARDIAC CYCLE

Summary -

The cardiogenic change in thoracic electrical impedance (ΔZ) was studied in 20 Kg, pentobarbitol anesthetized, closed-chest dogs with electromagnetic flowmeter probes placed about the main pulmonary artery and ascending aorta, and with balloon catheters in the right and left atria. ΔZ was measured with a 4 band (2 neck and 2 abdominal) electrode plethysmograph utilizing constant current 100 kHz excitation. ΔZ, pulmonic flow (PF) and aortic flow (AF) were recorded during periods of disassociation of PF and AF resulting from inflation of the atrial balloons, and also in a dog with a spontaneous left ventricular mechanical alternans and a stable right-ventricular ejection pattern. It was found in both the balloon and alternans experiments that the rapid systolic decrease in thoracic impedance occurred only in the presence of ejection of blood into the aorta, and that this result was independent of right ventricular ejection. Further experiments demonstrated the persistence of ΔZ when all branches of the aorta to the level of the diaphragm were ligated. These findings suggest that the rapid systolic decrease of thoracic impedance in the dog is related to intrathoracic systemic circulatory events. Further work indicates that aortic volume changes may be the origin of ΔZ.

The purpose of this chapter is to describe an investigation into one of the basic questions in the impedance cardiac output technique. That is, what produces the intrathoracic impedance variations seen across the chest during a cardiac cycle? The origin of these impedance variations is most likely dependent upon a particular electrode configuration and the results presented in this chapter deal with the particular electrode configuration show in figure 4-1.

Previous investigations by this laboratory into the origin of intrathoracic impedance variations were by means of detecting the paths of maximum current flux with the belief that the impedance variations would probably be caused by the medium in which most current flux was found. Results of earlier investigations (1) indicated that the majority of the current flux distributed itself through the lung field. Therefore, it was felt that the impedance variations across the chest were due to pulmonary blood volume changes since the impedance decreased during systole implying an increased blood volume and increased during diastole suggesting a run off of blood. This was the case for the pulmonary circulation. The purpose of this investigation was to evaluate this hypothesis.

A four electrode 100 kHz impedance system was used in this investigation. The excitation electrodes consisted of a band around the upper portion of the neck and the abdomen. The inner two sensing electrodes were placed at the lower boundary of the neck and approximately 1 cm below the xiphisternal joint. Positioning of the two excitation bands was not critical except for the fact that the excitation band on the neck must be at least 3 cm away from the sensing electrode band. The thorax was excited by a 100 kHz constant current source with an amplitude of 6 milliamps rms and with an output impedance of 100 K ohms at the end of 7 foot electrode leads. The sensing electrodes saw an input impedance of 100 K ohms at the end of 7 foot input leads.

For the experimental design it appeared that the most direct method of determining the origin of impedance variations was to dissociate right and left ventricular ejection in animals and observe resulting impedance changes of the thorax. It would then be possible to determine if the major contribution was coming from the systemic circulatory system or from the pulmonary system. Fig. 4-1 describes the methods used in the first approach to dissociating right and left ventricular ejections.

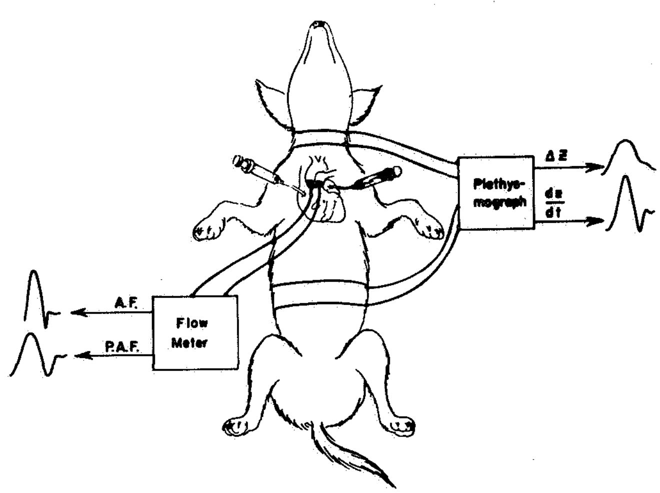

Figure 4-1 Electrode and balloon catheter placement

Twenty kilogram male mongrel dogs were anesthetized with penobarbitol at 30 milograms per kilogram and impedance determinations were made in the usual fashion. Then with the animal attached to a positive pressure respirator, a left thoracicotomy was performed and balloon catheters were placed in each atrium via the atrial appendage. Electromagnetic flowprobes for a Biotronix Model 410 electromagnetic flowmeter were acutely implanted on the main pulmonary artery and on the ascending aorta. After closure of the chest the animals were placed upon a continous suction to eliminate any pneumothorax. Simultaneous ΔZ, dZ/dt, aortic and pulmonary flow tracings were recorded while balloon catheters were inflated in various sequence so as to dissociate aortic from pulmonic flow for brief periods. Resulting impedance tracings were then examined for contributions from either pulmonic or systemic volume changes as indicated by the flowmeter tracings.

Fig. 4-2a indicates a control condition in which both balloons were deflated, the control or normal ΔZ waveform was characterized by the rapid decrease in impedance during systole, (impedance decreases upward in these tracings). Note the correlation between the onset of rapid decrease in impedance and the onset of systole as indicated by aortic flow or the EKG waveform. This rapid decrease of impedance during systole, or the systolic component of the ΔZ waveform, is the portion of the impedance waveform that is used in our laboratory as a means for estimating cardiac output and subsequently it is the origin of this portion of the waveform that is of interest. Fig. 4-2a is a control condition for the following sequence of events:

a) both balloons deflated

b) right atrial balloon inflated

c) left atrial balloon inflated

d) right atrial balloon deflated

e) left atrial balloon defalted returning to control condition

Results of this experimental run are described in figures 4-2b through 4-2e.

Figure 4-2b shows the condition of the animal when the right atrial balloon was inflated with the left atrial balloon still deflated. Blood was free to move from the pulmonary circulation into the left heart and out into the systemic circulation. It can be seen that the ΔZ waveform was still present in the first cardiac cycle of this figure and decreased as the aortic flow decreased. Fig. 4-2c depicts the results when both balloons were inflated. It can be seen that the aortic flow and ΔZ waveform had essentially gone to zero. When the right atrial balloon was deflated while the left atrial balloon remained inflated the pulmonary artery flow returned, aortic flow was still zero but a ΔZ waveform was present as seen in fig. 4-2d. Note that the ΔZ waveform was displaced in time, i.e. there was not the rapid decrease of impedance with the onset of systole as was characteristic of the control condition. This result was found essentially in all dogs in this experimental condition. In fig. 4-2e the left atrial balloon had been deflated. Pulmonary artery flow was now present, aortic flow had returned and the ΔZ waveform had

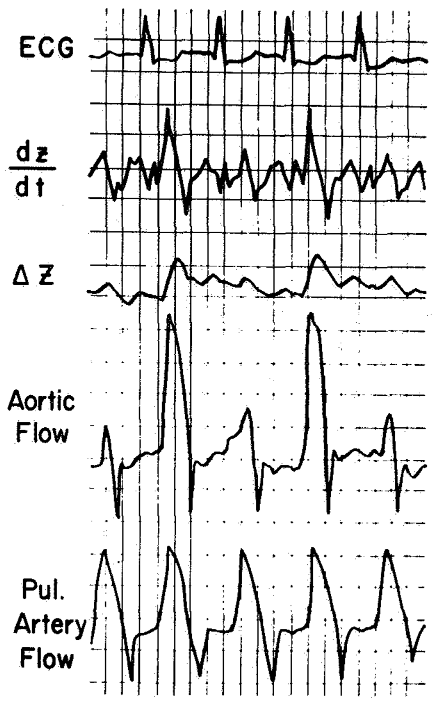

Fig. 4-2a Control, deflated balloon catheter in each atrium

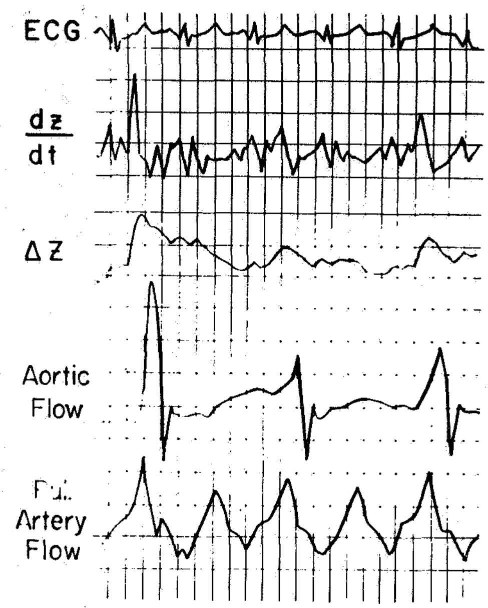

Fig. 4-2b Right atrial balloon inflated

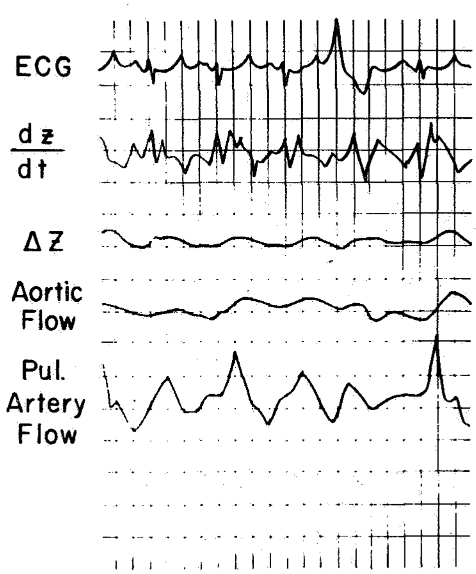

Fig. 4-2c Both atrial balloons inflated

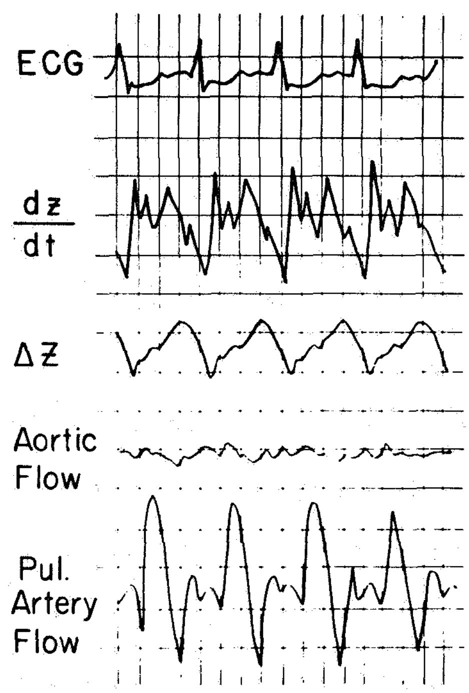

Fig. 4-2d Right atrial balloon deflated, left still inflated

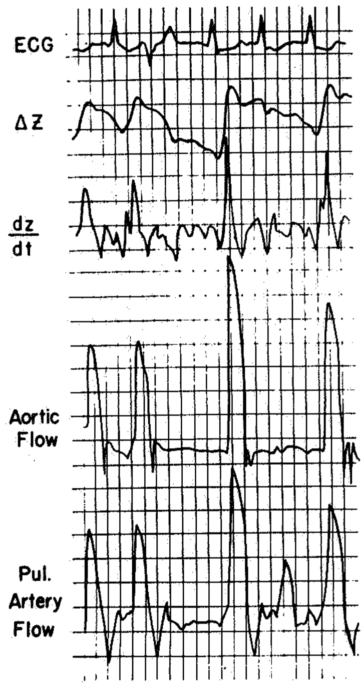

Figure 4-2e Left atrial balloon deflated (both balloons deflated

returned to its control characteristics. The dZ/dt waveform showed pronounced systolic peaking indicating fast or rapid decrease in impedance with systole.

These results were typical of those found in a series of ten experiments and subsequently the original pulmonary origin hypothesis was changed. It was now assumed that aortic flow, or some systemic circulatory function, is the origin of the rapid decrease of impedance during systole.

The preceding series of figures describe the results of an experiment in which it was possible to dissociate right and left ventricular functions although these functions occurred with balloon catheters in the animal's atria. Fortunately two animals exhibited spontaneous left ventricular mechanical alternans and stable right ventricular ejection patterns with the heart intact. The tracings obtained from one of these animals with the left mechanical alternans condition is show in fig. 4-3. The pulmonary artery flow occurred with the normal

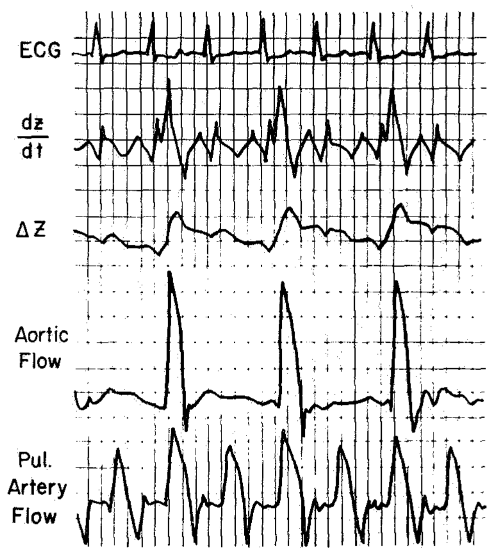

Figure 4-3 Left heart mechanical alternans, Dog No. 8

sinus rhythm of the ECG while aortic flow was present only with every second beat. The ΔZ waveform corresponded in time with the aortic flow and the rapid decrease of impedance occurred only with the onset of left ventricular ejection and was independent of right ventricular ejection. Fig. 4-4 shows the same alternans condition in another animal. Here the pulmonary flow was regular and the aortic flow varied. There was not the marked degree of mechanical alternans as there was in the previous animal but it can be seen that the ΔZ waveform, subsequently dZ/dt, varied with aortic but not the pulmonary artery flow.

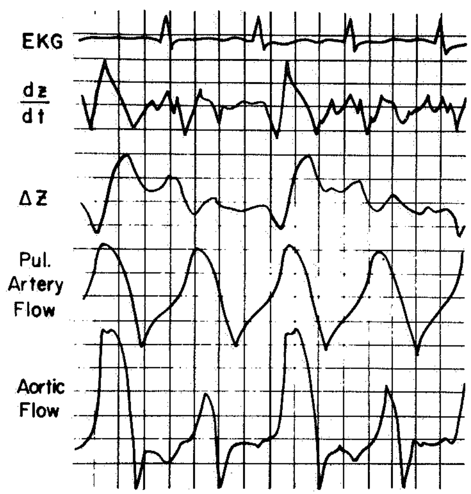

Figure 4-4 Left heart mechanical alternans, Dog No. 12

The previous evidence suggests that the ΔZ waveform occurs as a consequence of left-sided hemodynamic events. However it was not shown whether the site of origin of ΔZ waveform is intrathoracic; that is from the left ventricle, aorta or extrathoracic, that is from thoracic wall circulation. Although it remains to be conclusively demonstrated, evidence thus far indicates that it is unlikely that the left ventricle is the origin of the systolic decrease in impedance because its diminished blood volume during systole should cause decreased conductivity at this time. However, either the aorta or thoracic wall vasculature could account for a systolic impedance decrease since their blood volumes and hence conductivities, would be appropriately increased during systole. Therefore an experiment was planned which would eliminate the extra thoracic circulation so that observations of ΔZ could be made in its absence.

Twenty Kilogram male mongrel dogs were anesthetized with pentobarbitol at the rate of 30 millograms per kilogram and impedance determinations were made in the usual fashion as a control condition. Then, with the animals placed upon a positive pressure respirator, a left thoracotomy was performed and the aorta was exposed as competely as possible. Electromagnetic flowprobes were placed on the ascending aorta in all animals, and in some animals in this series of experiments a probe was placed about the main pulmonary artery. In addition balloon catheters of the type previously described were also placed in the right and left atria of some of the animals. Following the placement of the probes and catheters all branches from the aorta to the level of the diaphragm were ligated. The brachialcephalic vessels were ligated immediately prior to chest closure. After closure of the chest, the animals were placed on a continous suction to eliminate any pneumothorax and impedance determinations were then made in a controlled state.

The results of a series of these experiments is demonstrated in fig. 4-5. The impedance waveform, ΔZ, was found to persist in the experimental animals following thoractomy

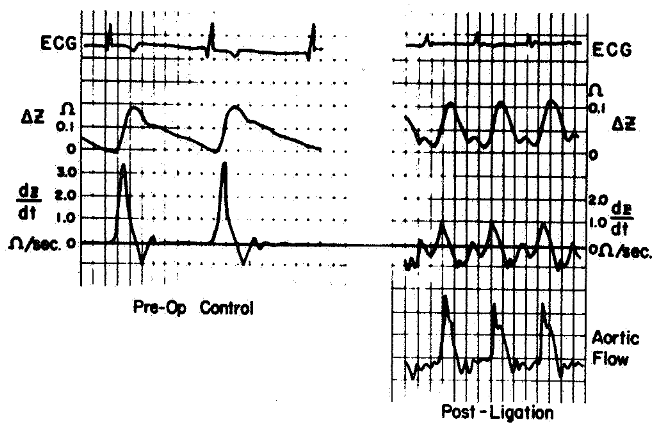

Figure 4-5 Impedance waveforms before and after ligation of aorta branch vessels

and aortic branch ligation. In addition it was also shown by means of balloon experiments (as described above) that the rapid systolic decrease which characteristics the normal waveform occurred only in the presence of the ejection of blood into the aorta. The differences between the pre-op and post ligation ΔZ waveform were no different than those in the ordinary post thoractomy animal in the absence of ligation. Fig. 4-6 describes a condition with balloons in the right and left atrium of an animal with ligated aortic branch vessels. It can be seen that the rapid decrease of impedance with the onset of systole occurred only when there was an aortic pulse. The impedance change waveform occurring with the cardiac cycle containing only pulmonary flow was again displaced in time and contained no rapid decrease of impedance with the onset of systole.

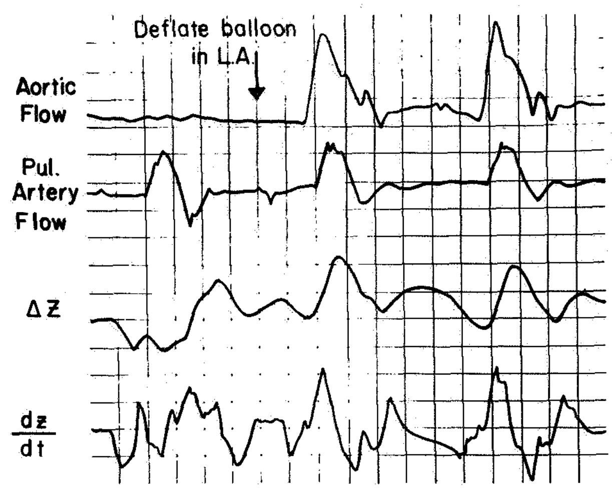

Figure 4-6 Atrial balloon experiment with ligated aortic branch vessels

The results of these ligation experiments indicate that the origin of impedance variations occurring during the cardiac cycle, as monitored by the four band electrode configuration, appeared to be from the systemic circulation and appeared to be primarily intrathoracic as opposed to being caused by volume changes in the thoracic wall.

As a further investigation of the origin of impedance variations, a pilot series of experiments was run in which left heart bypass was used to dissociate right and left ventricular functions. A Harvard Apparatus pulsatile pump (model 1403) was used to profuse the aorta allowing control over stroke volume and pulse rate for systemic flow. By setting the pulse rate of the pump equal to approximately one-half the pulse rate of the normal sinus rhythm of the animal and the stroke volume compensated such that right and left ventricular outputs were equal, it was found that the major contribution to the impedance change of the thorax was the volume change induced by the pulsatile pump as opposed to the normal cardiac rhythm volume changes produced by the right ventricular ejection (fig. 4-7).

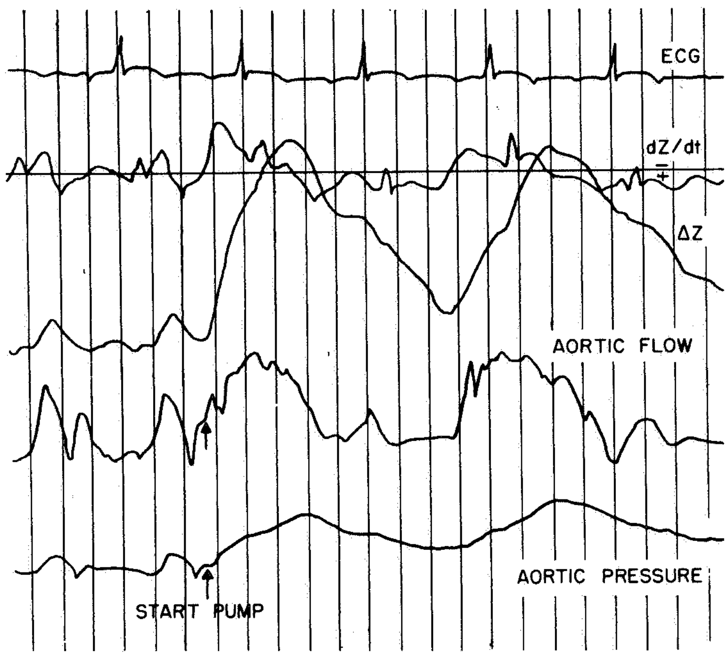

Fig. 4-7 Impedance response to left ventricular bypass with pulsatile pump

A modification of the pump experiment was carried out on one dog in which the heart was put into fibrillation to stop pulmonary circulation while the pump was allowed ro run, filling from a large blood reservoir. Thoracic impedance variations followed pump induced stroke volume changes in the aorta indicating that volume changes in the aorta could indeed produce thoracic impedance changes as monitored from the four band electrode configuration.

Further interesting results were obtained when the fluid pumped into the fibrillating dog was changed to 1/2 normal saline and then to tap water while keeping the rate and stroke volume of the pump constant. Considering as a reference the amplitude of impedance variations occurring with the profusion of blood the following observations were noted. Impedance amplitudes for the volume changes of 1/2 normal saline were approximately equal to the impedance amplitudes noted when blood was profused in the aorta. Profusion with tap water produced an increase in impedance during systole as opposed to the decrease in impedance during systole with blood and saline. The magnitude of the increase in impedance with systole for water profusion was considerably smaller than that for the changes in impedance occurring with profusion of blood or saline. These results indicate that changes in the volume of a volume conductor are responsible for thoracic impedance variations rather than such phenomena as pressure changes on the electrode interface or motion of the great heart or vessels. The fact that approximately the same amplitude impedance variations were obtained with 1/2 normal saline as compared to that with whole blood would indicate that the thoracic impedance variations were again due to changes of impedance with flow since the electrical properties of red blood cells was not contained in the half normal saline.

In conclusion the data indicate that the impedance variations observed with the four band electrode configuration have an intrathoracic systemic circulatory origin, and that the impedance variations may be due to changes in the aortic volume.

REFERENCE

1. Kinnen, E., Kubicek, W. G., and Witsoe, D.: Thoracic Cage Impedance Measurements: Impedance Plethysmographic Determination of Cardiac Output (an Interpretive Study). Technical Documentary Report No. SAM-TDR-64-23, USAF School of Aerospace Medicine, Brooks Air Force Base, Texas, May 1964.

CHAPTER FIVE

APPLICATIONS OF THORACIC IMPEDANCE VARIATIONS DURING THE CARDIAC CYCLE

SECTION I. Relationships between Impedance Changes and: a) Aortic Flow Velocity b) Aortic Flow Acceleration

Summary -

It has been shown in the dog that changes of peak dZ/dt and d^2Z/dt^2 reliably reflect changes in peak aortile flow (AF) and dF/dt under the experimental conditions described. The theoretical and practical implications of these findings have been discussed and further exploratory work proposed.

Introduction -

Following the demonstration of the relationship between ΔZ and left-sided hemodynamic events (Chap. 4) and the strong suggestion that ΔZ most probably resulted from thoracic aortic volume changes, the question arose as to whether there was any quantitative relationship between impedance events and aortic hemodynamic events.

It was hypothesized on the basis of the evidence that ΔZ was the electrical analog of continuous volume changes (ΔV) of a segment of the thoracic aorta. ΔV at any instant, for a segment of aorta, can be considered to be the difference between inflow to the given segment and outflow from the segment. During the early part of systole when aortic volume is increasing rapidly and ΔZ is decreasing rapidly, the most important influence on ΔV is obviously inflow to the aortic segment. Since inflow to the thoracic aorta can be continuously determined by means of the electromagnetic flowmeter, it therefore seemed logical to attempt to relate this hemodynamic parameter to the impedance events. Aortic inflow or the pattern of the ventricular ejection pulse is however a velocity phenomenon not a volume phenomenon, in a mathematical sense, so it therefore seems reasonable to compare the first time derivative of impedance dZ/dt (which would also by analogy represent a velocity phenomena) to aortic inflow velocity. Through similar reasoning it was decided to also compare the second time derivative of impedance d^2Z/dt^2 with the first time derivative of aortic flow velocity dF/dt (aortic acceleration). The question asked was whether the electrical events bore any quantitative relationship to the hemodynamic events.

Materials and Methods -

Twenty kg mongrel dogs were anesthetized with Pentobarbital (30 mg/kg), ventilated with a positive pressure respirator, and subjected to left thoracotomy at which time an electromagnetic flowmeter probe (Biotronex Model 410) of the appropriate size was placed about the ascending aorta, and pacemaker electrodes were sewn into the right or left atrial appendage. The thoracotomy wound was then closed and all air was evacuated from the thorax. Aortic flow velocity (AF) and its first time derivative dF/dt (obtained by continuous electronic differentiation) were recorded. ΔZ, dZ/dt, and d^2Z/dt^2 were also recorded in the usual fashion. The atria were stimulated with paired pulse pacemaker (Medtronic Model 5837) so that the heart rate could in most instances be varied between 60 and 150 beats per minute. The aforementioned parameters were recorded during periods of end expiratory apnea at each heart rate level. Peak AF in liters per minute was measured and plotted against peak dZ/dt in ohms per second. Peak dF/dt was measured in arbitrary units and plotted against peak d^2Z/dt^2 in ohms per second^2. The main effect of raising the heart rate by the pacing was to cause the stroke volume, peak aortic flow velocity and peak aortic acceleration to decrease. Thus a wide range of peak AF and dF/dt was achieved.

Results -

Fig. 5-1 shows the results of one experiment in which peak AF was plotted against peak dZ/dt. A least squares

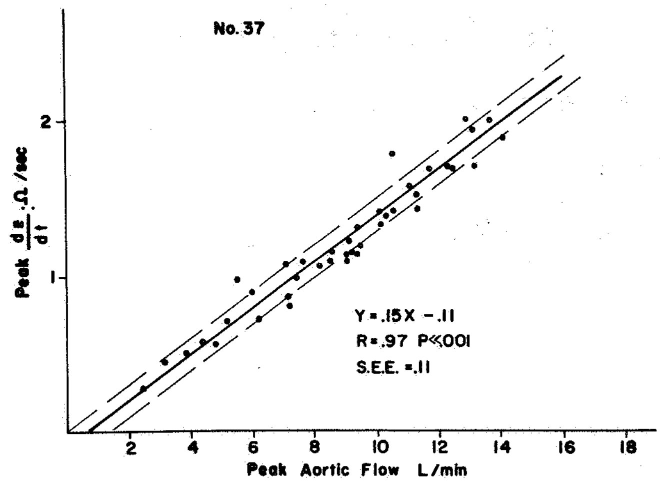

Fig. 5-1 Comparison of peak dZ/dt with peak ascending aorta flow; range obtained by pacing heart

fit (L.S.F.) line was drawn for each plot and the standard error of the estimate noted. As can be seen there is a good linear relationship between the two variables, and a relatively small degree of scatter. Fig. 5-2 shows a

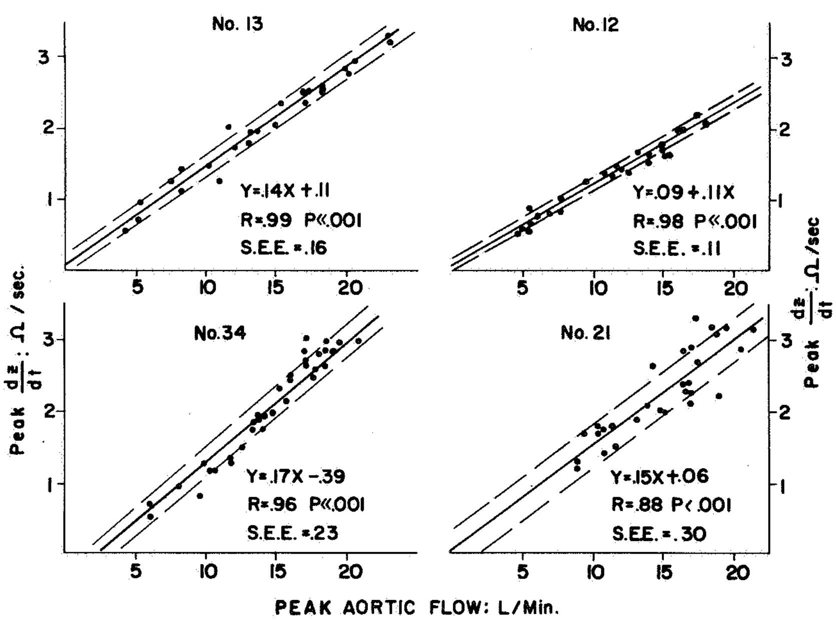

Fig. 5-2 Comparison of peak dZ/dt with peak ascending aorta flow, four dogs

composite of 4 such experiments (twelve were performed) and shows similar results to those found in fig. 5-1. However it can be noted that there is variation of the slope of the L.S.F. line from experiment to experiment. This point is important and will be discussed in some detail below.

Fig. 5-3 shows a plot of peak dF/dt (in arbitrary units) against peak d^2Z/dt^2. Again a striking linear relationship can be

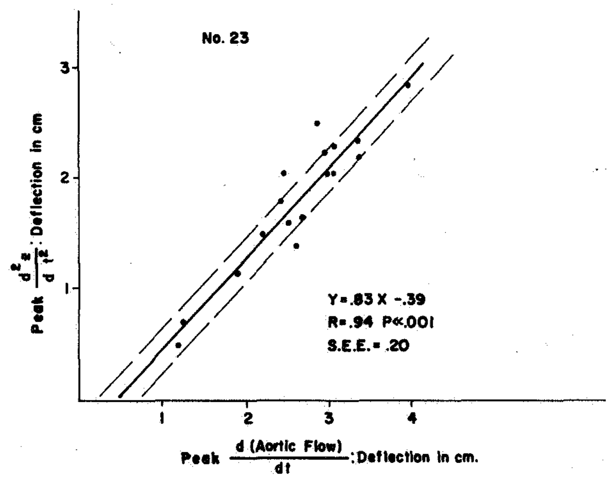

Fig. 5-3 Peak first derivative of ascending aorta flow vs. peak d^2Z/dt^2, range obtained by pacing

seen between the two variables. Fig. 5-4 shows a composite of four such experiments (seven were performed) and it has the same findings as found in fig. 5-3. Note however the increased scatter in these acceleration plots as compared to the velocity plots.

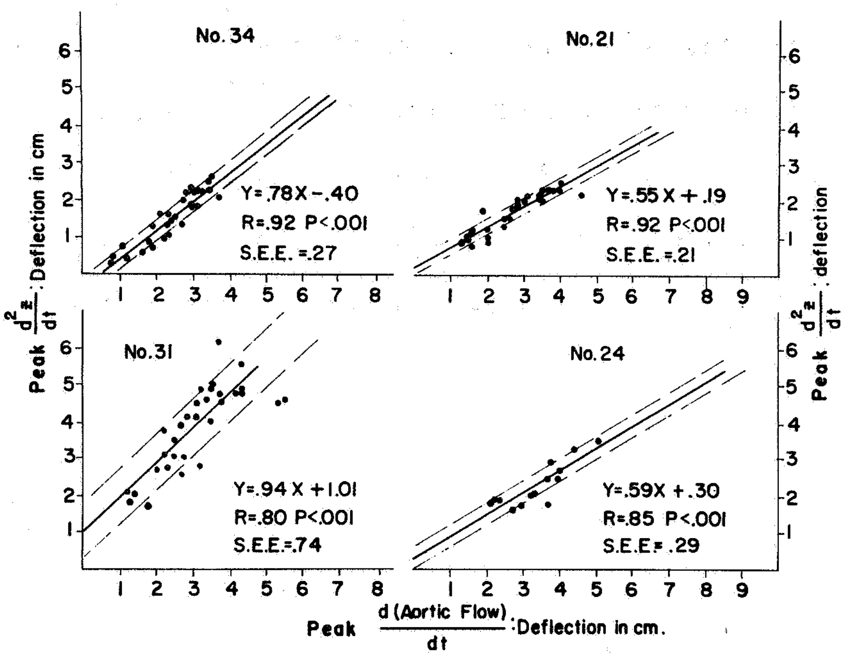

Fig. 5-4 Peak d(aortic flow)/dt vs. peak d^2Z/dt^2, four dogs

Discussion -

Recently Rushmer and his colleagues (1) have suggested that evaluation of what they term the "initial ventricular impulse" might yield valuable information about the level of function of the left ventricle. To substantiate this contention, Rushmer (2) and Noble (3) have published data which demonstrate that measurement of peak aortic flow velocity and acceleration in intact, awake dogs is useful in that changes in these parameters are sensitive indicators of changes in left ventricular contractility induced by drugs, exercise or ischemia. These workers have further suggested that such measurements might prove extremely useful in the clinical setting were they possible. Unfortunately the only methods available for making such determinations are catheterization techniques which are complex and require a level of technical competence which makes their widespread use unlikely.

The findings, reported here, suggest that changes in the peak magnitude of dZ/dt and d^2Z/dt^2 reflect changes in peak AF and dF/dt in the experimental situation described. Therefore it is suggested that these measurements may be valuable in obtaining information about the initial ventricular impulse in intact humans and animals.

However there are still several unanswered questions about the interpretation of the results which must be discussed and at the present time remain unanswered.

The first question concerns the general applicability of the method to other circulatory situations than the one described. It can fairly be asked whether the electrical impedance parameters, under circumstances when the peripheral resistance and stroke volume are changing rapidly (such as in exercise), will adequately reflect changes in the hemodynamics variables. This question has not been answered yet, but hopefully soon will be answered. This point is clearly of importance in determining whether the current results are accepted on empirical grounds, or on the basis of our hypothesis.

The next unanswered question is that of the cause of the variability of the slopes of the LSF lines in the velocity experiments. This question cannot be explored in the acceleration experiments unless real units are used for dF/dt. If the hypothesis concerning the origin of ΔZ is correct, then it can be assumed that any factor causing a variation in the capacitance of the aorta would cause a variation in the amount of blood stored in the aorta at any instant as compared to the amount that flows rapidly on. This variation in capacitance would also vary the absolute rates of storage, and therefore could give a constant bias to each experiment resulting in the aforementioned slope variation.

Another factor which could be of significance could be variation in resistivity of the blood from animal to animal. This factor was not evaluated.

The importance of this slope variation is that it precludes the use of the method for anything more than noting relative changes in the parameters in a given animal or man. Because of the inconstant slope, it is impossible to compare resting values of dZ/dt or d^2Z/dt^2 from subject to subject, or to assign a real hemodynamic value to any electrical impedance value. This does not obviate the potential usefulness of the technic since the determination of relative changes is extremely valuable as pointed out above.

The last question to be discussed is that of whether the observations described above further our understanding of the origin and mechanism of the thoracic electrical impedance waveform. Although the experimental findings are consistent with the hypothesis presented previously, they do not prove it conclusively. To further explore the relationship of the impedance derivative to aortic mechanics will require experiments in which instantaneous changes in aortic dimensions and aortic pressures at various levels (such as done by Patel and others (4) are correlated with the impedance changes. The time delays in the various transducer system will be critical as will the frequency responses of these systems. However this sort of experimental correlation may answer some of the basic questions about aortic mechanics and the relationship of the impedance waveform to them that are otherwise unanswerable.

REFERENCES

1. Rushmer, R. F.: Initial Ventricular Impulse, A Potential Key to Cardiac Evaluation, Circulation 29:268, 1964.

2. Rushmer, R. F., Watson, N., Harding, D., Baker, D.: Effects of Acute Coronary Occlusion on Performance on the Right and Left Ventricles in Intact Unanesthetized Dogs, Am. Heart J. 66:522, 1963.

3. Noble, M.I.M., Trenchard, D., Guz, A.: Left Ventricular Ejection in Conscious Dogs: 1. Measurement and Significance of the Maximum Acceleration of Blood from the Left Ventricle. Circ. Res. 19:139, 1966.

4. Patel, D. J., Mallos, A. J., Fry, D. L.: Aortic Mechanics in the Living Dog, J Appl Physiol 16:293, 1961.

SECTION II. Thoracic Impedance Change Indications of Ventricular Electromechanical Delay and Myocardial Contractility During Rest and Exercise

Summary -

The data obtained in this study indicate that changes in the time interval between the R spike of the ECG and the onset of the ΔZ waveform interval reflect primarily changes in the duration of the isometric period of ventricular contraction, and changes in peak (dZ/dt) and (d^2Z/dt^2) reflect changes in peak aortic flow velocity and acceleration. The electrical measurements obtained were consistent with the known physiological alterations occurring during the experimental period in normal man.

Introduction -

The use of the thoracic impedance technique as a potential indicator of left ventricular function has been explored in the past relative to the measurement of cardiac output (Chap 1). However, the relationship between the electrical events of the heart (as registered by means of the electrocardiograph) and mechanical cardiovascular events (as registered by the impedance technique) have not been examined. In the following study such an effort was made.

Methods -

Thoracic impedance changes (ΔZ) and the time derivatives of impedance (dZ/dt and d^2Z/dt^2) were determined in the usual fashion on five normal human volunteers, all of whom were in their early to mid twenties. Simultaneous electrocardiograph records were obtained. Measurements were made during four consecutive periods of the experiment: a) during supine rest, b) after five minutes of 45° feet-down tilt on a standard tilt table, c) after five minutes of rest in a sitting position on a bicycle ergometer and d) during a period of exercise after the subject had been pedaling for five minutes on the bicycle ergometer at 60 cycles a minute so as to do work at the rate of 100 watts per minute. During each period the (a) heart rate, (b) time between the peak of the R wave of the ECG and the beginning of the up stroke of ΔZ, as determined by the first zero crossing of dZ/dt, (c) peak magnitude of dZ/dt, (d) and the peak magnitude of d^2Z/dt^2 were measured.

Results -

The results are summarized in figs. 5-5 through 5-8. It can be seen that the R spike to ΔZ interval increased over the control values during the tilt period and the sitting rest and then decreased sharply during the exercise period. Peak (dZ/dt) and (d^2Z/dt^2) changed little during tilt and sitting rest but increased sharply in magnitude during the period of exercise.

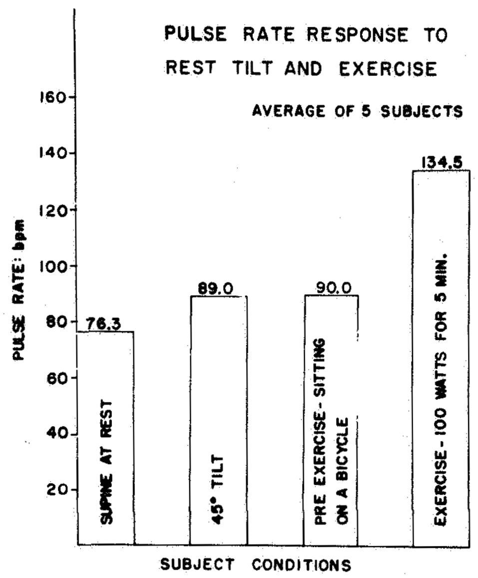

Fig. 5-5

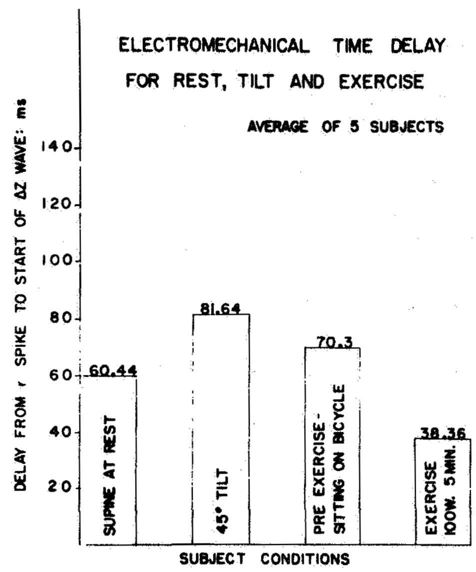

Fig. 5-6

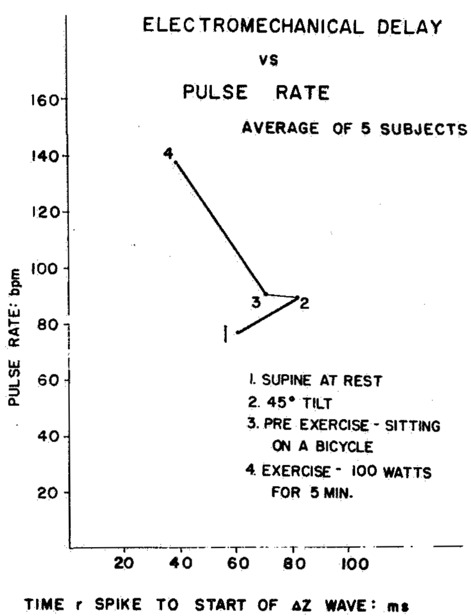

Fig. 5-7

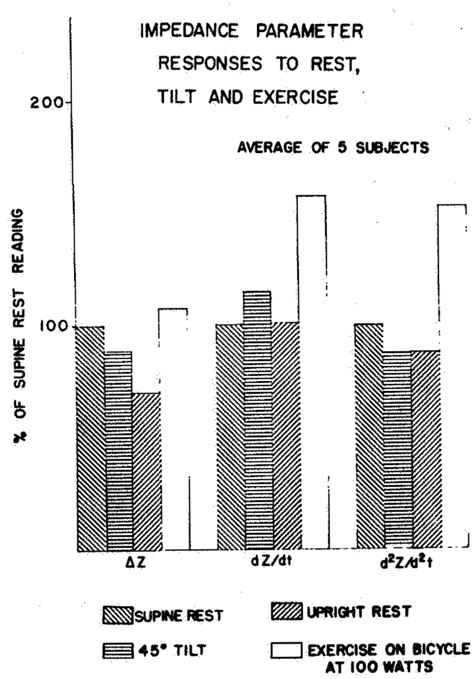

Fig. 5-8

Discussion -

As noted previously in this report, cardiogenic oscillations of thoracic impedance are assumed to be due primarily to changes in the volume of the thoracic aorta (Chap. 4). It would then appear likely that the rate of these volume changes reflects the rate of ventricular ejection. It would also seem likely on the basis of experimental work performed by others (1,2) that the onset of ejection relative to the onset of electrical activity in the myocardium is also related to the vigor of contraction. Thus, a heart with a high degree of contractility, whatever the mechanism, would be expected to have a shorter electromechanical interval and to eject blood more rapidly (1,2,3,4).

The electromechanical interval as measured in these experiments should reflect changes in both the isometric contraction period, and the initial rate of injection of blood. Since we are measuring from an electrical impedance event rather than from the beginning of the first heart sound, the R-ΔZ interval would also reflect, in part, the true electromechanical interval. There is, however, little evidence to show that the true electromechanical interval, i.e. the time from some point on the electrocardiogram to the beginning of the isometric contraction period, varies much under physiological conditions in the absence of conduction defects (2). It can therefore be assumed with some confidence that changes in the R-ΔZ interval reflects primarily changes in the isometric period of contraction.

Under controlled experimental conditions in the dog (1) it has been shown that the isometric period decreases with increasing stroke volume, increasing heart rate, and with ionotropic stimulation of the heart such as digitalis or catacholamines. The isometric period has been shown to increase (2) with increased mean aortic pressure when other variables are held constant.

Under the experimental conditions described above,the stroke volume is known to vary in the first three phases, -- supine, sitting rest, and tilting in a progressively decreasing direction; and in the light of the above discussion, the R-ΔZ interval would be expected to progressively increase as it did.

During exercise, however, other factors also come into play. Not only does the stroke volume increase significantly during sitting exercise, but there is also an increase in heart rate and catacholamine stimulation of the heart, all three factors which tend to shorten the isometric period, and such was noted in these data.

To summarize, this phase of the experiment suggested that there was an inverse relationship between the duration of the R-ΔZ interval and cardiac contractility. Furthermore the duration of the R-ΔZ interval was comparable to similar intervals determined by other investigators using the phonocardiogram and externally monitored carotid pulse wave (2).

The alterations of dZ/dt and d^2Z/dt^2 were also consistent with the known physiological changes occurring during the experimental periods (3,4). It is known that peak aortic flow velocity and acceleration increase with increasing stroke volume and ionotropic stimulation of the heart (3,4). It would be expected that if peak (dZ/dt) and (d^2Z/dt^2) reflect changes in the peak velocity and acceleration of aortic blood flow, then they should vary appropriately with the experimental manipulations, as indicated by the data shown in fig. 5-8. The rise in magnitude of the derivatives during exercise may therefore give a measure of the increase in contractility of the myocardium that occurred during this period.

REFERENCES

1. Wallace, A. G., Mitchell, J. H., Skinner, S. W. and Sarnoff, J. J.: Duration of phases of Left Ventricular Systole, Circulation Research 12:611, 1963.

2. Frank, M. N., and Kinlaw, W. B.: Indirect Measurement of Isovolumetric Contraction Time and Tension Period in Normal Subjects, American Journal of Cardiology 10:800, 1962.

3. Rushmer, R. F.: Initial Ventricular Impulse, A Potential Key to Cardiac Evaluation, Circulation 29:268, 1964.

4. Noble, M.I.M., Trenchard, D. and Guz, A.: Left Ventricular Ejection in Conscious Dogs: 1. Measurement and Significance of the Maximum Acceleration of Blood from the Left Ventricle. Circulation Research 19:139, 1966.

SECTION III. Investigation into the Use of Thoracic Impedance Techniques to Monitor Changes in Total Pulmonary Blood Volume

Summary -

Animal experiments have been carried out to assess the possibility of measuring shifts in mean pulmonary blood volume by monitoring changes in the total intrathoracic impedance Z_o between band electrodes around the neck and abdomen. Left ventricular output was controlled in anesthetized dogs by a balloon catheter in the left atrium and pulsatile blood volume input into the pulmonary circulation was monitored by an electromagnetic flowprobe placed around the main pulmonary artery. Results indicated that it is not feasible to monitor separately by impedance plethysmographic techniques the blood volume changes of the pulmonary-vascular bed since the Z_o signal apparently represents changes in total thoracic blood volume.

Introduction -

Early investigations into the origin of intrathoracic impedance variations (monitored by a four-band electrode configuration) had suggested that the major concentration of excitation current into the thorax would probably be found in the lungs (1). Based on these and other related observations the prevailing hypothesis was that the impedance variations seen across the chest were due to temporal changes in pulmonary blood volume. Decreases in the total impedance, Z_o, of the thorax were also observed with postural changes from upright to supine suggesting that changes in Z_o might represent changes in total pulmonary blood volume. A series of animal experiments was carried out to evaluate the probability of monitoring pulmonary blood volume shifts by measuring changes in Z_o. Results indicate that it is not feasible to separate intra and extra pulmonary blood volume change components contained in the Z_o signal.

Methods and Results -

Electromagnetic flowmeter probes were acutely placed about the main pulmonary artery and the ascending aorta of anethetized dogs. A balloon catheter was also placed in the left atrium as described in Chapter Four. It was assumed that when the left atrial balloon was inflated for a relatively short period of time blood would continue to be pumped into the lungs by the right ventricle and the venous return to the right side of the circulation would continue. It appeared possible that this experimental situation might allow the measurement of shifts of blood into the pulmonary circulation from the systemic circulation by the impedance technique and could be compared with the quantitative values obtained from the pulmonary artery flow probe.

The results of these experiments show that the thoracic impedance tended to increase following balloon inflation in the left atrium, suggesting that shifts of blood out of the thorax, as the blood left the left ventricle, aorta, and thoracic wall vessels, were more effective in changing thoracic impedance than the presumed inflow of blood which continued into the lungs and right heart and great veins. The data indicate that the value Z_o is a function of multiple factors and that blood volume changes in the pulmonary vascular bed probably cannot be separately determined.

Discussion

The basis for this experiment was planned around a hypothesis that the primary impedance waveforms reflected primarily changes in pulmonary vascular blood volume. Subsequent work, Chapter Four, has indicated that this initial hypothesis was incorrect and that the impedance variation observed across the chest originates from changes in systemic circulation and its primary determinant is most probably aortic volume change. However the total impedance, or Z_o of the thorax, should reflect changes in the total volume of blood contained between the sampling electrodes. Therefore changes in Z_o in a decreasing direction should indicate increasing blood volume within the thorax. Unfortunately, however, as indicated the electrodes do not only see the pulmonary circulation but also the entire thoracic systemic circulation including the thoracic wall and great vessel blood volumes. This being the case, Z_o may indicate shifts in blood volume in and out of the thorax but partition of such blood volumes into intra and extra pulmonary components is not feasible.

Another problem in estimating pulmonary blood volume changes arises in that Z_o is also strongly influenced by the state of the inflation of the lungs and the height of the diaphragm with the greater lung inflation being associated with the higher impedance. Respiratory shifts in the impedance magnitude are so great relative to the blood volume induced changes in impedance that they completely dwarf the latter. Although ΔZ, the pulsatile thoracic impedance change, tends to retain a relatively constant magnitude at several levels of lung inflation and therefore its determination during expiratory apnea is not critically affected by the lung volume change, the magnitude of Z_o is affected. For this reason transient changes in blood volume of the thorax would have to be studied during the period of one expiratory condition or exact changes in the lung volume would have to be monitored and controlled during such determinations.

Should there be an interest in pursuing the problem of qualitatively or semi-quantitatively assessing shifts of blood into the thorax from the body as opposed to into the pulmonary circulation, and if some effort were made to keep the lung volume constant from determination to determination, the technique might be feasible for making such measurements.

REFERENCE

1. Kinnen, E., Kubicek, W. G., and Witsoe, D.: Thoracic Cage Impedance Measurements: Impedance Plethysmographic Determination of Cardiac Output (an Interpretive Study). Technical Documentary Report No. SAM-TDR-64-23, USAF School of Aerospace Medicine, Brooks Air Force Base, Texas, May 1964.

SECTION IV Simultaneous Monitoring of Respiration and Cardiac Output with a Single Impedance Measuring System

Summary -

An electrode configuration has been found which will allow simultaneous monitoring of impedance cardiac output and respiration rate from one electronic system. The cardiac output four band configuration has remained unmodified while a single ECG spot electrode has been added on the left mid axillary line at the nipple level to obtain respiration signals. The cardiac output-respiration rate system requires only the thoracic 100 kHz current excitation from the original impedance cardiograph system. The cardiac output signal is obtained in the usual manner from band electrodes 2 and 3 while the respiration rate signal can be obtained from the impedance changes occurring between the spot electrode and band 3 with sensing electronics identical to the cardiac output system.

A 10 percent change in the static impedance between the spot electrode and band 3 has been noted for a one liter volume inspiration. The residual cardiogenic impedance change between band 3 and the spot electrode was found to be only 5 percent of the impedance change resulting from a one liter inspiration. Equivalent signals were found with thoracic and diaphragmatic inspiration of one liter and a linear relationship between inspired air volume and the respiration impedance change signal was noted for both thoracic and diaphragmatic breathing. The latter characteristic may allow monitoring

of tidal volumes during inflight conditions by calibration of the subject during preflight operations.

Introduction -

Impedance plethysmographic techniques for monitoring respiration rates have been used by the NASA (1) and others in the past and employ essentially the same basic hardware that is used in estimating cardiac output by impedance methods. It may be desirable to monitor both respiration rate and cardiac output simultaneously but existing methods would require two separate plethysmographs operating at different excitation frequencies and two separate electrode systems. The purpose of the pilot study described here was to determine the feasibility of obtaining both respiration rate and cardiac output data from a single electrode configuration using the thoracic current excitation of the cardiac output system. Since development of the electronics for such a system would only involve a modification of existing impedance cardiac output electronics, the major effort has been directed toward the establishment of an electrode system which would yield suitable signals for respiration rate while simultaneously monitoring cardiac output. Results indicate that a suitable respiration signal can be obtained over a wide range of tidal volumes by the addition of a single spot electrode to the four band electrode configuration (described in Chapter One, Section I) of the impedance cardiac output system.

Methods and Materials -

The following criteria were established as necessary for obtaining reliable and repeatable respiration rate and cardiac output signals when the thorax was excited by the 100 kHz cardiac output electrode system:

1. The electrode system for obtaining respiration rate should in no way affect the cardiac output measurements. Ideally respiration signals would be obtained from the cardiac output electrodes.
2. The percent thoracic impedance change due to respiration should be large enough to ensure the accurate monitoring of respiration rate with very shallow breathing. This was a problem of electrode placement not simply amplifying a small signal.
3. The respiration signal should be reliable for both abdominal and thoracic breathing patterns.

The first approach taken in this study was to determine if acceptable thoracic impedance changes due to respiration could be obtained from the signal sensing bands of the four band cardiac output electrodes. If suitable signals could not be obtained from the cardiac output signal sensing electrodes a modification of this configuration consisting of one additional spot electrode would be examined. The spot electrode was selected since any large surface area electrode would produce an equal potential surface on the thorax of sufficient area to alter cardiac output measurements. The type of spot electrode selected for this study was that which was employed by the NASA to monitor the electrocardiogram under inflight conditions.

Results and Discussion -

Observations of the respiration signal obtained from the four band cardiac output electrodes indicated that the major impedance change seen with this electrode system was due to the cardiac signal when the subject was at rest or taking shallow breaths. Typical tracings are shown in fig. 5-9a. The respiration signal has a period of approximately 4 seconds but the cardiac signal superimposed upon the slower respiration signal makes it difficult to evaluate the latter since there is only a factor of two difference in amplitude.

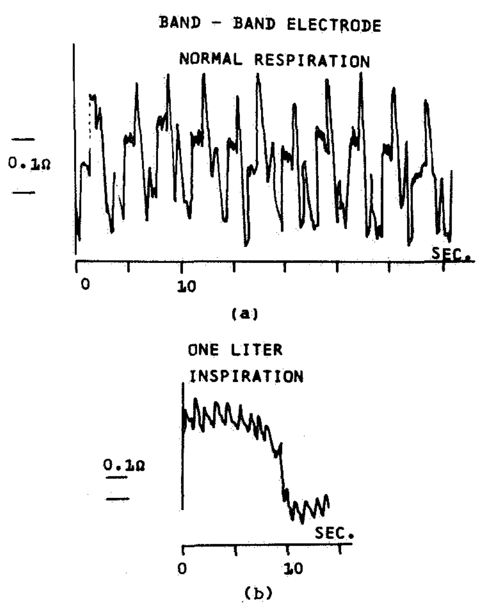

Fig. 5-9 Respiration signals from impedance cardiac output electrode bands 2 to 3

Attempts to filter out a signal due to respiration indicated that such a filtering technique would not be satisfactory since there is an overlap of frequency components of the respiration and cardiac signals. With the filter passing only frequencies well below the fundamental cardiac frequency, the impedance respiration signal was not reliable for rapid breathing rates. Fig. 5-9b shows the results when the subject inspired one liter of air. It can be seen that the respiration signal contains a significant ripple due to the cardiogenic impedance changes.

Since it was apparent that acceptable respiration signals could not be obtained from the cardiac signal sensing electrodes, the spot electrode configuration was explored. The spot electrode was placed on the mid-axillary line at the nipple level and the thoracic impedance changes were monitored between the spot electrode and band electrode 3. Fig. 5-10 is typical of the respiration signal obtained from the spot electrode to band 3 when the spot electrode was placed on the left side under the arm at the level of the nipple. Basic impedance between the spot electrode and band 3 was 4.7 ohms and .1 ohm steps are indicated on the record. Similar results (fig. 5-11) were observed when the spot electrode was placed on the right side under the arm at the nipple level. The percent change in impedance between the electrodes was approximately 10 percent for one liter air volume intake; a typical value was .5 ohm change out of a total impedance of 5 ohms for one liter air intake. The impedance change signal for the spot to band electrode configuration was primarily due to respiration and was characterized by about a 5 percent ripple due to the cardiac cycle for an impedance change corresponding to one liter air intake.

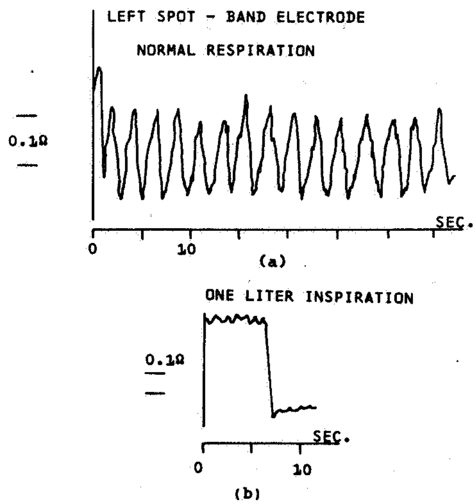

Fig. 5-10 Respiration signals from spot electrode on left mid-axillary line at nipple level to band 3

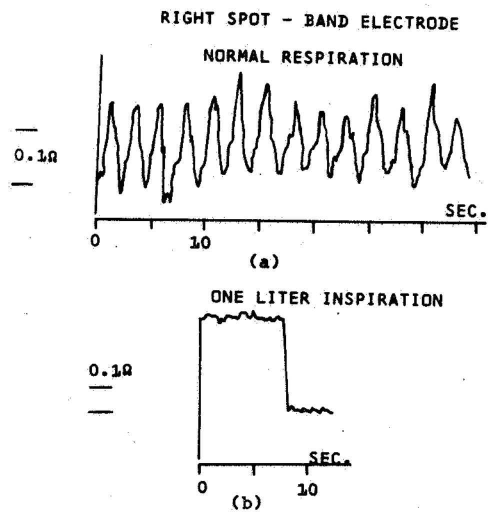

Fig. 5-11 Respiration signal from spot electrode on right mid-axillary line at nipple level to band 3

Measurement values using the spot-band electrode configuration were repeatable on a given subject and were approximately the same magnitude for two different subjects. Very little signal difference was noted when a subject breathed abdominally or thoracically. Fig. 5-12 shows the difference between a diaphragmatic breath of one liter of air and a thoracic breath of one liter of air.

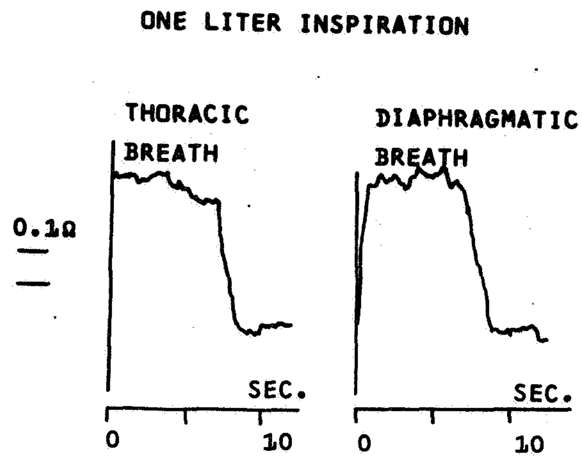

Fig. 5-12 Comparison of thoracic and diaphragmatic breath, left spot to band 3

One additional characteristic of the spot to band respiration impedance signal that may provide a basis for future investigation is that the amplitude of the impedance change noted between the spot electrode and band 3 appeared to be linearily related to inspired air volume. Although there are limited data, the possibility of calibrating the impedance signal with inspired air volume to give tidal volume values does exist. High precision probably could not be achieved but for some purposes recording of tidal volume under these circumstances may be of value. For example, during periods of anxiety or other stress this system probably could detect dangerous hyperventilation. Fig. 5-13 shows the relationship between inspired air volume and impedance measured between the spot electrode and band 3. This record was obtained by

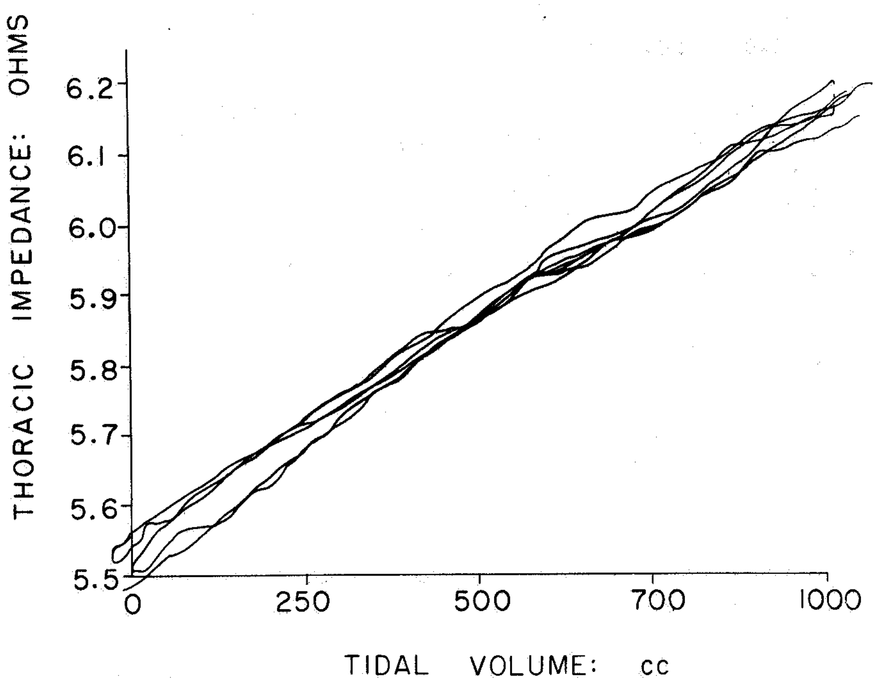

Fig. 5-13 Continuous respiration, left spot to band 3

plotting the output of the plethysmograph against the output of a Wedge Spirometer, (Med Science Inc.), on an XY plotter. The graph shows continuous inspiration and expiration over several respiratory cycles. Similar results were obtained when diaphragmatic breathing was compared with thoracic breathing in that they both indicated a linear relationship between inspired volume and impedance change. Linear relationships between transthoracic impedance and inspired air volume have been reported by other investigators. Hamilton, Beard and Kory (2) have shown a linear relationship using

6.25 x 1.25 cm electrodes placed on each mid-axillary line and coupled to a two electrode impedance plethysmograph. Although linear relationships were obtained with their electrode configurations it is felt that the spot electrode configuration has the distinct advantage of being less cumbersome since the band electrode does not inhibit motion by the subject and the spot electrode definitely does not interfere with the subject's motions.

REFERENCES

1. Experiment M-3 Inflight Exerciser on Gemini IV, NASA Proceedings of the Manned Space Flight Experiment Symposium Gemini Missions III and IV, Washington, D. C., October 18 and 19, 1965.

2. Hamilton, L. H., Beard, K. D., Kory, R. C.: Impedance measurements of tidal volume and ventilation. J Appl Physiol 20:565-568, 1965.

CHAPTER SIX

THE RESPONSE TO 70° PASSIVE TILT IN NORMAL HUMAN SUBJECTS USING IMPEDANCE PLETHYSMOGRAPHIC TECHNIQUES FOR MONITORING CARDIAC OUTPUT CHANGES

Summary -

A study was undertaken to evaluate the usefulness of the impedance plethysmographic method to measure cardiac output during 70° upright tilt. The experiment was performed using a protocol similar to the one the NASA uses in the evaluation of the cardiovascular system of the astronauts. Along with the cardiac output and stroke volume measured by impedance plethysmography, the blood pressure and pulse rate were recorded. Total peripheral resistance was calculated from the blood pressure and cardiac output values. The study was conducted on ten normal males without the use of any intravascular instrumentation.

The results of these studies showed the response to tilt as follows:

1. An increase in pulse rate
2. An increase in diastolic blood pressure and a small decrease in systolic pressure
3. Cardiac output decreased except for a transient increase at about ten minutes of tilt.
4. Stroke volume decreased
5. Total peripheral resistance increased

The results of these studies compare favorably with the

results of other investigators using other methods for determining cardiac output. Therefore the impedance method appears to be a reliable means for measuring changes in cardiac output.

Methods -

A total of twelve paid volunteers, University of Minnesota students, participated in this study. They ranged in age from 17 to 23 years, in weight from 104 to 178 pounds and in height from 63 to 75 inches. All participants were, at the time of the experiment, in good health and in no instance was a past history of fainting, serious illness or serious injury reported.

Their responses were observed during a 20 minute, 70° upright tilt while suspended from the hips on a padded motorcycle seat mounted on a Preston tilt table. With one exception all experiments were done between 8:00 A.M. and 12:00 noon, three days in succession. The first day was an orientation while the last two days were experimental trials. All reported data were from the last two days with the exception of subject 3 where three trials are reported and in cases of syncope during the orientation run.

During orientation, the participant was familiarized with the apparatus and the tile procedure, personal adjustments for maximum seat comfort, safety belt position and tightness, and electrode position were made. On succeeding experiments all adjustments were repeated as nearly as possible.

In an attempt to standardize conditions several variables were eliminated. Room temperature was held constant at 74°±1°F. All unnecessary noise and talking was eliminated. Subjects were requested to get a good night's rest prior to the experiment and to refrain from a heavy breakfast, use of tobacco and coffee on the morning of the experiment. All subjects wore loose fitting scrub trousers during the experiment.

The protocol of each tilt was as follows:

Minute	Position	Record Number
0-1	Supine	1
5-6	"	2
6-25	"	Rest
25-26	"	3
30-31	tilt in progress	
31-32	70° tilt	4
36-37	"	5
41-42	"	6
46-47	"	7
50-51	"	8
51-52	tilt down in progress	
52-53	supine	9
57-58	"	10
62-63	"	11

At the beginning of each reading, a cardiac output determination was taken followed by a blood pressure reading. During tilt, subjects were asked to be as relaxed as possible and not to move their legs or to talk unless absolutely necessary.

All instrumentation used in the experiment was non-traumatic to the subject. Blood pressure was recorded by the ausculatory method using a standard clinical cuff with an aneroid gauge. Heart sounds were recorded throughout all readings using a Beckman phonotransducer taped externally near the left third intercostal space. Electrodes for relative cardiac output determinations were the standard conductive Velcro bands developed in this laboratory and coated with Translyte* electrode paste. (See Methods Chapter 1, Section I).

All data were recorded on a two channel Sanborn recorder model 296. Stroke volume and cardiac output were determined using the impedance plethysmograph method described in Chapter One. Heart rate was determined by measuring the distance between successive impedance waveforms on calibrated recording paper which was demonstrated to be running at a constant speed of 50 mm per second. Total peripheral resistance was calculated using the formula:

$$\text{T.P.R.} = \frac{[1/3\ (\text{syst. press} - \text{diast. press})] + \text{Diast. Press}}{\text{Cardiac Output}}$$

For purposes of graphing, all data except heart rate and blood pressure were normalized using the 26 minute reading as baseline (100%).

Results -

The following results refer to the mean changes observed on subjects during tilt.

*Medtronic Inc., Minneapolis, Minnesota

The mean heart rate showed an immediate increase of 8 beats per minute upon tilting followed by a progressive increase throughout tilt reaching a maximum of 19 beats per minute.

The most characteristic change in blood pressure was a progressive increase of diastolic pressure reaching a maximum of 20 mm Hg above baseline just prior to tilt down. Mean systolic pressure showed a slight decrease from baseline during tilt which remained fairly constant except for a slight rise just prior to tilt down.

Cardiac output tended to decrease upon tilt to about 70 percent of baseline and remained fairly constant until tilt down except for a transient increase at 10 minutes of tilt. Following tilt down it returned to slightly less than baseline values.

Stroke volume tended to decrease to about 65 percent of baseline immediately after tilt followed by a further progressive decrease reaching a maximum decrease of 50 percent prior to tilt down.

Total peripheral resistance increased to approximately 140 percent of baseline upon tilt and increased progressively to 180 percent before tilt down except for a transient decrease at the 10 minute reading.

Fig. 6-1 is the mean response of ten individuals completing a total of 19 tilts without syncopal reactions.

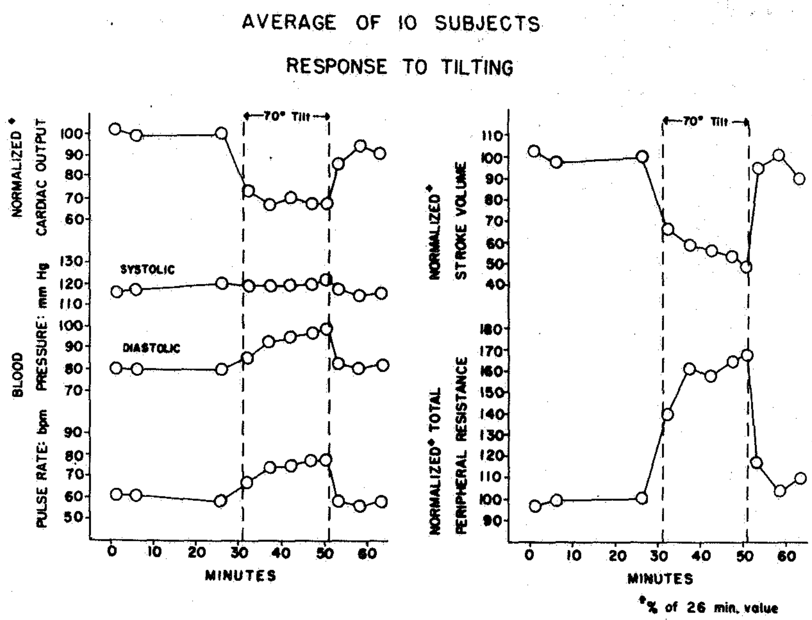

Fig. 6-1

The following graphs (figs. 6-2 to 6-11) illustrate the individual responses of ten subjects completing nineteen 70°, 20 minute tilt experiments without syncopal reactions. On all graphs the solid lines and X data points represent the first experimental run and the dashed lines and circle data points the second. The only exception to the above is subject number three who was unable to complete the second tilt due to syncopal symptoms.

SUBJECT NO. 1

RESPONSE TO TILTING

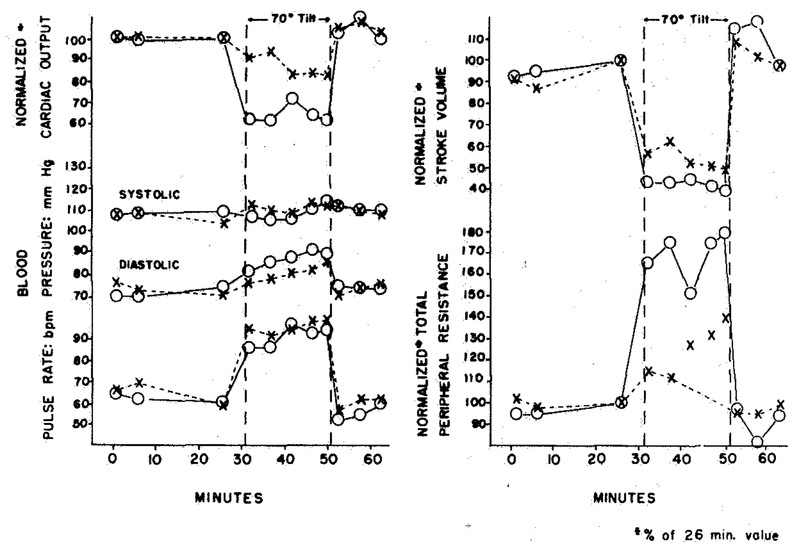

Fig. 6-2

SUBJECT No. 2

RESPONSE TO TILTING

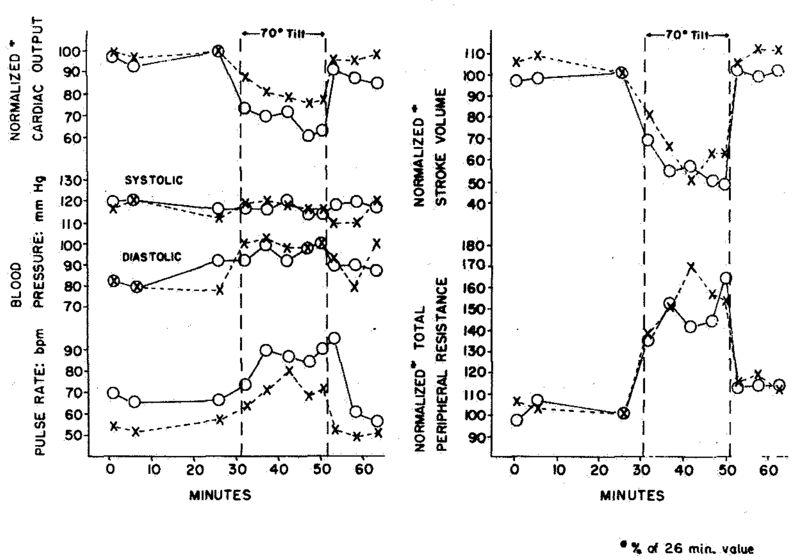

Fig. 6-3

SUBJECT NO. 3

RESPONSE TO TILTING

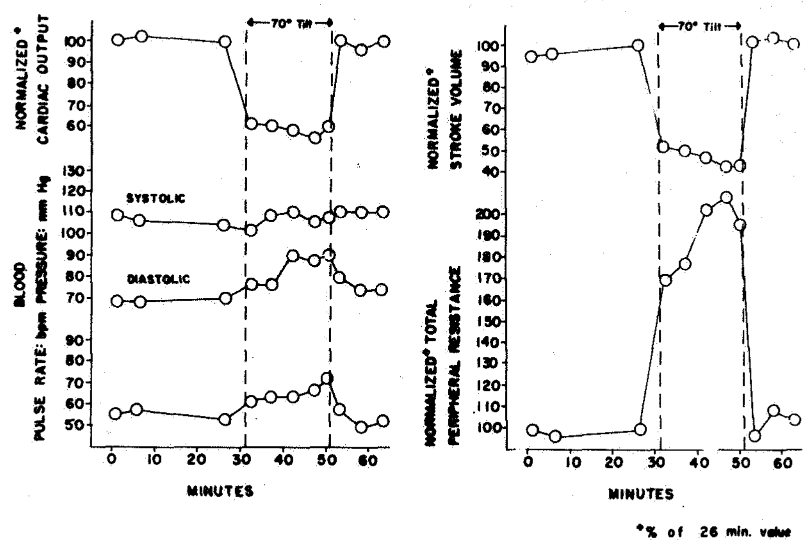

Fig. 6-4

SUBJECT NO. 4

RESPONSE TO TILTING

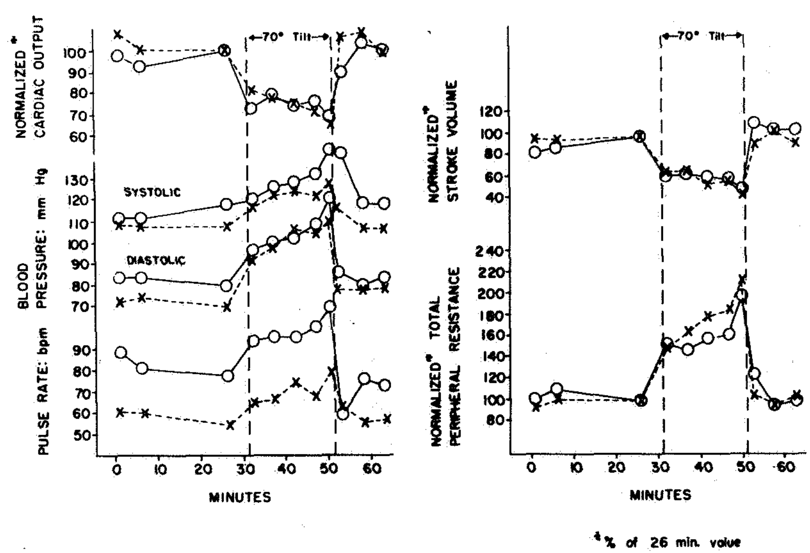

Fig. 6-5

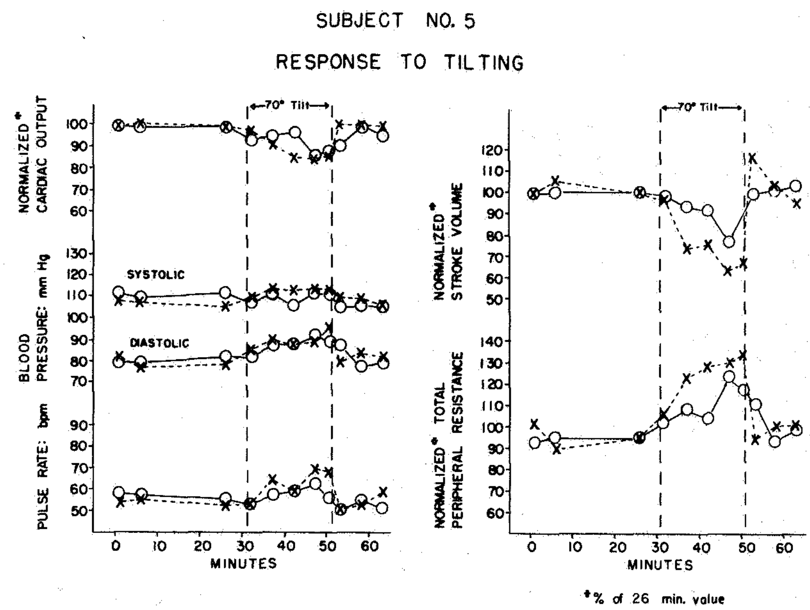
SUBJECT NO. 5
RESPONSE TO TILTING
70° Tilt
NORMALIZED* CARDIAC OUTPUT
BLOOD PRESSURE: mm Hg
SYSTOLIC
DIASTOLIC
PULSE RATE: bpm
MINUTES
NORMALIZED* STROKE VOLUME
NORMALIZED* TOTAL PERIPHERAL RESISTANCE
*% of 26 min. value

Fig. 6-6

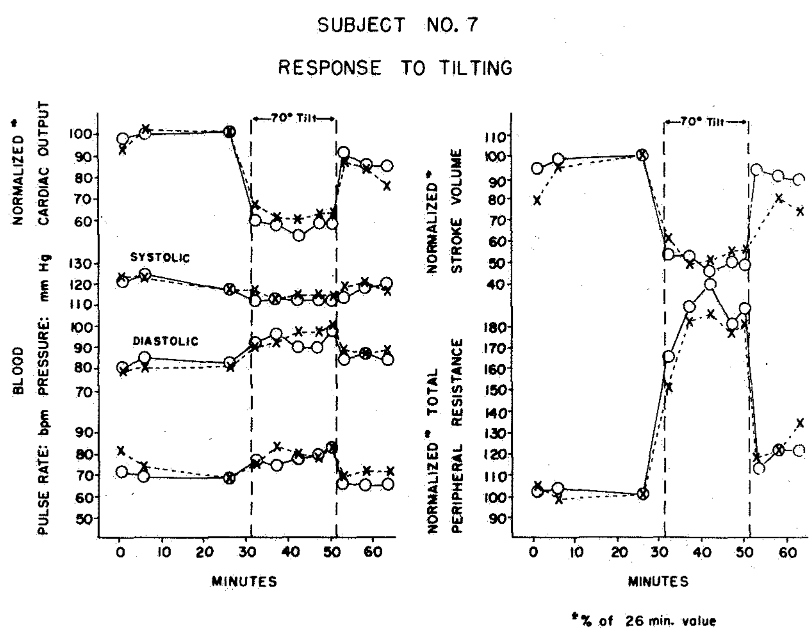
SUBJECT NO. 7
RESPONSE TO TILTING
70° Tilt
NORMALIZED* CARDIAC OUTPUT
BLOOD PRESSURE: mm Hg
SYSTOLIC
DIASTOLIC
PULSE RATE: bpm
MINUTES
NORMALIZED* STROKE VOLUME
NORMALIZED* TOTAL PERIPHERAL RESISTANCE
*% of 26 min. value

Fig. 6-7

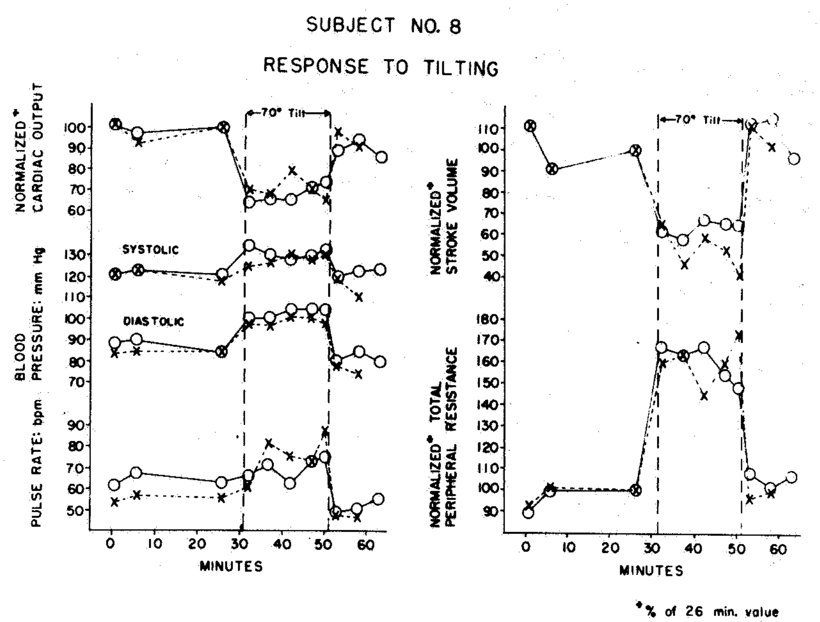
SUBJECT NO. 8
RESPONSE TO TILTING
70° Tilt
NORMALIZED* CARDIAC OUTPUT
SYSTOLIC
DIASTOLIC
BLOOD PRESSURE: mm Hg
PULSE RATE: bpm
MINUTES
NORMALIZED* STROKE VOLUME
NORMALIZED* TOTAL PERIPHERAL RESISTANCE
*% of 26 min. value

Fig. 6-8

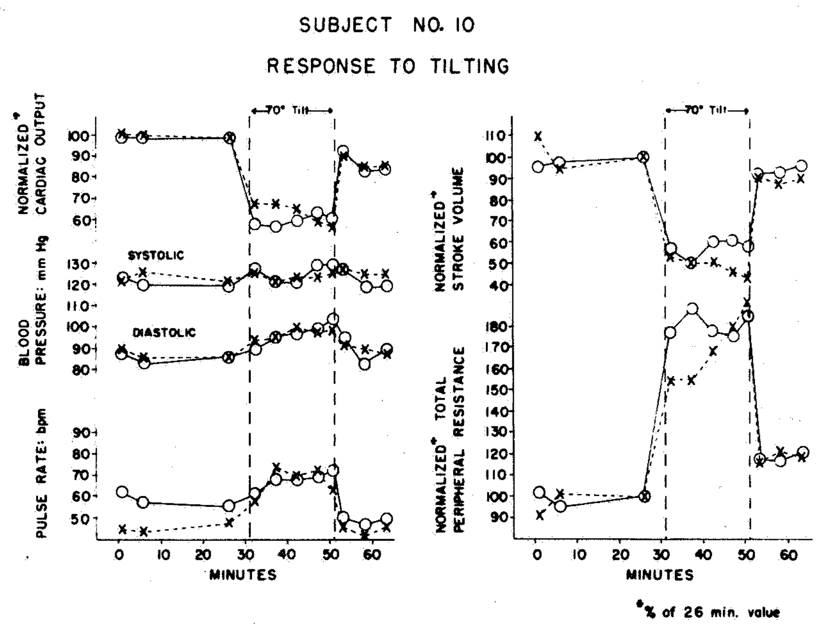
SUBJECT NO. 10
RESPONSE TO TILTING
70° Tilt
NORMALIZED* CARDIAC OUTPUT
SYSTOLIC
DIASTOLIC
BLOOD PRESSURE: mm Hg
PULSE RATE: bpm
MINUTES
NORMALIZED* STROKE VOLUME
NORMALIZED* TOTAL PERIPHERAL RESISTANCE
*% of 26 min. value

Fig. 6-9

SUBJECT NO. 11

RESPONSE TO TILTING

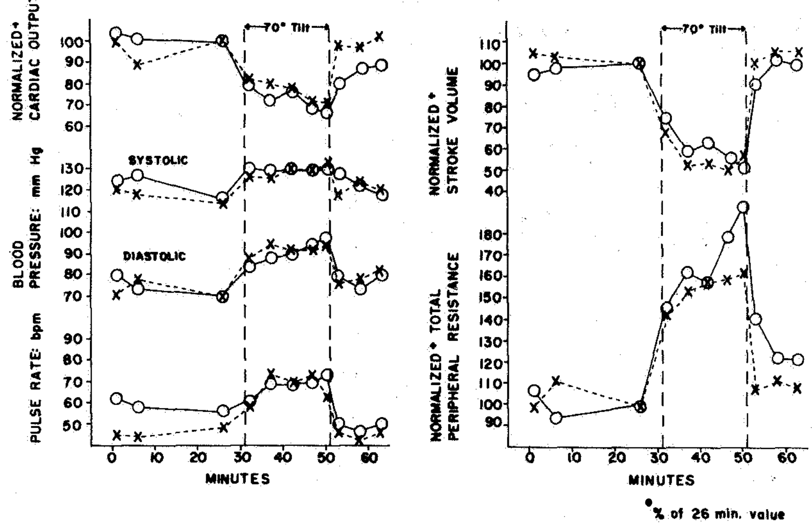

Fig. 6-10

SUBJECT NO. 12

RESPONSE TO TILTING

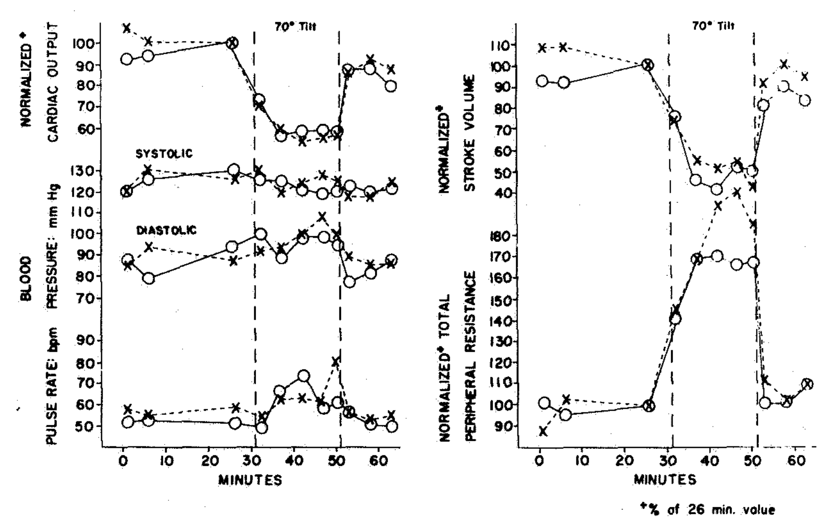

Fig. 6-11

With three of the participants, syncopal reactions to tilt were observed. At the onset of syncopal symptoms (pallor, sweating, nausea, and dizziness) recordings were taken followed by tilt down prior to actual syncope. The following explanations and graphs depict individuals who experienced the above reactions.

Fig. 6-12 illustrates two presyncopal responses of subject three. This subject had previously tolerated a complete 20 minute tilt (fig. 6-4). Due to scheduling problems both experimental runs that resulted in syncopal reactions took place at times other than the normal 8:00 a.m. to 12:00 noon time period set fourth in the protocol. The solid lines are plots of data obtained at 6:30 a.m. while the dashed lines are plots of data obtained at 1:30 p.m.

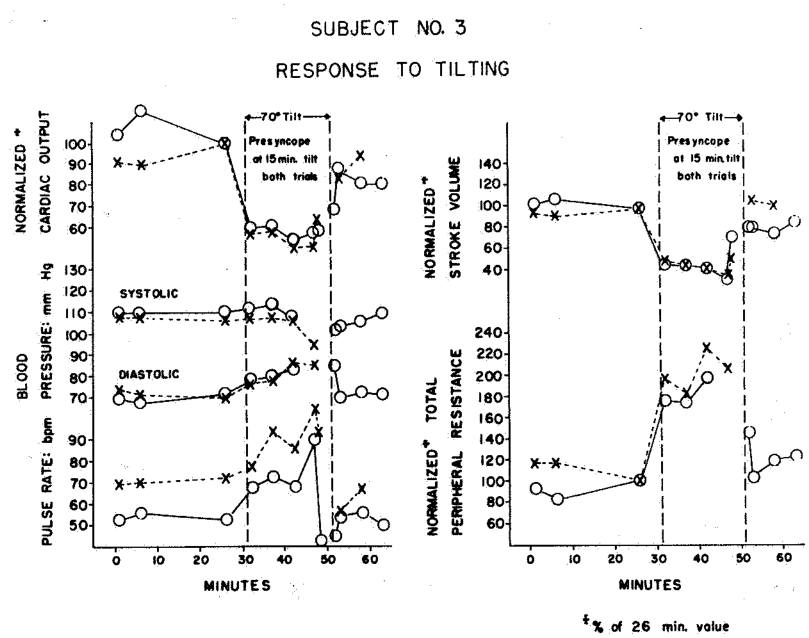

Fig. 6-12

To avoid a complete syncopal reaction during the 6:30 a.m. experiment, which at the time seemed imminent, blood pressure reading was omitted and tilt down began immediately after the 47 minute reading (15-16 minutes of tilt). The 47 minute reading showed a slight rise in cardiac output, a slight decrease in stroke volume, and a large increase in pulse rate. During tilt down further recordings were attempted as indicated on the graphs by circle data points at minute 48. Reference to those values show a slight increase in cardiac output, a marked increase in stroke volume, and a large decrease in heart rate. Following tilt down one extra reading was taken prior to the regular 53 minute reading. That reading indicated that the subject was beginning to assume the normal values of the supine position.

The second presyncopal reaction of subject three (dashed line on fig. 6-12) occurred at the 47 minute reading. Following the cardiac output recording and while his blood pressure was being taken, the subject first complained of presyncopal symptoms. The 47 minute reading showed a slight rise in cardiac output, a marked decrease in systolic blood pressure, a great increase in heart rate, a decrease in stroke volume, and a substantial decrease in total peripheral resistance. Prior to tilt down another reliable recording of cardiac output was obtained omitting only the blood pressure reading. This latter recording, indicated by X data points at minute 48, showed cardiac output and stroke volume to rise substantially while the pulse rate declined. Following tilt down the subject returned to normal supine values.

Fig. 6-13 depicts the syncopal reaction of subject six which occurred during his orientation run. Following the 37 minute recording (5-6 minutes tilt), syncopal symptoms were experienced. Prior to tilt down another recording at minute

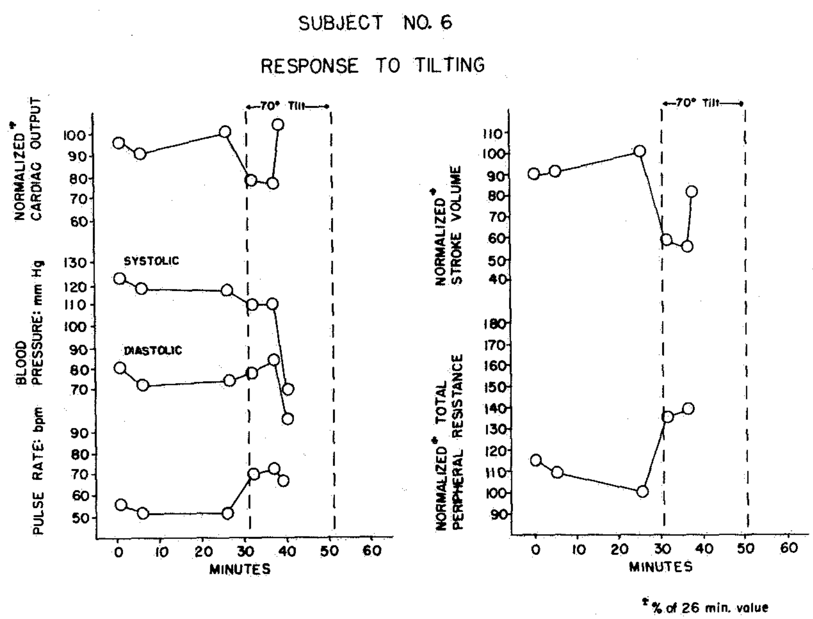

Fig. 6-13

38 was obtained. This final reading showed marked increases in cardiac output and stroke volume while pulse rate declined slightly. Furthermore, a large reduction of both systolic and diastolic blood pressure components was noted. The subject was then tilted down and the experiment was terminated

after normal supine values were reached. In our estimation, this subject appeared to be nearer actual syncope than any other subject.

Like subject six, subject nine showed early syncopal symptoms during his orientation; fig. 6-14 illustrates his response. Just before the 42 minute recording (10 minutes tilt) was to be taken, the subject complained of nausea and dizziness. The regular 42 minute ratings were taken followed

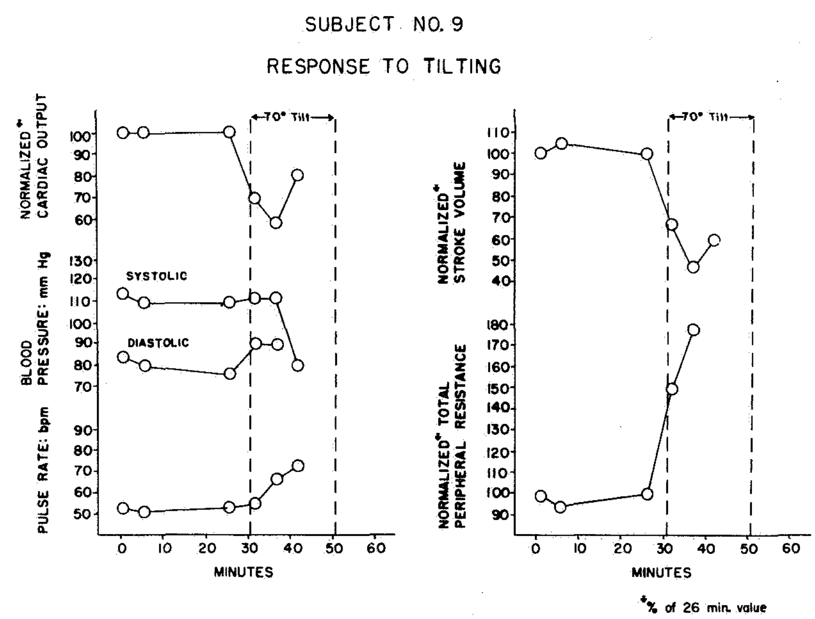

Fig. 6-14

by tilt down. At this reading cardiac output, stroke volume, and pulse rate all increased. Systolic blood pressure showed a marked decline while a diastolic reading was not obtained. The subject was tilted down and the experiment terminated.

Discussion -

The literature contains many reports of experiments attempting to determine the changes in cardiac output during orthostatsis. It is generally accepted that cardiac output decreases upon changing from the horizontal to an upright posture or upon tilt. However, reports we have investigated concerning the magnitude of this decrease vary from 11-30 percent depending upon the protocol of the particular experiment. Smith, in 1966, tilting subjects passively at 70° for 20 minutes using the green dye injection method found cardiac index to decrease by a mean value of 12.5 percent and stroke index to decrease by a mean value of 22 percent (1). Stead, et al, using a 70 percent standing tilt for five to eight minutes and the Fick method of cardiac output determination found a mean decrease in cardiac index of 23 percent (2). Stevens performed a 90°, 20 minute tilt with subjects suspended in a parachute harness using the green dye injection method and found cardiac output to decrease by a mean value of 19 percent and stroke volume to decrease by a mean of 39 percent in non-fainters (3).

In contrast to most other reports with similar protocol, we have found relative cardiac output to decrease by greater magnitudes. In experiments of this type, it is most important that the subject be completely relaxed and free of anxiety and discomfort. Stevens has demonstrated that orthostatic tolerance is decreased by the use of intravascular instrumentation (3). With the instrumentation used in this study, the anxiety and discomfort of other methods was eliminated. In no instances did subjects complain of pain or show signs of fear due to instrumentation. To illustrate the sensitivity of the cardivascular system, subject two on day one at the 42 minute reading (fig. 6-3) showed a marked response to a dynamite blast from a nearby construction project which vibrated the building. Therefore, it is possible that the apparently greater decrease in cardiac output without syncope tolerated by subjects in this study when compared to the results of other investigators may lie in the absence of physical and psychic trauma throughout these experiments.

However, it is also possible that the apparently greater decrease in cardiac output observed in these experiments was an inherent error in the impedance method. For example, a factor for accurate impedance cardiac output determinatons is an accurate measurement of the distance between the two inner bands. Even when securely taped in position to the subject the distance between them varies from the supine to the tilt position. Nevertheless, previous experiments done in this laboratory (Chapter 1) have shown good correlation in relative cardiac output values between the impedance method and the dye dilution method.

Previously mentioned in these results was a transient increase in mean cardiac output values at the 42 to 47 minute readings (10 to 15 minutes tilt). This observation has been reported by other investigators (3).

In conclusion, the findings of this study indicate the impedance method to be a reliable means of determining relative cardiac output during orthostasis in the same individual from day to day. Further, the subject to subject variation appears within the expected range of normal variation. From all indications, the results appear satsifactory.

REFERENCES

1. Smith, W. M., Hyatt, K. H., Kamenetsky, L. G.: The Role of 9 - α - Fluorohydrocortisone as a Countermeasure to Postrecumbency Orthostatism, February 1966 NASA Contractors Meeting.

2. Stead, E. A., Elbert, R. V.: Postural Hypotension, A Disease of the Sympathetic Nervous System. Arch Int. Medicine, 67:546, 1941.

3. Stevens, P. M.: Cardiovascular Dynamics during Orthostatsis and the Influence of Intravascular Instrumentation. The American Journal of Cardiology, Vol. 17, February 1966.

AN OXYGEN CONSUMPTION RATE COMPUTING SYSTEM USING MASS SPECTROMETRY FOR ANALYSIS OF RESPIRATORY GASES

Chapter Summary -

A new system has been developed for determining oxygen consumption rates of human subjects. The block diagram of the system is shown in fig. 7-1. Gas analysis is accomplished with a high degree of sensitivity by means of a quadrupole mass spectrometer which provides a complete quantitative and qualitative analysis of the respiratory gases every 20 milliseconds. Flow rate of gases is measured by means of a Sanborn pneumotachograph system. A Pace TR-20 analog computer is used for the "on-line" computation of oxygen consumption rate. Breath-by-breath determination of oxygen consumption rate can be accomplished if desired. The average oxygen consumption rate per minute can also be determined by integration.

This system provides an excellent means for accurate breath-by-breath analyses of respiratory gases and gas flow rates for:

A. Studies of oxygen consumption rates on human subjects under various conditions and metabolic activities.

B. Pulmonary function tests; for example, the determination of the degree of inequality of gas distribution in the lungs, measurement of the degree of uniformity of the ventilation-perfusion ratio and the variation in respiratory quotient during expiration.

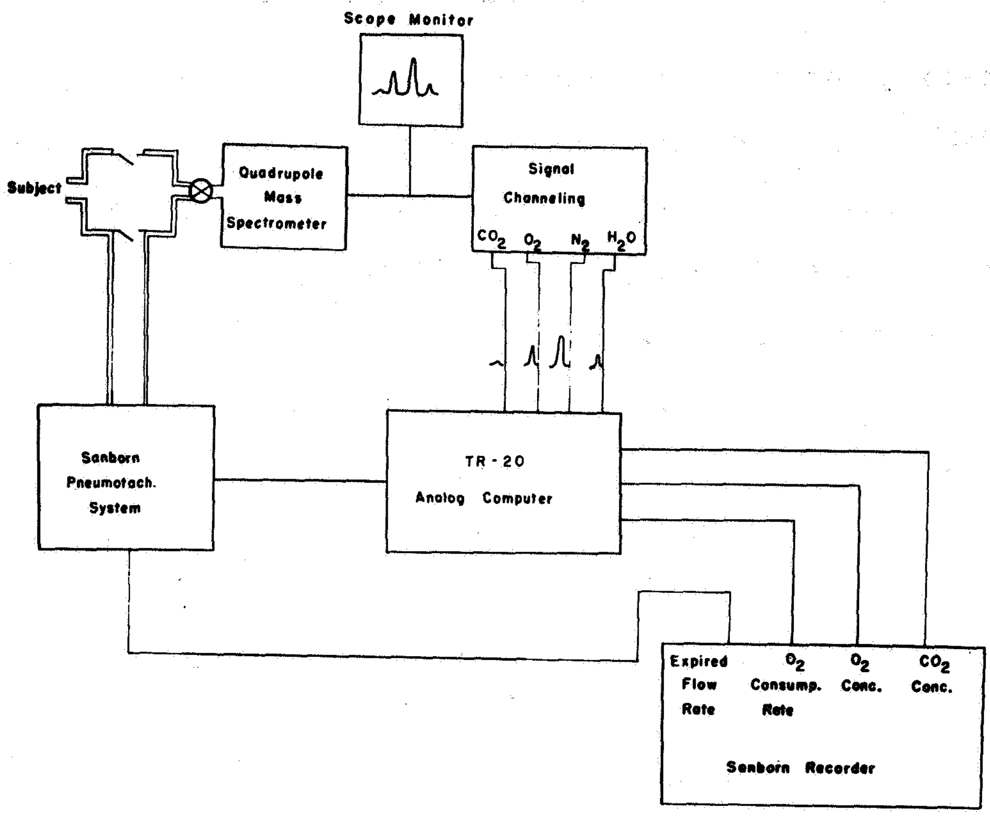

BLOCK DIAGRAM OF MASS-SPECTROMETER
OXYGEN CONSUMPTION RATE SYSTEM

Fig. 7-1

C. Research in respiratory physiology: This system, combined with regional measurements through bronchoscopy should open up wide research possibilities in the elucidation of the changes in pulmonary blood flow associated with various diseases.

D. The mass spectrometer can also be used as a rapid and accurate analyzer for substances in the mass range (1-100)

E. The gas flow rate system can be used independently for studies on pulmonary ventilation dynamics.

SECTION I. Basic Considerations

The determination of the oxygen consumption rate of a human subject while breathing room air or any other gas mixture requires the accurate quantitative and qualitative analysis of expired and inspired gases, as well as the measurement of inspired or expired gas flow rate.

Neglecting pressure differences during the breathing cycle, the mathematical relationship for oxygen consumption rate can be derived from the conservation of mass equation and gas laws.

Let: P_a = atmospheric pressure

C_{i_1} = fractional concentration of oxygen in inspired gas

C_{i_2} = fractional concentration of CO_2 in inspired gas

C_{i_3} = fractional concentration of water vapor in inspired gas

T_i = temperature of inspired gas in degrees Kelvin

$\dot{V}_i$ = flow rate of inspired gas in liters per minute

C_{e_1} = fractional concentration of oxygen in expired gas

C_{e_2} = fractional concentration of CO_2 in expired gas

C_{e_3} = fractional concentration of water vapor in expired gas

T_e = temperature of expired gas in degrees Kelvin

$\dot{V}_e$ = flow rate of expired gas in liters per minute

$\dot{V}_{O_2}$ = oxygen consumption rate in liters per minute

The oxygen consumption rate at STP can be written as:

$$\dot{V}_{O_2} = \left(\frac{273}{Ti}\right)\left(\frac{P_a}{760}\right)\dot{V}_i \left[\frac{\left(C_{i_1}-C_{e_1}\right) + \left(C_{i_3}C_{e_1}-C_{i_1}C_{e_3}\right) + \left(C_{e_1}C_{i_2}-C_{i_1}C_{e_2}\right)}{\left(1 - C_{e_1} - C_{e_2} - C_{e_3}\right)}\right]$$

in terms of inspired gas flow rate.

or:

$$\dot{V}_{O} = \left(\frac{273}{Te}\right)\left(\frac{P_a}{760}\right)\dot{V}_e \left[\frac{\left(C_{i_1}-C_{e_1}\right) + \left(C_{i_3}C_{e_1}-C_{i_1}C_{e_3}\right) + \left(C_{e_1}C_{i_2}-C_{i_1}C_{e_2}\right)}{\left(1 - C_{i_1} - C_{i_2} - C_{i_3}\right)}\right]$$

in terms of expired gas flow rate.

The main desirable features in a system for determining oxygen consumption rate are the following:

1. High speed of response: Breath-by-breath analyses enable studies of dynamic changes in oxygen consumption rate due to physical efforts such as exercise. Time relationships during the breathing cycle can also yield valuable information regarding the functional behavior of the lungs. Such studies require a system with a high response speed based on rapid gas analyses.

2. Accuracy: To meet physiological criteria.

3. Sensitivity of the gas analyzing system: A high degree of sensitivity of the gas analyzing system is desirable in studies covering a wide dynamic range of gas concentrations.

4. The simultaneous analysis of several gases in a gas mixture.

The system described here was designed and built to fulfill the above requirements for studies on oxygen consumption rates of human subjects under various levels of physical activities.

SECTION II Description of the Oxygen Consumption Rate Computing System

The system comprises three main components:

A. The quadrupole mass spectrometer for rapid quantitative and qualitative analyses of respiratory gases

B. The gas flow-rate measuring system

C. The oxygen consumption computing system

A. The Quadrupole Mass Spectrometer

Continuous quantitative and qualitative analysis of respiratory gases is accomplished by means of a quadrupole mass spectrometer (3), which was designed and built in our laboratories. The gas analysing system is therefore composed of the following parts.

1) The gas inlet section:

The gas inlet section is show diagrammatically in fig.7-2. Respiratory gases are sampled from a small compartment attached to a mouthpiece via a stainless steel tube, 0.020" I.D. and 8 feet in length. Two unidirectional rubber valves are mounted in the compartment to separate inspired and expired gas flows, since the measurement of flow rate of either type only is required for oxygen consumption rate determinations. The sampling end of the stainless steel tube is pinched to form a small orifice in order to control the volume of the gas sample while maintaining the highest practical differential pressure gradient. This method has the advantage over the use of capillary tubing in that it has a smaller response time. The sampling tube is, in turn, connected via a high-vacuum valve to an intermediary compartment which is pumped differentially by means of a Welch mechanical pump. The majority of the gas sample is lost to the pump and a very small fraction (of the order of 1μ L/sec at 2 Torr) is allowed to enter the mass analyzer section via a small (100μ diameter) orifice. Differential pumping in this manner is necessary for maximizing the response speed of the system for breath-by-breath analysis of respiratory gases. Provisions are made for heating the sampling tube electrically in order to facilitate the introduction of water vapor into the mass spectrometer for analysis.

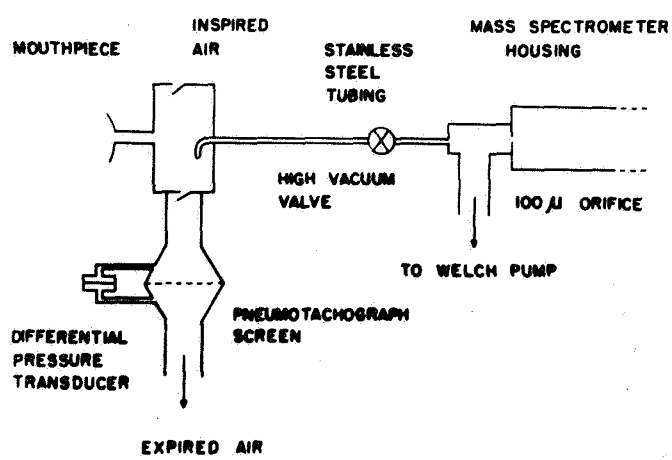

Fig. 7-2 Respiratory gas inlet to the mass spectrometer

2) The mass analyzing section:

The mass analyzing section is enclosed in a glass vacuum system and consists of the following:

a) The ion source:

A Nier-type electron bombardment source (1,2) is used for ionizing the sampled respiratory gas molecules. A heated Tungsten filament (5 watts heating power) provides the necessary electron beam current for ionization by electron impact. A schematic representation of the ion source is shown in fig. 7-3. The positive ions formed in the ionization chamber by the 90 eV electrons are accelerated into the quadrupole mass spectrometer by applying a positive potential (about 20V) to the repeller plate. This potential constitutes, therefore, the accelerating potential for the ions in the mass spectrometer since the entrance to the quadrupole analyzing field is at ground potential due to the symmetry of the applied electric fields.

ION SOURCE

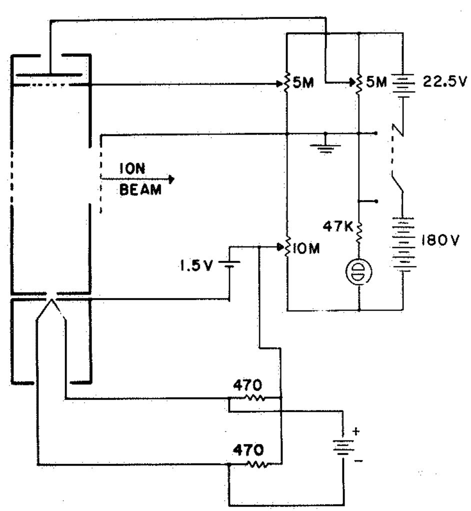

Fig. 7-3

b) The quadrupole analyzing field:

1. Principle of operation:

Positively charged particles are separated in the quadrupole analyzing section according to their mass-to-charge ratio. The basic principle upon which separation is achieved can be explained from a crude physical standpoint as follows:

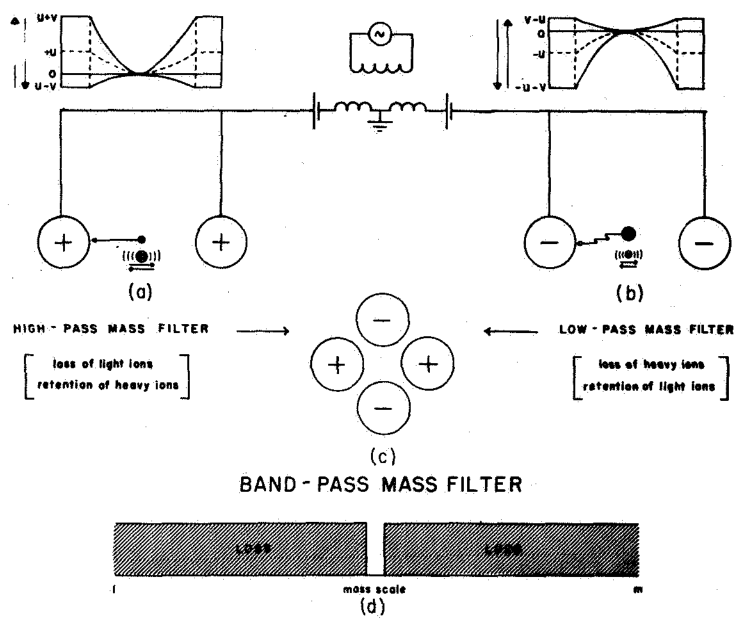

PRINCIPLE OF OPERATION OF
THE QUADRUPOLE MASS SPECTROMETER

Fig. 7-4

Consider two circular rod-shaped electrodes of equal length L and distance $2r_o$ centimeters apart as shown in fig. 7-4(a). Assume a positive d.c. potential (+U) is applied to both electrodes simultaneously with respect to the axis of symmetry (i.e. the midpoint between the two rods is assumed to be maintained at ground potential). A positive ion injected in this electric field region will be restricted near the central axis by the repulsive forces due to the positive potential on the two electrodes. In other words, the positive ion will oscillate, but tend to remain at the bottom of the "valley" created by the potential distribution. This electric field configuration corresponds to a "stable" condition for positive ions, independent of their mass-to-charge ratio (M).

Considering now the case of two electrodes identical to the previous configuration, however, with a negative applied d.c. potential (-U) as shown in fig. 7-4 (b). Similar analogy shows that positive ions will be swept to the rods and are therefore in an "unstable" condition since they are positioned on a "hill" created by the potential distribution.

If an a.c. field is superimposed on the stable configuration (a) with a peak amplitude (V) larger than U, and a positive ion of small mass-to-charge ratio is injected very near the symmetry axis of the field, it is able, due to its light mass, to respond easily to the changes in the electric field. Hence as the resultant field becomes negative during part of the negative half cycle of the a.c. field, the positive ion will be accelerated towards the electrodes gaining a substantial amount of velocity. The following positive half cycle of the a.c. field will have an even greater influence on the motion of the ion, causing it to reverse its direction and accelerate away from the electrodes with a larger force. The net result is that the ion will exhibit oscillations with increasing amplitudes until it finally strikes one of the two electrodes. The lighter the ion in mass, the smaller the number of a.c. cycles elapsed before it is collected by the electrode. Hence, positive ions with small mass-to-charge ratios become "unstable." On the other hand, positive ions with large mass-to-charge ratios (heavy ions) would move very slowly in the field and their velocity is virtually unaffected by the short period of attractive forces during the a.c. cycle. They will tend to oscillate in the field and remain "stable." The field configuration represented in fig. 7-4(a) can therefore be considered as a "High-pass Mass Filter." Heavy positive ions injected parallel to the axis of the field will therefore oscillate with a finite amplitude and exit from the far end of the field, while light positive ions will be swept away from the field and collected by the electrodes.

Considering now the field geometry 7-4(b) with an a.c. field superimposed on this unstable configuration with a peak amplitude V larger than the magnitude of U. In this case, it is easily seen that positive ions with small mass-to-charge ratios will become stable, while heavy positive ions will gradually drift toward the electrodes since they will not respond to any significant extent to the small repulsive force existing during part of the positive half cycle of the a.c. field. This field geometry corresponds therefore to a "Low-pass Mass Filter."

These two field geometries (7-4a and 7-4b) are combined in two perpendicular directions as shown in fig. 7-4c, to produce a "Band-pass Mass Filter." Motion of the positive ions in the x-direction is controlled by the high-pass filter, while that in the y-direction is controlled by the low-pass filter. Therefore, in order for a positive ion entering at one end of this combined field geometry to penetrate through the field and exit from the other end, it must undergo stable oscillations in both the x and y directions. With all other parameters maintained constant, this stability is dependent upon the ion's mass-to-charge ratio (M). Other particles with different mass-to-charge ratios are swept out of the electric field and collected by the rod-shaped electrodes. This is the principle upon which the quadrupole mass spectrometer, or more appropriately designated as the "Mass filter," operates.

The pass-band of this filter is ideally infinitely sharp as shown in fig. 7-4d. In practice, the degree of sharpness of the band is influenced by the initial entrance conditions of the ions, such as their radial energy and initial displacement. This deviation of infinite sharpness conditions appears as tails in the peaks of mass spectra. The width of the pass-band is determined mainly by the ratio of the magnitudes of a.c. to d.c. voltages, i.e. $|V/U|$. It is evident that for $|V| \leq |U|$ the width of the pass-band is zero. Since the mass-to-charge ratio for positive ions is a discrete, and not continuous function, it is also evident that, from a practical standpoint, the width of the band would be zero for $V>U$ up to $M=1$. (This corresponds to the atomic hydrogen ion). There is also a maximum practical limit to the $|V/U|$ ratio, namely that the amplitude of oscillation of stable ions for large $\left|\frac{V}{U}\right|$

would exceed the physical dimensions of the field ($2r_o$) resulting in these ions striking the rod-shaped electrodes.

The position of the pass-band at optimum resolution, i.e. the desired stable mass-to-charge ratio ions (M_s), is determined by the following relationships:

$$M_s = 0.1372V/r_o^2f^2$$

and

$$M_s = 0.8176U/r_o^2f^2$$

where

M_s = mass-to-charge ratio in atomic units of the desired stable ion. (e.g. $O_2^+ = 32$, $O_2^{++} = 16$)

V = a.c. peak voltage amplitude in volts

U = d.c. voltage amplitude in volts

r_o = field radius in centimeters, and is equal to 1/2 the distance between any two opposite electrodes.

f = frequency of applied a.c. voltage in MHz.

<u>General design considerations for the quadrupole mass spectrometer:</u>

A detailed report on the theory of the quadrupole mass spectrometer has been given by M. Mosharrafa and H. J. Oskam (4). It will suffice here, therefore, to outline a general design procedure together with a summary of the basic formulae used in the design of an instrument of this type.

<u>Summary of design formulae:</u>

The relationships between the various "mass filter" parameters which determine the stability of an ion of a specific mass-to-charge ratio (M_s) are summarized in the following design formulae:

$$(\Delta r_o/r_o)_{max} \approx (\Delta M_s/4M_s) \quad (1)$$

$$U_{acc._{max.}} = 4.26 \times 10^2 L^2 f^2 M_s \text{ volts} \quad (2)$$

$$V = 7.287 r_o{}^2 f^2 M_s \text{ volts} \quad (3)$$

$$U = 1.223 r_o{}^2 f^2 M_s \text{ volts} \quad (4)$$

$$P = 6.5 \times 10^{-4} \times CM_s{}^2 f^5 r_o{}^4/Q \text{ watts} \quad (5)$$

$$U_{r_{max.}} = 0.667V(\Delta M_s/M_s) \text{ electron volts} \quad (6)$$

where

r_o = field radius of quadrupole analyzing field in cms.

Δr_o = maximum allowable dimensional tolerance in r_o in cms.

$U_{acc._{max.}}$ = maximum allowable ion accelerating potential in volts.

L = length of quadrupole analyzing field in meters.

f = frequency of applied a.c. voltage in MHz.

M_s = mass-to-charge ratio of desired stable ion.

ΔM_s = width of the stable mass peak (M_s) at 50% of its height ($M_s/\Delta M_s$) is therefore a definition for the resolution of the mass spectrometer.

P = r.f. driving power required in watts.

C = capacity of the system in µµf.

Q = quality factor of the output circuit

$U_{r_{max.}}$ = maximum allowable radial energy of the ions at the entrance to the analyzing field in electron volts.

Design Procedure (5)

1. The desired mass range and maximum resolving power of the instrument should be known.
2. The maximum desired resolving power sets the upper limit on allowable machining and construction tolerances, therefore providing a minimum practical value of field radius r_o to be considered.
3. The field radius r_o is chosen, based on a compromise between mechanical tolerance on the one hand, and radio frequency power requirements which increase proportional to r_o^4 on the other.
4. A choice of the length of the quadrupole analyzing field is made, based on a compromise between the power requirements, which increased linearly with length (the capacity of the system is proportional to length), and the minimum practical required accelerating potential for a defined resolving power.
5. Choice of operating frequency and necessary rf and dc applied voltages: It is evident that the mass filter could be "tuned" to any stable mass-to-charge ratio M_s utilizing several combinations of frequencies and voltage amplitudes. It is therefore important to take the following considerations into account when choosing the most appropriate values. a) Examination of equation 3 reveals that, for the same desired value of M_s higher frequencies will require less voltage amplitudes. However, equation 5 shows that rf power requirements increase proportional to f^5.

Therefore a compromise has to be made again to employ practical power and voltage values. b) Since scanning of the mass range can be accomplished by either a frequency or voltage amplitude sweep, consideration must be taken with regards to upper limiting values of either and their demands on power requirements. Voltage amplitude sweep, however, offers the advantage of a linear mass scale as shown by equations 3 and 4. c) The frequency of operation should be chosen such that the maximum allowable accelerating potential $U_{acc._{max.}}$ given by equation 2 lies within reasonable limits for each required M_s value and resolving power.

6. Mechanical design considerations:

   The type of construction of the quadrupole analyzing field depends entirely on the type of application for which it is to be used. Fields of smaller radii and lengths constructed utilizing circular rods are feasible when the ultimate required resolving power is not high. The construction can therefore be made very simple, compact and light in weight. This type of construction would be quite favorable for space vehicle installation. On the other hand when a high resolving power is required, quadrupole field accuracy necessitates larger dimensions and extreme precision in construction and alignment.

7. Vacuum system design:

   Due to the relative insensitivity of the spectrometer to the background pressure, a distinct feature which permits satisfactory operation up to pressures of 10^{-3} Torr, the vacuum system requirements are not critical. If clean ultra-high vacuum is required, however, facilities for system bakeout have to be introduced and precautions have to be made with regards to choice of materials, impurity traps, etc. It is important to note that in this case an added precaution has to be made for bakeable systems, namely the close matching of thermal expansion coefficients for all materials involved. This is necessary in order not to affect the original tolerances and alignment of the spectrometer upon bakeout.

The quadrupole mass spectrometer used for oxygen consumption rate determinations was designed and built with the following specifications:

Length of analyzing field L	= 10 centimeters
Field radius r_o	= 0.5 centimeters
Operating rf frequency f	= 2.1 MHz.
Range of mass analysis	= 1-50
Operating resolution $M_s/\Delta M_s$	= 50
Maximum resolution	= 100
Peak rf voltage amplitude	= 8.033 volts per unit M_s
dc voltage amplitude	= $\pm$1.348 volts per unit M_s
Voltage amplitude sweep rate	= 50 Hz.

Vacuum system: glass enclosure, 8 liters/sec differential ionization pump. Background pressure less than 10-8 Torr.

Ion acceleration voltage = 22.5 volts dc.

3) The Detection System:

The mass filtered ions arriving at the exit of the quadrupole analyzing field are amplified by a 10-stage Dumont electron multiplier with Cu-Be Dynodes operating at 200 volts per stage. The gain of the multiplier is approximately 10^5. The output current (mass spectrum) from the electron multiplier is further amplified via a high gain solid state amplifier shown schematically in fig. 7-5.

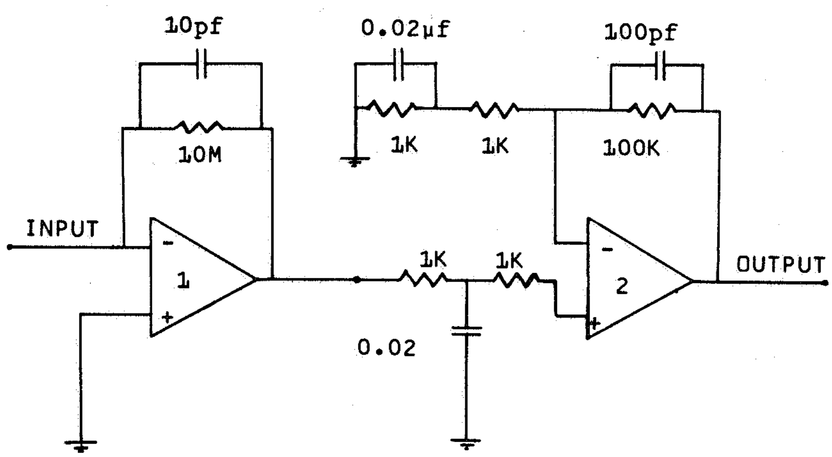

Fig. 7-5 Mass spectrum current amplifier

This amplifier consists of two stages, a high input impedance stage using a differential operational amplifier (Analog Devices Model 301) operating as a current amplifier with unit voltage gain followed by a second stage which provides adequate voltage gain using a Nexus Model SA-2 operational amplifier. The amplified mass spectral current consists of a series of Gaussian shaped current pulses (peaks), each peak signal corresponding to one of the constituents of the gas mixture being analyzed. This current is subsequently channeled through the use of a multivibrator-relay switching circuit. This circuit shown in figs. 7-6, 7-7 serves to separate the mass spectrum into the pertinent component peaks and enables the continuous monitoring and measurement of the components of the respiratory gas mixtures. Four channels are available for monitoring CO_2, O_2, N_2, H_2O respectively.

The General Radio type 1201C master pulse generator which triggers the mass spectrometer sweep voltage also triggers the channeling multivibrator circuit in order to maintain constant time relationships. A Tektronix model 260 monitor oscilloscope is attached to the output of the solid state amplifier for visual monitoring of the mass spectrum.

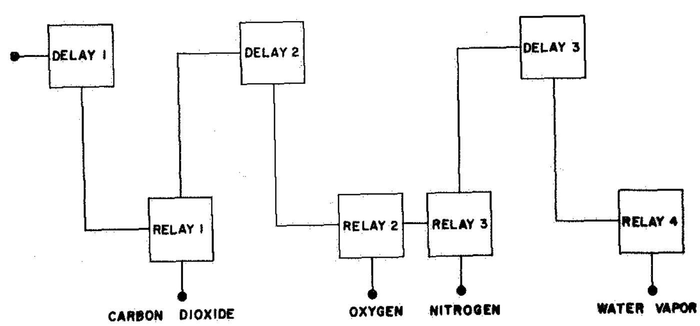

BLOCK DIAGRAM OF CHANNELING CIRCUITS

Fig. 7-6

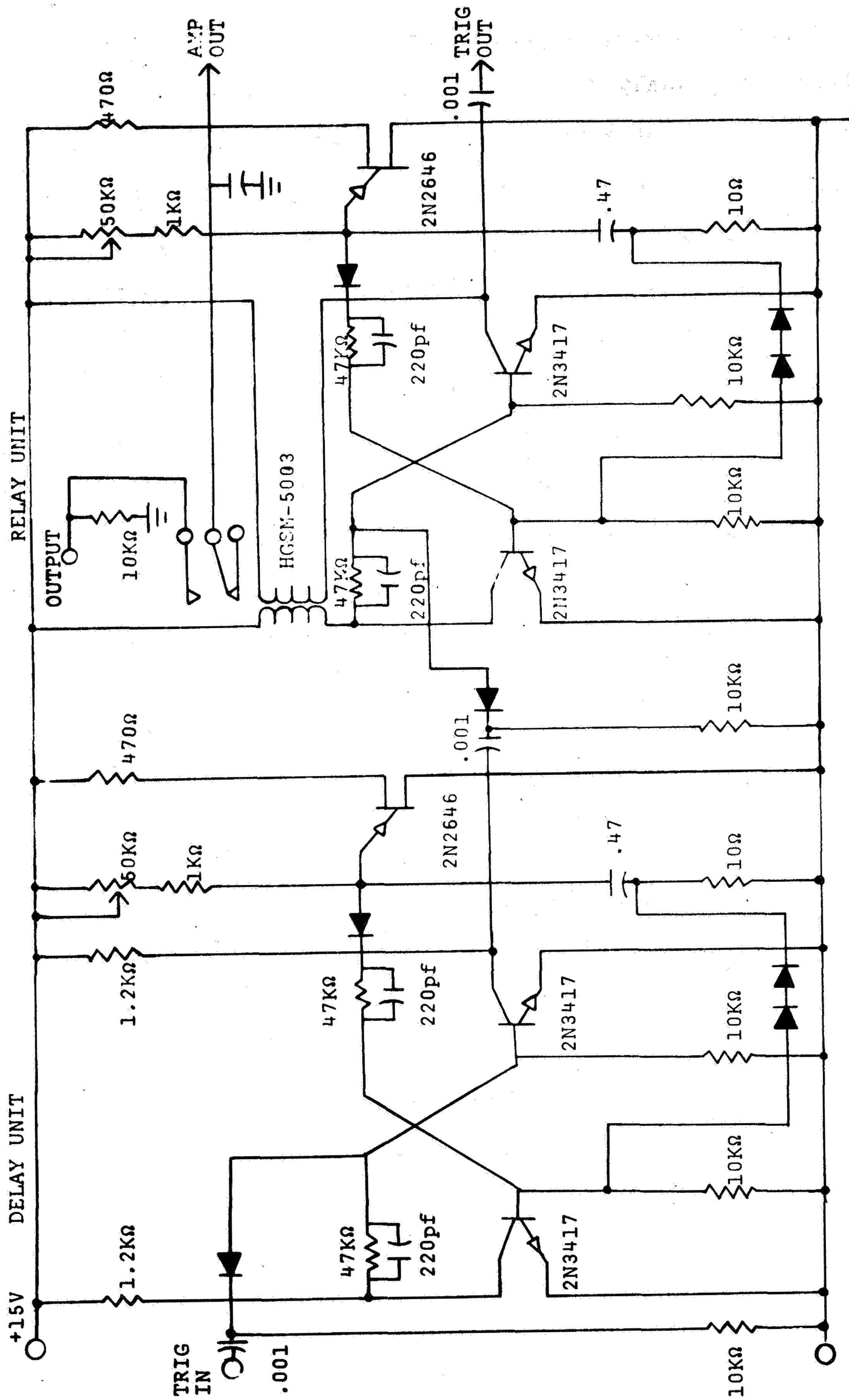

MULTIVIBRATOR - RELAY UNIT

Fig. 7-7

B. Flow rate measuring system:

The flow rate of expired air during the breathing cycle is measured with a Sanborn pneumotachograph system. This consists of a Sanborn pneumotachograph screen which develops a differential pressure proportional to the rate of flow of air through the screen. Three such screens are available for covering flow rates ranging from 0 to 600 litres/min. The differential pressure is measured with a Model 270 Sanborn differential pressure transducer and a Sanborn model 350-3000C carrier pre-amplifier. The output signal of the carrier pre-amplifier which is proportional to the instantaneous flow rate of expired air is used for computation of the oxygen consumption rate, and can also be recorded on a Sanborn model 296 strip-chart recorder. This permits time interval correlation analysis of gas flow rate, CO_2, 0_2 concentrations, and oxygen consumption rate, provided the response time of the gas analyzing system is taken into account.

C. Computing system:

A simplified expression for oxygen consumption rate was used in which the water vapor content in inspired and expired air, temperature, and pressure were neglected. The previous expression in terms of expired gas flow rate, therefore, reduces to:

$$\dot{V}_{O_2} = \dot{V}_2 \left[\frac{\left(C_{i_1} - C_{e_1}\right) + \left(C_{e_1} C_{i_2} - C_{i_1} C_{e_2}\right)}{\left(1 - C_{i_1} - C_{i_2}\right)} \right]$$

Computation of oxygen consumption was performed using a Pace TR-20 analog computer. The computer program is shown in fig. 7-8.

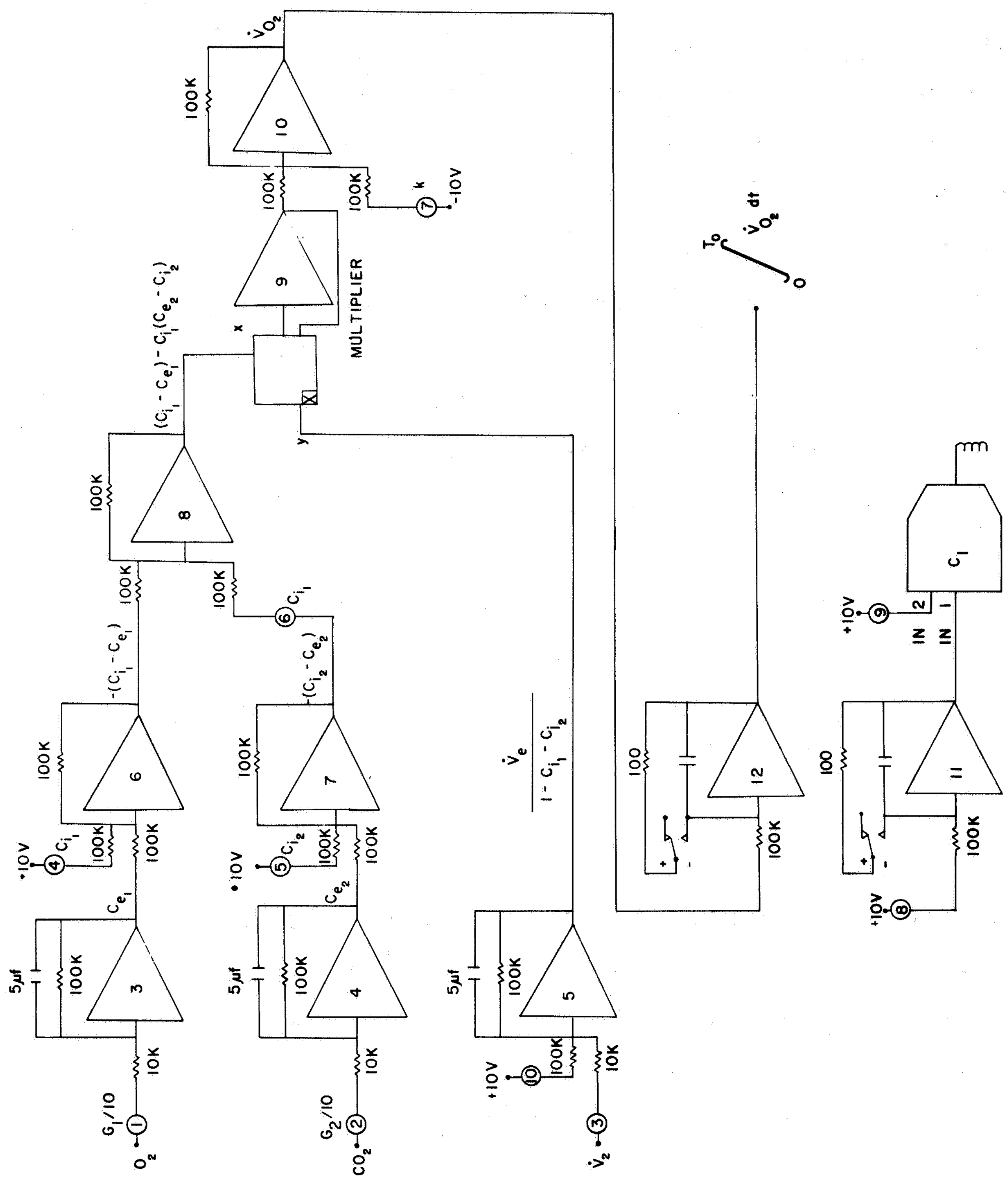

Fig. 7-8 Analog computer program for oxygen consumption calculations

The computer amplitude scaling factor for concentration was taken as: +10 volts corresponds to 100% concentration.

Let

x_1 = mass spectrometer output voltage corresponding to inspired oxygen concentration (C_{i_1}) in volts

x_2 = mass spectrometer output voltage corresponding to oxygen concentration in expired air (C_{e_1}) in volts

y_1 = mass spectrometer output voltage corresponding to inspired CO_2 concentration (C_{i_2}) in volts

y_2 = mass spectrometer output voltage corresponding to CO_2 concentration in expired air (C_{e_2}) in volts

z = output voltage of pneumotachograph system corresponding to flow rate $\dot{V}_2$ in volts

K = amplitude scaling factor for flow rate

Therefore

Gain factor for oxygen: $G_1 = \frac{2.09}{x_1}$

assuming 20.9% O_2 in the inspired gas.

Gain factor for CO_2 : $G_2 = \frac{0.004}{y_1}$

assuming .04% CO_2 in the inspired gas.

These gain factors will be constants since the mass spectrometer system is highly linear throughout the range of oxygen and CO_2 variation. This choice of scaling factor is very advantageous since the analog multiplier provides the necessary division by a factor of 10 and hence the output represents true fractional concentrations. The sensitivity of the system is therefore determined by the scaling factor for flow rate, i.e. scaling factors for flow rate and oxygen consumption rate are identical.

$$\text{Gain factor for flow rate } G_3 = \frac{K}{z}$$

For tests on human subjects under resting conditions, K was taken as 5.0 volt/liter/sec which is also the scaling factor for oxygen consumption rate as described above.

The mass spectrometer output signals corresponding to oxygen and CO_2 are fed into the operational amplifiers 3 and 4 respectively (fig. 7-8) which serve as averaging amplifiers and provide the gain for proper scaling. After appropriate summing to amplifiers 6, 7 and 8, the signal is fed into the X axis of the analog multiplier. Amplifier 5 provides the proper gain scaling factor for the output signal from the pneumotachograph system corresponding to the expired flow rate of air. This in turn is fed into the Y section of the multiplier and the resultant output of the multiplier is fed into amplifier 10, a unity gain amplifier acting as an inverter. In addition, a signal corresponding to the setting of potentiometer 7 (k) serves to correct for the zero offset of the multiplier. The output voltage of amplifier 10 is therefore proportional to the instantaneous oxygen consumption rate, the proportionality constant being K.

It is usually desirable to determine oxygen consumption rates of human subjects averaged over longer periods of time, rather than breath-by-breath values. For this purpose an automatic reset integrator of breath-by-breath oxygen consumption rates has been included in the computing circuitry. This integrator (12) resets automatically after any desired integration time (up to 2 minutes) via the ramp generator (11) and the relay comparator (C_1). A step voltage is applied to amplifier 11 through potentiometer 8, the output of amplifier 11 is a ramp function with a slope determined by the step voltage amplitude (i.e. setting of potentiometer 8). This ramp function is compared with a constant voltage, determined by the setting of potentiometer 9, using the relay comparator. At the instant the two voltages become equal, the relays are activated thereby resetting the oxygen consumption rate integrator (12) as well as the ramp function generator. The integration time T_o is controlled by the setting of both potentiometers 8,9. The output of integrator 12, therefore, represents the total oxygen consumed during the time period selected and can be recorded on a suitable recorder.

SECTION III. Performance Characteristics

The oxygen consumption rate computing system has been successfully tested and adjusted for optimum performance. Typical operating conditions are as follows:

Mass spectrometer operating pressure: 2×10^{-5} Torr.

Mass spectrometer sensitivity: approximately 50 milliamps per torr with 5 watts of dissipation in the ion source filament and an anode current of 5 microamps.

Speed of response: Defined as the time interval between the change in concentration of a constituent of the respiratory gas at the inlet, and the recording of the corresponding change in mass stectrometer output signal. This response time was measured to be approximately 30 milliseconds. This time interval constitutes a constant lag between physical change and observed signal. The actual transit time of the ions in the mass spectrometer is, however, of the order of 20 microseconds.

Good stability, low noise level, and reproducibility of the system ($\pm 1\%$) have been achieved.

The oyxgen consumption rate computing system has been tested in experiments on human male and female subjects at various levels of metabolic activity. Measurements of oxygen consumption rates averaged over one minute time intervals were made on subjects at rest, sitting on a bicycle ergometer, and at 50 watt and 100 watt levels of exercise. Fig. 7-9 shows the results of an experiment performed on a healthy male human subject, age 31.

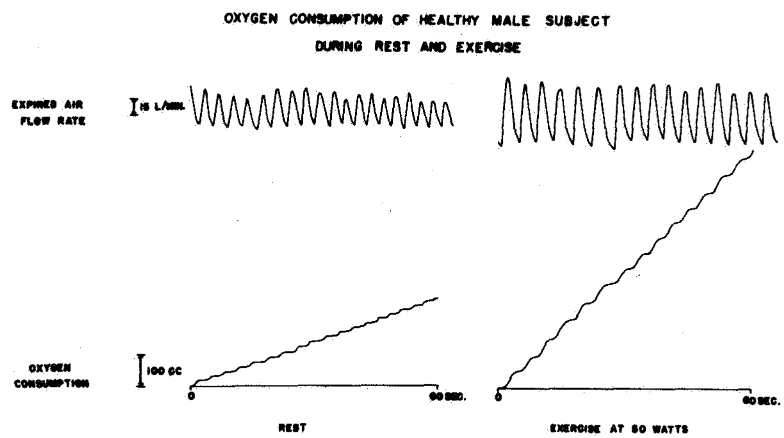

Fig. 7-9

The subject was allowed to rest in a sitting position for 15 minutes prior to the start of the experiment. His total oxygen consumption was then measured over successive one minute time intervals in order to test the reproducibility of the system. This value was found to be 234 STP cc/minute ±1% over a total period of 6 minutes. (In an experiment with another subject, however, rest values of oxygen consumption varied over ±25% during the same time period of 6 minutes.)

The subject commenced exercising on a bicycle ergometer with a 50 watt load for a period of 4 minutes. Oxygen consumption was then measured for the duration of the fourth minute, and for the succeeding three minutes of recovery following exercise. Fig. 7-9 shows tracings of strip-chart recordings of average expired air flow rate and oxygen consumption at rest (234 STPcc/min) and for the fourth minute of exercise at 50 watts (667 STPcc/min). The amount of oxygen consumed during the first and second minutes of recovery from exercise were measured to be 470 STPcc and 371 STPcc respectively.

The exercising load was subsequently increased to 100 watts for the same period of time (4 minutes) and the procedure was repeated in an identical manner to the 50 watt exercise load. The oxygen consumption during the various one minute intervals were found to be as follows:

4th minute exercise: 895 STPcc

1st minute recovery: 800 STPcc

2nd minute recovery: 468 STPcc

3rd minute recovery: 332 STPcc

REFERENCES

1. Nier, A. O.: Rev. Sci. Instr. 11:212, 1960

2. Nier, A. O.: Rev. Sci. Instr. 18:398, 1947

3. Paul, W., Steinwedel, H.: Z. Naturforschg 8a:448, 1953

4. Mosharrafa, M., Oskam, H. J.: Technical Report No. 2, Contract No. Nonr - 710(37), 1961.

5. Mosharrafa, M., Oskam, H. J.: Technical Report No. 5, Contract No. Nonr -710(37), 1964.